Title
Novel strategies for prophylactic viral vaccines enabled by lipid nanoparticle technology

Author
Lam, Alex Ka-Shing

Publication Date
2022

Peer reviewed|Thesis/dissertation

UNIVERSITY OF CALIFORNIA

Los Angeles

Novel strategies for prophylactic viral vaccines enabled by lipid nanoparticle technology

A dissertation submitted in partial satisfaction of the requirements for the degree

Doctor of Philosophy in Molecular and Medical Pharmacology

by

Alex Ka-Shing Lam

2022

ABSTRACT OF THE DISSERTATION

Novel strategies for prophylactic viral vaccines enabled by lipid nanoparticle technology

by

Alex Ka-Shing Lam

Doctor of Philosophy in Molecular and Medical Pharmacology

University of California, Los Angeles, 2022

Professor Ting-Ting Wu, Chair

Lipid nanoparticles (LNPs) are at the forefront of scientific thought due to the SARS-CoV-2 pandemic. While mRNA-LNPs have been studied for years, there is still much to be learned about their uses in translational medicine. Here, we expand the application of this technology for prophylactic viral vaccines and study factors that impact the immunogenicity of mRNA-LNP vaccines.

First, we discuss the prospects for vaccines against the tumor-associated Kaposi sarcoma-associated herpesvirus (KSHV) using knowledge obtained from previous herpesvirus studies. We highlight the need for immune responses in addition to neutralizing antibodies, such as antibodies with effector functions and cellular immunity. We apply LNPs as an adjuvant for a protein-based vaccine against KSHV using virus-like vesicles (VLVs), noninfectious viral particles that present viral envelope proteins. We find that adjuvanted VLVs generate KSHV-specific antibody and T cell responses in mice. Importantly, we highlight an important role of antibodies that target the

complement control protein ORF4 for complement-dependent neutralization of KSHV. This forms a basis for LNP-adjuvanted KSHV VLVs to be developed as a vaccine.

We next studied the impacts of type I interferons (IFN-I) on the immunogenicity of mRNA-LNPs. Using genetic knockout and antibody blockade of IFN-I in mice, we find antigen-specific alterations in immunogenicity against three viral antigens delivered by mRNA-LNPs: influenza hemagglutinin (HA), SARS-CoV-2 Spike receptor binding domain (RBD), and SARS-CoV-2 RNA-dependent RNA polymerase (RdRp). HA antibody responses are largely unaffected by IFN-I, but T cells responding to inactivated viruses are deficient without IFN-I. Antibody responses to RBD appear strain-dependent, but IFN-I is necessary for T cell responses. Finally, RdRp-specific T cell responses are unchanged or enhanced when IFN-I is not present. These results highlight the need for antigen-specific studies to better understand the role of IFN-I in immunogenicity of mRNA-LNPs.

Finally, we study whether mRNA-LNPs that target the highly conserved SARS-CoV-2 RdRp can protect against infection. The RdRp mRNA-LNP is immunogenic in wildtype and transgenic mice, but there was minimal protection conferred by RdRp immunization against high dose SARS-CoV-2 infection of K18-hACE2 transgenic mice. Further studies are necessary to elucidate whether RdRp is a promising candidate for next-generation SARS-CoV-2 vaccines.

The dissertation of Alex Ka-Shing Lam is approved.

Samson A Chow

Robert M Prins

Maureen An-Ping Su

Ting-Ting Wu, Committee Chair

University of California, Los Angeles

2022

DEDICATION

This dissertation is dedicated to my family, who sacrificed so much to build a better life in the United States.

To my dad, Andy, who believed that more education is always better. He would be so proud of this achievement.

To my mom, Christy, who supported me through all these years.

To my sister and built-in friend for life, Michelle. I hope you enjoy the poofy hat.

TABLE OF CONTENTS

LIST OF FIGURES

LIST OF TABLES

ACKNOWLEDGMENTS

This dissertation would not be possible without the support and guidance of my advisor Dr. Ting-Ting Wu. She has constantly challenged me to be a better scientist and expand my boundaries. Thank you for all the time you've spent giving me pep talks, arguing with me, reading my writing, and following my progress. You are truly dedicated to ensuring an excellent training experience for all students in our program. Any student would be lucky to have you as a mentor.

Much of the work in this dissertation was a collaborative effort with many other research groups. I would like to thank Dr. Samson Chow, who opened his lab space to us and supported me throughout my PhD. I would also like to thank the laboratories of Dr. Denise Whitby (NIH/NCI), Dr. Hong Zhou (UCLA), and Dr. Jeffrey Johnson (Mt. Sinai) for their participation in our VLV project. I also thank Drs. Caius Radu and Owen Witte (UCLA) for their support of our work and for pulling us into their studies on mRNA vaccines.

I need to thank the mentees I have been able to teach during my PhD – Claire Harelson, (future) Dr. Shirley Zhang, and Celine Cheng. Thank you for keeping me company in the lab and telling me stories about your lives. I hope you found this experience as rewarding as I have. I would also like to thank Pu-Lin Teng, who has provided much experimental support and assistance.

I am glad to have scientific colleagues who I am also able to call my friends. I would like to thank Dr. Raymond Lim, Dr. Vida Zhang, and (soon to be) Dr. Kathy Situ for listening to my complaints about lab and being supportive friends. To all my other friends who have been there for me along the way – Michelle Lam, Emilio Uranga III, Dr. Chris Alvarado, Daniel Zamora, (soon to be) Dr. Karen Lo, Andrea Tam, James Nguyen, (soon to be) Dr. Emani Stanford, and Sandy Chen – thank you for all the brunches, dinners, and hangouts. I hope we'll have many more soon.

Lastly, I suppose I should acknowledge SARS-CoV-2. The COVID-19 pandemic has disrupted all our lives and caused innumerable tragedies, including in my own life. However, I must begrudgingly acknowledge the fact that much of this work would not have taken place had the pandemic not occurred. This situation interrupted our plans to study our KSHV vaccine platform and pivoted us toward mRNA vaccines. For that reason, this dissertation first explores the potential for vaccination against KSHV. Then, it discusses novel knowledge about mRNA vaccines and the type I interferon system, and finally explores a potential vaccine target for SARS-CoV-2.

Chapter 1 is expanded from “Lam AK and Wu T. Learning from family: how other herpesviruses can inform vaccine design for KSHV. 2022”.

Chapter 2 is expanded from “Lam AK, Roshan R, Miley W, Labo N, Zhen J, Kurland AP, Cheng C, Huang H, Teng P, Harelson C, Gong D, Tam YK, Radu CG, Epeldegui M, Johnson JR, Zhou ZH, Whitby D, and Wu T. Immunization of mice with virus-like vesicles of Kaposi sarcoma-associated herpesvirus reveals a role for antibodies targeting ORF4 in activating complement-mediated neutralization. 2022”.

Chapter 3 is a version of “Lam AK, Teng P, Rashid K, Noguchi MA, Jeyachandran AV, Nesterenko PA, Abt ER, Lee HR, Garcia G Jr, Zhang S, Creech AL, Tam YK, Arumugaswami V, Witte ON, Radu CG, and Wu T. Antigen-specific impact of type I interferons on the immunogenicity of mRNA lipid nanoparticle vaccination. 2022”.

Chapter 4 is a section from a manuscript describing a project still in progress. We thank Dr. Ellie Taus and Dr. Otto Yang for providing human CD8 T cells used in this chapter. SARS-CoV-2 challenge studies were performed by Jill Henley under the supervision of Dr. Lucio Comai at the University of Southern California Biosafety Level 3 Animal Core Facility. Other contributors

include Pu-Lin Teng, Khalid Rashid, Miyako Noguchi, Pavlo Nesterenko, Evan Abt, Hailey Lee, Amanda Creech, Ying Tam, Owen Witte, Caius Radu, and Ting-Ting Wu.

Much of this work was supported by National Institutes of Health grant R01DE028774 to Ting-Ting Wu. The VLV project was further supported by NIH grant R01DE025567 to Z. Hong Zhou and Ting-Ting Wu and by federal funds from the National Cancer Institute under contract 75N91019D00024/HHSN261201500003I to Denise Whitby. Human serum samples used in the VLV project were obtained from the Multicenter AIDS Cohort Study (MACS), which is supported by NIH grants U01-HL146333 to Roger Detels and Matthew Mimiaga and UL1-TR001881 for the UCLA CTSI. mRNA vaccine studies were supported by COVID-19 Research Awards from the W.M. Keck Foundation and Broad Stem Cell Research Center OCRC#20-12 to Caius Radu and Ting-Ting Wu and OCRC#21-100 to Owen Witte and by a grant from the California HIV/AIDS Research Program #H22BD4466 to Ting-Ting Wu. SARS-CoV-2 neutralization studies were supported by NIH grants R01EY032149 and R01DK132735 in addition to COVID-19 Research Award OCRC#20-15 to Vaithilingaraja Arumugaswami. I was supported by the NIH Ruth L. Kirschstein Institutional Research Award for Interdisciplinary Training in Virology and Gene Therapy T32AI060567 and by a graduate student fellowship from the Jonsson Comprehensive Cancer Center.

VITA

Education

2017 B.S. Chemistry – University of California, Los Angeles

Departmental Highest Honors

Awards and Honors

2021 Best Poster Presentation, UCLA Department of Molecular and Medical Pharmacology Annual Retreat

2019 Jonsson Comprehensive Cancer Center Graduate Student Fellowship

2018 Ruth L. Kirschstein Institutional National Research Service Award (Virology and Gene Therapy)

2017 Graduate Dean's Scholar Award

2016 Norman Smith Science Scholarship

Publications

Lam AK, Teng P, Rashid K, Noguchi MA, Jeyachandran AV, Nesterenko PA, Abt ER, Lee HR, Garcia G Jr, Zhang S, Creech AL, Tam YK, Arumugaswami V, Witte ON, Radu CG, and Wu T. Antigen-specific impact of type I interferons on the immunogenicity of mRNA lipid nanoparticle vaccination. 2022; Manuscript in preparation.

Lam AK, Roshan R, Miley W, Labo N, Zhen J, Kurland AP, Cheng C, Huang H, Teng P, Harelson C, Gong D, Tam YK, Radu CG, Epeldegui M, Johnson JR, Zhou ZH, Whitby D, and Wu T. Immunization of mice with virus-like vesicles of Kaposi sarcoma-associated herpesvirus reveals a role for antibodies targeting ORF4 in activating complement-mediated neutralization. 2022; Submission in progress.

Salvatore B, Resop RS, Gordon BR, Epeldegui M, Martinez-Maza O, Comin-Anduix B, **Lam A**, Wu T, and Uittenbogaart CH. Characterization of T Follicular Helper Cells and T Follicular Regulatory Cells in HIV-Infected and Sero-Negative Individuals. 2022 In Review.

Abt ER, Rashid K, Le TM, Li S, Lee HR, Lok V, Li L, Creech AL, Labora AN, Mandl HK, **Lam AK**, Cho A, Rezek V, Wu N, Abril-Rodriguez G, Rosser EW, Mittelman SD, Hugo W, Mehrling T, Bantia S, Ribas A, Donahue TR, Crooks GM, Wu T, and Radu CG. Purine nucleoside phosphorylase enables dual metabolic checkpoints that prevent T cell immunodeficiency and TLR7-dependent autoimmunity. *J Clin Invest*. 2022; 132(16):e160852

Brar G, Farhat N, Sukhina A, **Lam AK**, Kim YH, Hsu T, Tong L, Lin WW, Ware CF, Blackman MA, Sun R, and Wu T. Deletion of immune evasion genes provides an effective vaccine design for tumor-associated herpesviruses. *npj Vaccines*. 2020; 5: 102

Angarita SAK, Truong B, Khoja S, Nitzahn M, Rajbhandari AK, Zhuravka I, Duarte S, Lin MG, **Lam AK**, Cederbaum SD, and Lipshutz GS. Human Hepatocyte Transplantation Corrects the Inherited Metabolic Liver Disorder Arginase Deficiency in Mice. *Mol Genet Metab*. 2018; 124(2): 114-123

Lee PC, Truong B, Vega-Crespo A, Gilmore WB, Hermann K, Angarita SA, Tang JK, Chang KM, Wininger AE, **Lam AK**, Schoenberg BE, Cederbaum SD, Pyle AD, Byrne JA, and Lipshutz GS. Restoring Ureagenesis in Hepatocytes by CRISPR/Cas9-mediated Genomic Addition to Arginase-Deficient Induced Pluripotent Stem Cells. *Mol Ther Nucleic Acids*, 2016; 5(11): e394

CHAPTER 1:

Learning from family: how other herpesviruses can inform vaccine design for KSHV

Abstract

Kaposi Sarcoma-associated Herpesvirus (KSHV) is a gammaherpesvirus that is the etiological agent for cancers such as Kaposi Sarcoma and primary effusion lymphoma. Vaccination against KSHV would reduce the disease burden associated with infection, but an effective vaccine is still not yet available. Because of a relatively small number of vaccine studies on KSHV, research on other herpesviruses provides informative guidance for the design of KSHV vaccine candidates. While most herpesvirus vaccine candidates focused on the induction of neutralizing antibodies that block viral attachment and entry through the antigen-binding (Fab) region, recent data underscore antibody-mediated protection through the constant (Fc) region. Moreover, herpesviruses can spread through a cell-to-cell mechanism, allowing them to evade neutralizing antibodies during dissemination within a host. An effective prophylactic herpesvirus vaccine will likely need to induce multifaceted immunity, consisting of antibody and T-cell responses against a spectrum of viral antigens. Here, we highlight important advancements in human herpesvirus vaccine research and knowledge gleaned from other gammaherpesvirus studies and discuss the implications to the development of a prophylactic KSHV vaccine.

Introduction

Kaposi sarcoma-associated herpesvirus (KSHV) is the etiological agent for Kaposi sarcoma (KS), a cancer that is largely composed of endothelial cells and can appear on the skin, lymph nodes, lungs, and digestive tract. Like all herpesviruses, the life cycle of KSHV has two distinct phases: lytic replication that leads to virion production and latency where the viral genome is maintained in an episomal manner. KSHV belongs to the gamma subfamily of herpesviruses, which establishes latency mainly in lymphocytes and unlike viruses of the other two subfamilies, alpha and beta, is associated with the development of cancers. While the majority of tumor cells in KS are latently-infected, a small fraction of cells express the lytic gene program, inducing angiogenesis and promoting the proliferation and survival of tumor cells[1]. After being discovered in 1994 in an AIDS KS lesion[2], KSHV was also found to be associated with several diseases, including B cell proliferative disorders such as primary effusion lymphoma (PEL) and multicentric Castleman disease (MCD)[3,4], and more recently KSHV inflammatory cytokine syndrome (KICS)[5]. It is estimated that over 40,000 new cases of KS and 20,000 deaths from KS per year[6]. Most of cases and deaths occur in sub-Saharan Africa where KSHV seroprevalence is high, ranging from 30-60%, and resources are limited[6]. Therefore, a vaccine to prevent KSHV-associated diseases is especially beneficial for people living in this area. However, an effective vaccine has not yet been developed. A vaccine that induces sterilizing immunity may not be achievable due to the virus's ability to avoid immune detection during latency. Since the vast majority of KSHV infections are asymptomatic, a more attainable goal for a KSHV vaccine would be the prevention of KSHV related disease by minimizing latent viral load. In order to achieve such a goal, a better understanding of the role of immune responses to KSHV during its natural history and pathogenesis is needed.

Given the fairly recent discovery of KSHV, vaccine research is still at an early stage. The only human herpesvirus for which an effective vaccine has been developed is the alphaherpesvirus varicella zoster virus (VZV). Considerable efforts have also been made on other alphaherpesviruses, herpes simplex viruses (HSV-1 and HSV-2), the betaherpesvirus human cytomegalovirus (hCMV), as well as the other human gammaherpesvirus, Epstein-Barr virus (EBV). Despite decades of effort, effective vaccines for these viruses remain elusive. Nevertheless, valuable lessons that have been learned from these efforts can inform the design of a KSHV vaccine. Meanwhile, it is imperative to be mindful of a fundamental difference in the viral pathogenesis between gammaherpesviruses and the other herpesvirus families. Alpha- and betaherpesviruses cause diseases via lytic replication, whereas cancers associated with gammaherpesviruses are composed of mostly latently infected cells, where expression of latency-associated genes from the viral genome predisposes cells for transformation by driving the proliferation of infected cells[1]. However, lytic replication can also contribute to the pathogenesis of gammaherpesviruses indirectly, for example, by expressing lytic genes that facilitate the proliferation of latently-infected tumors cells and by replenishing the pool of latently infected cells[7]. Therefore, unlike vaccines for VZV, HSV, and hCMV, which aim to control lytic replication to protect against diseases, vaccines for KSHV and EBV may need to prevent or at the very least reduce viral latency to protect against cancers. Prevention of latent infection is extremely challenging but is the ultimate goal for all herpesvirus vaccines. Alternatively, a KSHV vaccine might function to enhance immune control of latently infected cells to prevent cancer development. Because there is no small animal model for KSHV and EBV, a closely related rodent herpesvirus, murine gammaherpesvirus-68 (MHV-68), has been exploited as a model to study vaccine strategies and the immune mechanisms needed to prevent latency[8]. Here, we will highlight recent developments in prophylactic human herpesvirus vaccine research with the focus on how they differ from traditional approaches, summarize the knowledge gained from the MHV-

68 studies, and discuss how they can be applied to developing a prophylactic vaccine for KSHV in the future.

Lessons from alpha- and beta-herpesviruses

Primary VZV lytic infection causes varicella (chickenpox), a once common childhood disease; reactivation of latent VZV into lytic replication causes herpes zoster (shingles), which occurs more frequently in older adults. The live attenuated Oka strain has been used for vaccination to protect against chickenpox in children and shingles in older adults. More recently, an adjuvanted recombinant glycoprotein E (gE) vaccine, Shingrix, was developed to prevent shingles[9,10]. gE is the most abundant viral protein on the viral envelope and in infected cells[11]. Levels of antibodies binding to gE correlate well to protection against varicella in children immunized with the live VZV vaccine[12]. In addition, post-exposure administration of VARIZIG (Varicella Zoster Immune Globulin), prepared from plasma of donors containing high titers of anti-VZV antibodies, has been shown to reduce the severity and incidence of varicella in high risk populations[13]. Therefore, vaccine-elicited humoral immunity is likely important for protection against varicella. However, cell-mediated immunity (CMI) also plays a critical role in preventing shingles, which is associated with a decline in CMI and not antibody[14]. The live vaccine is generally thought to elicit a broad cellular and humoral immune response against a spectrum of viral antigens. And yet, the gE subunit vaccine offers better efficacy of protection against shingles than the live VZV vaccine[15]. This could be because gE-specific T cell responses were over ten times higher in people who received the gE subunit vaccine than those who received the live VZV vaccine[16]. In addition, the gE vaccine also boosted gE-specific antibody responses more than the live vaccine[17]. Therefore, the single viral antigen gE vaccine that boosts gE-specific cellular and humoral immunity in infected individuals is sufficient to protect against shingles caused by VZV reactivation.

Nevertheless, it remains to be determined whether this vaccine is also effective against varicella, which is caused by primary infection in naïve individuals.

Numerous efforts have been made to develop vaccines for HSV-1, HSV-2, and hCMV (reviewed in [18–20]). HSV vaccines have attempted subunit, live attenuated, or inactivated whole virus vaccine strategies in preclinical studies, and some have advanced to clinical trials. gD, essential for HSV entry of cells, is the major target for vaccine development[21]. The Herpevac Trial investigated the protection afforded by an adjuvanted HSV-2 gD (gD2) subunit vaccine against primary infection. This vaccine, which elicited a high titer of neutralizing antibodies, showed vaccine efficacies of 58% against genital HSV-1 disease and 35% against HSV-1 infection but no protection against HSV-2[22]. It was later found that antibodies, not T cells, are the correlate of protection against disease[23]. Although it is not surprising to observe protection against HSV-1, as gD of HSV-1 shares >80% amino acid sequence homology to gD2, it is not completely clear why the gD2 vaccine is not effective for HSV-2 despite robust neutralizing antibody levels. An important lesson from the Herpevac Trial is that neutralizing antibodies may not be the only component of effective protection, as certain individual with high levels of neutralizing antibodies were still infected. One explanation could be because herpesviruses can spread independently of cell-free virions such as through cell-cell spread, which is unaffected by neutralizing antibodies[24]. Thus, additional antibody functions should be explored, such as protection through other antiviral mechanisms mediated by their Fc regions: antibody-dependent cellular cytotoxicity, antibody-dependent phagocytosis, and complement-dependent neutralization and cytotoxicity[25,26]. HSV-2 expresses two immune evasion glycoproteins, gC and gE, which block complement and Fc-receptor mediated antibody effector functions, respectively[27–29]. In preclinical studies, when gC and gE are also included in subunit vaccines in addition to gD, the protection against HSV-2 is significantly improved compared to a vaccine with gD alone[29,30]. Built on these studies, a trivalent nucleoside-modified mRNA vaccine encoding gD, gC, and gE was generated and has demonstrated superior

efficacy of protection in preclinical models[31–34]. This trivalent vaccine elicits antibodies that block the immune evasion mechanisms of gC and gE, thereby enhancing the effector functions of gD antibodies[29,30]. Therefore, while gC and gE have not been traditionally targeted by HSV vaccines, it appears that blocking their functions by vaccination would enhance protective humoral immunity of the vaccine. Another HSV-2 vaccine candidate that emphasizes the important of antibody effector functions is based on an attenuated single-cycle gD-deleted virus (ΔgD-2). Immunization with ΔgD-2 provides complete protection against lethal challenge of HSV-2 in mice[35]. The sera from the ΔgD-2 immunized mice possessed very little neutralization activity but contained antibodies that have both Fc-receptor and complement effector functions[36,37]. Moreover, passive transfer of the ΔgD-2 immune serum protected wild-type (WT) mice but not Fc-receptor knockout mice against HSV-2 challenge, suggesting that the effector functions of antibodies are vital to protection[35,38,39]. Together these studies indicate that while conventional neutralizing antibodies that block entry and fusion through their Fab regions is a major component of protective immunity, other antiviral functions through the Fc-region of antibodies can also contribute to vaccine-mediated protection.

For hCMV, many vaccine candidates based on a variety of platforms have been studied (reviewed in [40]). A recent vaccine candidate, V160, is a live attenuated AD169 strain that only replicates in the presence of a synthetic compound[41]. Therefore, this virus is replication deficient and unable to persist beyond one cycle of replication *in vivo*. In addition to safety, V160 is further improved from the previous AD169 attenuated strains by the restoration of viral pentameric protein complex (gH/gL/pUL128/pUL130/pUL131) that is required for hCMV infection of epithelial and endothelial cells[42,43]. Immunization of seronegative patients with V160 resulted in both neutralizing and non-neutralizing antibodies against a variety of targets including the restored pentameric complex[44]. In addition, subunit vaccines have also been studied, especially those targeting gB, which is required for viral fusion. Interestingly, while gB-based vaccines generate neutralizing antibodies

in humans, this neutralizing activity is significantly enhanced by complement[45,46]. Analysis of sera from vaccinated humans indicated that the protection provided by an adjuvanted gB vaccine could be attributed to non-neutralizing effector functions[47]. More recently, due to the advent of mRNA vaccines, Moderna's mRNA-1647, which combines six viral targets (gB and the viral pentameric complex), has entered Phase 3 studies. Overall, the recent developments in HSV and hCMV vaccines have emphasized approaches that include multiple viral targets and harness the Fc-mediated functions of antibodies.

Guidance from the MHV-68 model

Due to the restricted host range of KSHV and EBV, the MHV-68 mouse infection model has been widely used to test various "proof-of-principle" vaccination strategies for gammaherpesviruses. Like KSHV and EBV, MHV-68 also establishes long-term latent infection in B cells[48,49]. Following intranasal infection, MHV-68 first undergoes acute lytic replication in epithelial cells of the respiratory tract. Subsequently, the virus spreads to secondary lymphoid organs and infects B cells, likely via trafficking of infected myeloid cells[50–52]. Viral latency in the spleen peaks at 2-3 weeks after inoculation and is accompanied by splenomegaly, a syndrome similar to infectious mononucleosis associated with EBV primary infection. MHV-68 then establishes a steady, low level persistent infection 4-6 weeks later. Because the oncogenic potential of gammaherpesviruses is associated with their latent infection, the goal for vaccines is to identify a strategy that will prevent the establishment of latency in B cells. The only strategy that has shown to afford the desired protection so far is based on live attenuated viruses, which for safety reasons were engineered to be latency-deficient through (i) overexpression of the viral replication and transcriptional activator (RTA), (ii) removal of latency-associated gene encoded by ORF73, or (iii) both[53–58]. Recently, to further increase the safety of a latency-deficient virus, our laboratory has minimized the ability of the vaccine virus to replicate *in vivo* by removing multiple viral immune

evasion mechanisms. This generated a severely attenuated vaccine virus that has no detectable productive or latent infection in vivo but is highly efficacious in protecting against latency establishment from a WT challenge virus[59]. However, the same protection was not attained by vaccination of another latency-deficient virus that was made replication-deficient by eliminating RTA expression[60]. These studies demonstrate that latency is not required for a live attenuated virus to elicit protective immunity, but antigen expression from the vaccine virus is critical.

Due to the potential oncogenic risk of an infectious gammaherpesvirus, alternative, safer vaccine candidates, such as subunit vaccines have been investigated. The first type of subunit vaccines focused on generating antibodies against viral glycoprotein 150 (gp150), which has significant homology to EBV's gp350, the protein responsible for mediating EBV attachment to host B cells[61,62]. Although immunization with a gp150-expressing vaccinia virus was able to generate MHV-68-neutralizing antibodies that lessened mononucleosis-like symptoms, the challenge virus was nonetheless able to establish latency[63]. Other subunit vaccines were designed to elicit T cell responses against viral lytic antigens. Vaccination with DNA encoding for viral protein M3, vaccinia viruses expressing major T cell targets (lytic proteins ORF6 and ORF61), or adenoviruses encoding known viral $CD8^+$ T cells epitopes were able to inhibit lytic replication and reduce but not eliminate latency after WT virus challenge[64–66]. Other groups have attempted vaccinations with latent antigens instead of lytic ones. Using either DNA vaccines or adenoviruses to generate cellular immunity against the latent antigen M2 led to a lower latent load, but was still unable to completely prevent latency establishment by a WT challenge virus[67,68]. The major latency-associated gene of gammaherpesviruses is known to have evolved to reduce its expression and antigen presentation by MHC class I, which avoids the detection and elimination by CD8 T cells[69,70]. Therefore, efforts were also made to increase the CD4 T cell control of latently infected B cells, which express MHC class II and can be targets for cytotoxic CD4 T cells. However, an elegant study using a recombinant MHV-68 virus to express and present a defined

MHC class II-restricted OVA epitope under the control of latent gene ORF73 promoter has shown that while OVA-specific CD4 T cells were elicited and could eliminate B cells artificially coated with the OVA peptide, they had no impact on latently infected cells that endogenously expressed the same epitope[71]. Thus, it may be difficult to directly eliminate latently infected cells and instead, vaccination to prevent the lytic replication that precedes latency establishment may be a more effective strategy. This is consistent with the conclusion from studies of live attenuated virus vaccine candidates that latent infection and latency-associated genes are not required for eliciting protective immunity against latency establishment. While subunit vaccines have some impact on MHV-68 replication, they can reduce peak latent infection, but are ultimately unable to prevent, or even impact long-term latency on their own.

A compromise between live attenuated viruses and subunit vaccines could be whole inactivated viruses (WIVs). WIVs containing the complete set of viral envelope proteins and have been used as effective vaccines for other viruses. Immunization with unadjuvanted inactivated MHV-68 is able to induce immune responses that limit lytic challenge WT infection, but cannot prevent latency establishment[72,73]. Studies using formalin-inactivated virions of HSV showed that adjuvants improved protection, potentially due to the induction of cellular immunity[74,75]. Thus, WIVs have the potential to present a diversity of viral antigens for antibody and CD4 T cell responses if appropriate adjuvants are used. Overall, vaccination strategies that induce a broad spectrum of immune responses could be better candidates to prevent latency establishment compared to subunit vaccines based on individual viral antigens.

Recent advances in human gammaherpesvirus vaccine development

Compared to KSHV, much more vaccine research has been performed on EBV, likely due to a higher incidence of associated diseases in the United States[76,77]. EBV vaccine candidates have been focused on recombinant proteins, virus like particles (VLPs), or viral vectors encoding an

EBV protein. EBV's gp350 is the attachment protein for B cell infection and the major target for antibodies that neutralize B cell infection in humans[78,79]. As a result, gp350 has drawn the most attention for vaccine development. In human studies, gp350-based vaccine candidates have so far demonstrated a potential protection against the symptomatic primary EBV infection disease, infectious mononucleosis, but are unable to prevent infection[80] similar to the MHV-68 gp150 study[63]. The effect on long-term EBV latent load in gp350-vaccinated individuals is yet to be determined. However, immunization with the gp350 homologue of the rhesus lymphocryptovirus (LCV) resulted in lower levels of long-term viral DNA in the blood after LCV challenge[81], suggesting some benefit from gp350 immunization. In addition to gp350, antibodies to the EBV fusion machinery, gH/gL or gH/gL/gp42, also contribute to neutralizing activities of human plasma[82]. A ferritin-based nanoparticle that incorporates EBV gH/gL and gp42 is able to elicit high levels of neutralizing antibodies that block viral fusion in immunized mice and nonhuman primates[82]. Antibodies from mice immunized with ferritin-based gH/gL/gp42 nanoparticles or with self-assembling gH/gL particles are able to protect humanized mice from EBV infection[83,84]. While these subunit vaccines have achieved success in preclinical studies, a parallel approach to generate broad immune responses toward multiple EBV proteins has also been followed, utilizing virus-like particles (VLPs) produced from viral mutants deficient in genome packaging or viral maturation. These VLPs are devoid of viral DNA but contain viral structural proteins, including all envelope proteins[85,86]. Vaccination of these non-infectious EBV VLPs reduced the chance of humanized mice being infected with EBV, and the protection was enhanced by the incorporation of epitopes from the EBV latent proteins EBNA1 into the VLP vaccine[87]. These EBV vaccine studies emphasize the trend toward multivalent vaccines, rather than focusing on a singular protein target.

For KSHV, one main avenue of vaccine research under active investigation is VLPs generated through the Newcastle Disease Virus (NDV) platform, which was used previously to incorporate

EBV glycoproteins[88,89]. This platform uses the NDV fusion (F) protein to display antigens, which are assembled into VLPs through interactions with the viral matrix protein (M) and nucleoprotein (NP). NDV VLPs were generated to display KSHV glycoproteins individually (except where gL must be expressed with gH to be displayed) and used to immunize mice and rabbits[90,91]. Neutralizing antibodies were elicited with the highest level detected when VLPs of K8.1, gB, and gH/gL were all included for immunizations[90]. This NDV VLP platform demonstrates that multivalent vaccines would be the optimal approach for a KSHV vaccine and is now awaiting testing in nonhuman primate models. Recently, our laboratory identified a KSHV mutant that generates non-infectious KSHV virus-like particles, which we named virus-like vesicles (VLVs)[92]. Like EBV VLPs mentioned above, KSHV VLVs display a spectrum of antigens including those on the surface of virions, providing a safe multi-antigen vaccine candidate for KSHV. Others have proposed an epitope-based KSHV vaccine strategy by immunizing against multiple T and B epitopes selected through bioinformatics analysis, but this strategy has yet to be tested in animals[93]. While few preclinical candidates for KSHV vaccines have been developed so far, platforms that can elicit cellular and humoral immunity toward multiple viral antigens would be the way forward.

Potential immune components of an effective KSHV vaccine

Neutralizing antibodies that block viral attachment or entry are generally thought to be the correlate of protection for most commercial vaccines[94,95]. KSHV's K8.1 is one of the major targets of antibodies in infected individuals[96]. Although antibodies against K8.1 provide some neutralizing activity[97], K8.1 is not needed for infection of epithelial cells[98]. For KSHV, neutralizing antibodies should target K8.1 and gB to block attachment via heparan sulfate moieties on the cell surface, and target gH/gL and gB to block entry and fusion. The NDV-based VLP platform mentioned above is designed to achieve the goal of generating KSHV neutralizing antibodies. Because

KSHV, like other herpesviruses, can probably spread through a cell-to-cell mechanism that evades neutralization, neutralizing antibodies should not be the only focus of vaccine research. Studies from HSV and hCMV highlighted above provide evidence that other mechanisms of antibodies could make important contributions to vaccine-mediated protection, and this lesson should be considered in the development of a KSHV vaccine.

Fc-mediated antiviral functions of antibodies has been shown to play a major role in controlling MHV-68 infection[99,100]. For KSHV, the importance of non-neutralizing antibodies is implicated from mother-child transmission studies, where maternal antibodies are generally thought to protect young children from infection. One study of KSHV-infected mother-child pairs showed that mothers of seroconverted children had an average lower KSHV-specific antibody titers compared to those of seronegative children[101]. Only few seropositive mothers had detectable neutralizing antibodies, 3/54 mothers of KSHV seropositive children and 2/32 mothers of KSHV seronegative children. This low prevalence of neutralizing antibodies implies other antiviral functions of antibodies may be important for controlling KSHV infection or transmission. A similar notion is also derived from studies in EBV and hCMV, which showed that neutralizing antibodies were not necessarily the mechanism of protection against transmission in mother-child pairs[102,103]. Only one study has been conducted on KSHV to analyze a different Fc-mediated function, antibody-dependent cellular cytotoxicity (ADCC). It showed that while many patients had ADCC-capable antibodies, there was no correlation between these antibodies, patient characteristics, or disease[104]. Finally, there are currently no published studies regarding the role of complement in infected individuals. A preliminary study from our laboratory indicates that KS patient sera do not possess significant complement-mediating activities. However, it is known that KSHV encodes a modulator of complement activity via ORF4[105], and that antibodies towards ORF4 can inhibit its complement regulatory functions[106,107]. Thus, more studies are required to understand how KSHV antibodies can contribute to protection beyond blocking virus attachment and entry.

While much attention has been paid to eliciting antibody responses by prophylactic vaccination, it is generally thought that vaccine efficacy will be enhanced by stimulating T cell immunity to control infected cells. T cell responses against KSHV in infected individuals are low and disparate[108], especially when compared to those in EBV-infected individuals[109–111]. K8.1 is a more consistent target of T cell responses compared to other viral proteins, but still only a third of patients exhibit K8.1-specific T cells[111]. However, that does not mean T cells do not play a role in protection against KSHV and instead suggests that perhaps KSHV-associated diseases can be kept in control with relatively low cellular immunity. This also suggests the opportunity for vaccines to elicit a more robust T cell immunity than natural infection, which may enhance the immune control of KSHV infection, especially in already infected individuals. Studies using the MHV-68 model have demonstrated that T cells alone can reduce both lytic infection and the peak latent viral load[59,66,112]. Ideally, this T cell protection would supplement that provided by antibodies. Moreover, with a possible progressive decay of antibody level after immunization, vaccine-induced T cells could eliminate newly infected cells and contribute to protection. Like other viruses, KSHV has evolved multiple mechanisms to evade T cell immunity. For example, two virally encoded ubiquitin ligases, K3 and K5, promote the degradation of MHC class I molecules[113,114]. Furthermore, the latency-associated nuclear antigen (LANA), in addition to being resistant to processing for MHC-I presentation[70], downregulates MHC class II at the transcriptional level, leading to reduced antigen presentation for immune surveillance[115]. However, in the context of infection, MHC class I downregulation in endothelial cells takes at least 24 hours[116] while in primary human tonsillar B cells neither MHC class I nor class II is downregulated[115,117]. Moreover, KSHV-infected tonsillar B cells can be recognized by LANA-specific CD4+ T cells resulting in the production of IFNγ[117]. Although studies in MHV-68 demonstrate that latently-infected B cells could be a difficult target for elimination by effector T

cells[71], T cells that can recognize latent proteins are still desirable for vaccines in order to control latently infected B cells early in infection, before antigen presentation is compromised.

Discussion

Herpesviruses have been notoriously difficult pathogens for vaccine development. The vast armaments of immune evasion genes and the ability to enter latency largely contribute to this challenge. Vaccine development is an especially daunting task for gammaherpesviruses because an effective vaccine will need to prevent or reduce latent infection where the expression and presentation of antigens that can be targeted by the immune system is limited. As implicated by the MHV-68 studies, controlling lytic replication leading up to the establishment of latency in B cells should be considered as part of vaccine strategies. In addition, immune responses such as cytotoxic cellular immunity and Fc-mediated antiviral activities of antibodies should supplement neutralizing antibodies that block attachment and fusion. However, selecting the viral proteins included in a vaccine to elicit protection could be challenging. Two platforms to present a repertoire of viral proteins are live attenuated viruses and whole inactivated viruses. Live attenuated viruses have advantages of self-adjuvanticity and the ability to present proteins expressed throughout the viral life cycle, showing much promise in the MHV-68 model. However, the risk associated with viral DNA and latent infection poses a significant safety concern for using live attenuated viruses to vaccinate healthy individuals. Whole inactivated viruses present a lower risk but have shown reduced efficacy in the MHV-68 model[73]. This may be ameliorated by co-administration with adjuvants to stimulate immune responses, but this is yet to be shown. One alternative to whole inactivated viruses is VLPs produced from EBV and KSHV mutants. These non-infectious EBV and KSHV VLPs mimic the viral structure and contains an array of viral structural proteins, but lack viral DNA[85,92]. Using these VLPs as vaccines can avoid the predicament of selecting viral antigens while still being able to be engineered to induce immune

responses to nonstructural antigens as well. Moreover, to improve protection against latent infection, these viral VLPs can also be modified to incorporate antigens expressed during latency[87]. With multiple platforms available to prime not only humoral but also cellular immunity against a variety of viral antigens, vaccines for KSHV and EBV could be across the horizon, leading us to the ability to control these viruses and the diseases they cause.

Author Contributions

A.K.L. drafted the manuscript. A.K.L. and T.W. edited the manuscript and approved its submission.

Acknowledgements

We would like to acknowledge the numerous articles we were unable to reference in this review. This work was supported by grant R01DE028774 to TTW from the National Institutes of Health. AKL was partially supported by a fellowship from the UCLA Jonsson Comprehensive Cancer Center (JCCC) and the Ruth L. Kirschstein Institutional National Research Service Award (Virology and Gene Therapy Training Grant) T32AI060567. We thank Denise Whitby for a critical reading of this review.

References

1. Ganem, D. KSHV-induced oncogenesis. in *Human Herpesviruses: Biology, Therapy, and Immunoprophylaxis* (eds. Arvin, A., Campadelli-Fiume, G. & Mocarski, E.) (Cambridge University Press, 2007).
2. Chang, Y. *et al.* Identification of herpesvirus-like DNA sequences in AIDS-associated Kaposi's sarcoma. *Science* **266**, 1865–1869 (1994).
3. Cesarman, E., Chang, Y., Moore, P. S., Said, J. W. & Knowles, D. M. Kaposi's Sarcoma–Associated Herpesvirus-Like DNA Sequences in AIDS-Related Body-Cavity–Based Lymphomas. *N Engl J Med* **332**, 1186–1191 (1995).
4. Soulier, J. *et al.* Kaposi's sarcoma-associated herpesvirus-like DNA sequences in multicentric Castleman's disease. *Blood* **86**, 1276–1280 (1995).
5. Uldrick, T. S. *et al.* An Interleukin-6–Related Systemic Inflammatory Syndrome in Patients Co-Infected with Kaposi Sarcoma–Associated Herpesvirus and HIV but without Multicentric Castleman Disease. *CLIN INFECT DIS* **51**, 350–358 (2010).
6. Grabar, S. & Costagliola, D. Epidemiology of Kaposi's Sarcoma. *Cancers* **13**, 5692 (2021).
7. Aneja, K. K. & Yuan, Y. Reactivation and Lytic Replication of Kaposi's Sarcoma-Associated Herpesvirus: An Update. *Front. Microbiol.* **8**, 613 (2017).
8. Dittmer, D. P., Damania, B. & Sin, S.-H. Animal models of tumorigenic herpesviruses--an update. *Curr Opin Virol* **14**, 145–150 (2015).
9. Wang, L., Zhu, L. & Zhu, H. Efficacy of varicella (VZV) vaccination: an update for the clinician. *Ther Adv Vaccines* **4**, 20–31 (2016).
10. Maltz, F. & Fidler, B. Shingrix: A New Herpes Zoster Vaccine. *P T* **44**, 406–433 (2019).
11. Levin, M. J. & Weinberg, A. Immune responses to zoster vaccines. *Human Vaccines & Immunotherapeutics* **15**, 772–777 (2019).
12. Habib, M. A. *et al.* Correlation of protection against varicella in a randomized Phase III varicella-containing vaccine efficacy trial in healthy infants. *Vaccine* **39**, 3445–3454 (2021).
13. Levin, M. J., Duchon, J. M., Swamy, G. K. & Gershon, A. A. Varicella zoster immune globulin (VARIZIG) administration up to 10 days after varicella exposure in pregnant women, immunocompromised participants, and infants: Varicella outcomes and safety results from a large, open-label, expanded-access program. *PLoS ONE* **14**, e0217749 (2019).
14. Weinberg, A. & Levin, M. J. VZV T Cell-Mediated Immunity. in *Varicella-zoster Virus* (eds. Abendroth, A., Arvin, A. M. & Moffat, J. F.) vol. 342 341–357 (Springer Berlin Heidelberg, 2010).
15. Tricco, A. C. *et al.* Efficacy, effectiveness, and safety of herpes zoster vaccines in adults aged 50 and older: systematic review and network meta-analysis. *BMJ* k4029 (2018) doi:10.1136/bmj.k4029.
16. Levin, M. J. *et al.* Th1 memory differentiates recombinant from live herpes zoster vaccines. *Journal of Clinical Investigation* **128**, 4429–4440 (2018).

17. Schmid, D. S. *et al.* Comparative Antibody Responses to the Live-Attenuated and Recombinant Herpes Zoster Vaccines. *J Virol* **95**, (2021).

18. Whitley, R. J. & Roizman, B. Herpes simplex viruses: is a vaccine tenable? *J. Clin. Invest.* **110**, 145–151 (2002).

19. Dropulic, L. K. & Cohen, J. I. The challenge of developing a herpes simplex virus 2 vaccine. *Expert Rev Vaccines* **11**, 1429–1440 (2012).

20. Nelson, C. S., Herold, B. C. & Permar, S. R. A new era in cytomegalovirus vaccinology: considerations for rational design of next-generation vaccines to prevent congenital cytomegalovirus infection. *NPJ Vaccines* **3**, 38 (2018).

21. Eisenberg, R. J. *et al.* Herpes Virus Fusion and Entry: A Story with Many Characters. *Viruses* **4**, 800–832 (2012).

22. Belshe, R. B. *et al.* Efficacy Results of a Trial of a Herpes Simplex Vaccine. *N Engl J Med* **366**, 34–43 (2012).

23. Belshe, R. B. *et al.* Correlate of Immune Protection Against HSV-1 Genital Disease in Vaccinated Women. *Journal of Infectious Diseases* **209**, 828–836 (2014).

24. Johnson, D. C. & Huber, M. T. Directed Egress of Animal Viruses Promotes Cell-to-Cell Spread. *J Virol* **76**, 1–8 (2002).

25. Burton, D. R. Antibodies, viruses and vaccines. *Nat Rev Immunol* **2**, 706–713 (2002).

26. Krammer, F. The human antibody response to influenza A virus infection and vaccination. *Nat Rev Immunol* **19**, 383–397 (2019).

27. Harris, S. L. *et al.* Glycoprotein C of Herpes Simplex Virus Type 1 Prevents Complement-Mediated Cell Lysis and Virus Neutralization. *Journal of Infectious Diseases* **162**, 331–337 (1990).

28. Judson, K. A. *et al.* Blocking Immune Evasion as a Novel Approach for Prevention and Treatment of Herpes Simplex Virus Infection. *J Virol* **77**, 12639–12645 (2003).

29. Awasthi, S., Huang, J., Shaw, C. & Friedman, H. M. Blocking Herpes Simplex Virus 2 Glycoprotein E Immune Evasion as an Approach To Enhance Efficacy of a Trivalent Subunit Antigen Vaccine for Genital Herpes. *Journal of Virology* **88**, 8421–8432 (2014).

30. Awasthi, S. *et al.* Immunization with a Vaccine Combining Herpes Simplex Virus 2 (HSV-2) Glycoprotein C (gC) and gD Subunits Improves the Protection of Dorsal Root Ganglia in Mice and Reduces the Frequency of Recurrent Vaginal Shedding of HSV-2 DNA in Guinea Pigs Compared to Immunization with gD Alone. *Journal of Virology* **85**, 10472–10486 (2011).

31. Awasthi, S. *et al.* An HSV-2 Trivalent Vaccine Is Immunogenic in Rhesus Macaques and Highly Efficacious in Guinea Pigs. *PLoS Pathog* **13**, e1006141 (2017).

32. Awasthi, S. *et al.* Nucleoside-modified mRNA encoding HSV-2 glycoproteins C, D, and E prevents clinical and subclinical genital herpes. *Sci Immunol* **4**, (2019).

33. Awasthi, S. *et al.* Trivalent nucleoside-modified mRNA vaccine yields durable memory B cell protection against genital herpes in preclinical models. *Journal of Clinical Investigation* **131**, e152310 (2021).

34. LaTourette, P. C. *et al.* Protection against herpes simplex virus type 2 infection in a neonatal murine model using a trivalent nucleoside-modified mRNA in lipid nanoparticle vaccine. *Vaccine* **38**, 7409–7413 (2020).

35. Petro, C. *et al.* Herpes simplex type 2 virus deleted in glycoprotein D protects against vaginal, skin and neural disease. *eLife* **4**, e06054 (2015).

36. Petro, C. *et al.* HSV-2 ΔgD elicits FcγR-effector antibodies that protect against clinical isolates. *JCI Insight* **1**, (2016).

37. Visciano, M. L., Mahant, A. M., Pierce, C., Hunte, R. & Herold, B. C. Antibodies Elicited in Response to a Single Cycle Glycoprotein D Deletion Viral Vaccine Candidate Bind C1q and Activate Complement Mediated Neutralization and Cytolysis. *Viruses* **13**, 1284 (2021).

38. Ramsey, N. L. M. *et al.* A Single-Cycle Glycoprotein D Deletion Viral Vaccine Candidate, ΔgD-2, Elicits Polyfunctional Antibodies That Protect against Ocular Herpes Simplex Virus. *J Virol* **94**, (2020).

39. Burn Aschner, C., Pierce, C., Knipe, D. M. & Herold, B. C. Vaccination Route as a Determinant of Protective Antibody Responses against Herpes Simplex Virus. *Vaccines* **8**, 277 (2020).

40. Plotkin, S. A. & Boppana, S. B. Vaccination against the human cytomegalovirus. *Vaccine* **37**, 7437–7442 (2019).

41. Wang, D. *et al.* A replication-defective human cytomegalovirus vaccine for prevention of congenital infection. *Science Translational Medicine* **8**, 362ra145-362ra145 (2016).

42. Hahn, G. *et al.* Human Cytomegalovirus UL131-128 Genes Are Indispensable for Virus Growth in Endothelial Cells and Virus Transfer to Leukocytes. *J Virol* **78**, 10023–10033 (2004).

43. Wang, D. & Shenk, T. Human cytomegalovirus virion protein complex required for epithelial and endothelial cell tropism. *Proceedings of the National Academy of Sciences* **102**, 18153–18158 (2005).

44. Li, L. *et al.* A conditionally replication-defective cytomegalovirus vaccine elicits potent and diverse functional monoclonal antibodies in a phase I clinical trial. *npj Vaccines* **6**, 79 (2021).

45. Li, F. *et al.* Complement enhances in vitro neutralizing potency of antibodies to human cytomegalovirus glycoprotein B (gB) and immune sera induced by gB/MF59 vaccination. *npj Vaccines* **2**, 36 (2017).

46. Cui, X. *et al.* Novel trimeric human cytomegalovirus glycoprotein B elicits a high-titer neutralizing antibody response. *Vaccine* **36**, 5580–5590 (2018).

47. Nelson, C. S. *et al.* HCMV glycoprotein B subunit vaccine efficacy mediated by nonneutralizing antibody effector functions. *Proc Natl Acad Sci USA* **115**, 6267–6272 (2018).

48. Sunil-Chandra, N. P., Efstathiou, S. & Nash, A. A. Murine gammaherpesvirus 68 establishes a latent infection in mouse B lymphocytes in vivo. *Journal of General Virology* **73**, 3275–3279 (1992).

49. Flaño, E., Husain, S. M., Sample, J. T., Woodland, D. L. & Blackman, M. A. Latent Murine γ-Herpesvirus Infection Is Established in Activated B Cells, Dendritic Cells, and Macrophages. *J Immunol* **165**, 1074–1081 (2000).

50. Gaspar, M. *et al.* Murid Herpesvirus-4 Exploits Dendritic Cells to Infect B Cells. *PLoS Pathog* **7**, e1002346 (2011).

51. Frederico, B., Milho, R., May, J. S., Gillet, L. & Stevenson, P. G. Myeloid Infection Links Epithelial and B Cell Tropisms of Murid Herpesvirus-4. *PLoS Pathog* **8**, e1002935 (2012).

52. Frederico, B., Chao, B., May, J. S., Belz, G. T. & Stevenson, P. G. A Murid Gamma-Herpesviruses Exploits Normal Splenic Immune Communication Routes for Systemic Spread. *Cell Host & Microbe* **15**, 457–470 (2014).

53. Rickabaugh, T. M. *et al.* Generation of a Latency-Deficient Gammaherpesvirus That Is Protective against Secondary Infection. *Journal of Virology* **78**, 9215–9223 (2004).

54. May, J. S., Coleman, H. M., Smillie, B., Efstathiou, S. & Stevenson, P. G. Forced lytic replication impairs host colonization by a latency-deficient mutant of murine gammaherpesvirus-68. *Journal of General Virology* **85**, 137–146 (2004).

55. Boname, J. M., Coleman, H. M., May, J. S. & Stevenson, P. G. Protection against wild-type murine gammaherpesvirus-68 latency by a latency-deficient mutant. *Journal of General Virology* **85**, 131–135 (2004).

56. Fowler, P. & Efstathiou, S. Vaccine potential of a murine gammaherpesvirus-68 mutant deficient for ORF73. *Journal of General Virology* **85**, 609–613 (2004).

57. Jia, Q. *et al.* Induction of Protective Immunity against Murine Gammaherpesvirus 68 Infection in the Absence of Viral Latency. *Journal of Virology* **84**, 2453–2465 (2010).

58. Lawler, C., Simas, J. P. & Stevenson, P. G. Vaccine protection against murid herpesvirus-4 is maintained when the priming virus lacks known latency genes. *Immunol Cell Biol* **98**, 67–78 (2020).

59. Brar, G. *et al.* Deletion of immune evasion genes provides an effective vaccine design for tumor-associated herpesviruses. *npj Vaccines* **5**, 102 (2020).

60. Lawler, C. & Stevenson, P. G. Limited protection against γ-herpesvirus infection by replication-deficient virus particles. *Journal of General Virology* **101**, 420–425 (2020).

61. Nemerow, G. R., Mold, C., Schwend, V. K., Tollefson, V. & Cooper, N. R. Identification of gp350 as the viral glycoprotein mediating attachment of Epstein-Barr virus (EBV) to the EBV/C3d receptor of B cells: sequence homology of gp350 and C3 complement fragment C3d. *J. Virol.* **61**, 1416–1420 (1987).

62. Stewart, J. P. *et al.* Identification and characterization of murine gammaherpesvirus 68 gp150: a virion membrane glycoprotein. *J Virol* **70**, 3528–3535 (1996).

63. Stewart, J. P., Micali, N., Usherwood, E. J., Bonina, L. & Nash, A. A. Murine gamma-herpesvirus 68 glycoprotein 150 protects against virus-induced mononucleosis: A model system for gamma-herpesvirus vaccination. *Vaccine* **17**, 152–157 (1999).

64. Obar, J. J. *et al.* T-Cell Responses to the M3 Immune Evasion Protein of Murid Gammaherpesvirus 68 Are Partially Protective and Induced with Lytic Antigen Kinetics. *Journal of Virology* **78**, 10829–10832 (2004).

65. Samreen, B., Tao, S., Tischer, K., Adler, H. & Drexler, I. ORF6 and ORF61 Expressing MVA Vaccines Impair Early but Not Late Latency in Murine Gammaherpesvirus MHV-68 Infection. *Front. Immunol.* **10**, 2984 (2019).

66. Boilesen, D. R. *et al.* CD8+ T cells induced by adenovirus-vectored vaccine are capable of preventing establishment of latent murine γ-herpesvirus 68 infection. *Vaccine* **37**, 2952–2959 (2019).

67. Usherwood, E. J., Ward, K. A., Blackman, M. A., Stewart, J. P. & Woodland, D. L. Latent Antigen Vaccination in a Model Gammaherpesvirus Infection. *Journal of Virology* **75**, 8283–8288 (2001).

68. Hoegh-Petersen, M., Thomsen, A. R., Christensen, J. P. & Holst, P. J. Mucosal immunization with recombinant adenoviral vectors expressing murine gammaherpesvirus-68 genes M2 and M3 can reduce latent viral load. *Vaccine* **27**, 6723–6730 (2009).

69. Kwun, H. J. *et al.* Kaposi's Sarcoma-Associated Herpesvirus Latency-Associated Nuclear Antigen 1 Mimics Epstein-Barr Virus EBNA1 Immune Evasion through Central Repeat Domain Effects on Protein Processing. *Journal of Virology* **81**, 8225–8235 (2007).

70. Kwun, H. J. *et al.* The central repeat domain 1 of Kaposi's sarcoma-associated herpesvirus (KSHV) latency associated-nuclear antigen 1 (LANA1) prevents cis MHC class I peptide presentation. *Virology* **412**, 357–365 (2011).

71. Smith, C. M. *et al.* CD4+ T cells specific for a model latency-associated antigen fail to control a gammaherpesvirusin vivo. *Eur. J. Immunol.* **36**, 3186–3197 (2006).

72. Aricò, E. *et al.* Humoral Immune Response and Protection from Viral Infection in Mice Vaccinated with Inactivated MHV-68: Effects of Type I Interferon. *Journal of Interferon & Cytokine Research* **22**, 1081–1088 (2002).

73. Aricò, E., Robertson, K. A., Belardelli, F., Ferrantini, M. & Nash, A. A. Vaccination with inactivated murine gammaherpesvirus 68 strongly limits viral replication and latency and protects type I IFN receptor knockout mice from a lethal infection. *Vaccine* **22**, 1433–1440 (2004).

74. Morello, C. S. *et al.* Inactivated HSV-2 in MPL/alum adjuvant provides nearly complete protection against genital infection and shedding following long term challenge and rechallenge. *Vaccine* **30**, 6541–6550 (2012).

75. Hensel, M. T. *et al.* Prophylactic Herpes Simplex Virus 2 (HSV-2) Vaccines Adjuvanted with Stable Emulsion and Toll-Like Receptor 9 Agonist Induce a Robust HSV-2-Specific Cell-Mediated Immune Response, Protect against Symptomatic Disease, and Reduce the Latent Viral Reservoir. *J Virol* **91**, (2017).

76. Balfour, H. H. Progress, prospects, and problems in Epstein-Barr virus vaccine development. *Current Opinion in Virology* **6**, 1–5 (2014).

77. Cui, X. & Snapper, C. M. Epstein Barr Virus: Development of Vaccines and Immune Cell Therapy for EBV-Associated Diseases. *Front. Immunol.* **12**, 734471 (2021).

78. Thorley-Lawson, D. A. & Poodry, C. A. Identification and isolation of the main component (gp350-gp220) of Epstein-Barr virus responsible for generating neutralizing antibodies in vivo. *J Virol* **43**, 730–736 (1982).

79. Sashihara, J., Burbelo, P. D., Savoldo, B., Pierson, T. C. & Cohen, J. I. Human antibody titers to Epstein–Barr Virus (EBV) gp350 correlate with neutralization of infectivity better than antibody titers to EBV gp42 using a rapid flow cytometry-based EBV neutralization assay. *Virology* **391**, 249–256 (2009).

80. Sokal, E. M. *et al.* Recombinant gp350 Vaccine for Infectious Mononucleosis: A Phase 2, Randomized, Double-Blind, Placebo-Controlled Trial to Evaluate the Safety, Immunogenicity, and Efficacy of an Epstein-Barr Virus Vaccine in Healthy Young Adults. *J INFECT DIS* **196**, 1749–1753 (2007).

81. Sashihara, J. *et al.* Soluble Rhesus Lymphocryptovirus gp350 Protects against Infection and Reduces Viral Loads in Animals that Become Infected with Virus after Challenge. *PLoS Pathog* **7**, e1002308 (2011).

82. Bu, W. *et al.* Immunization with Components of the Viral Fusion Apparatus Elicits Antibodies That Neutralize Epstein-Barr Virus in B Cells and Epithelial Cells. *Immunity* **50**, 1305-1316.e6 (2019).

83. Wei, C.-J. *et al.* A bivalent Epstein-Barr virus vaccine induces neutralizing antibodies that block infection and confer immunity in humanized mice. *Sci. Transl. Med.* **14**, eabf3685 (2022).

84. Malhi, H. *et al.* Immunization with a self-assembling nanoparticle vaccine displaying EBV gH/gL protects humanized mice against lethal viral challenge. *Cell Reports Medicine* **3**, 100658 (2022).

85. Ruiss, R. *et al.* A virus-like particle-based Epstein-Barr virus vaccine. *J. Virol.* **85**, 13105–13113 (2011).

86. Pavlova, S. *et al.* An Epstein-Barr virus mutant produces immunogenic defective particles devoid of viral DNA. *J Virol* **87**, 2011–2022 (2013).

87. van Zyl, D. G. *et al.* Immunogenic particles with a broad antigenic spectrum stimulate cytolytic T cells and offer increased protection against EBV infection ex vivo and in mice. *PLoS Pathog* **14**, e1007464 (2018).

88. Ogembo, J. *et al.* A chimeric EBV gp350/220-based VLP replicates the virion B-cell attachment mechanism and elicits long-lasting neutralizing antibodies in mice. *J Transl Med* **13**, 50 (2015).

89. Perez, E. M., Foley, J., Tison, T., Silva, R. & Ogembo, J. G. Novel Epstein-Barr virus-like particles incorporating gH/gL-EBNA1 or gB-LMP2 induce high neutralizing antibody titers and EBV-specific T-cell responses in immunized mice. *Oncotarget* **8**, 19255–19273 (2017).

90. Barasa, A. K. *et al.* BALB/c mice immunized with a combination of virus-like particles incorporating Kaposi sarcoma-associated herpesvirus (KSHV) envelope glycoproteins gpK8.1, gB, and gH/gL induced comparable serum neutralizing antibody activity to UV-inactivated KSHV. *Oncotarget* **8**, 34481–34497 (2017).

91. Mulama, D. H. *et al.* A multivalent Kaposi sarcoma-associated herpesvirus-like particle vaccine capable of eliciting high titers of neutralizing antibodies in immunized rabbits. *Vaccine* **37**, 4184–4194 (2019).

92. Gong, D. *et al.* Virus-Like Vesicles of Kaposi's Sarcoma-Associated Herpesvirus Activate Lytic Replication by Triggering Differentiation Signaling. *Journal of Virology* **91**, (2017).

93. Chauhan, V., Rungta, T., Goyal, K. & Singh, M. P. Designing a multi-epitope based vaccine to combat Kaposi Sarcoma utilizing immunoinformatics approach. *Sci Rep* **9**, 2517 (2019).

94. Plotkin, S. A. Correlates of protection induced by vaccination. *Clin. Vaccine Immunol.* **17**, 1055–1065 (2010).

95. Plotkin, S. A. Updates on immunologic correlates of vaccine-induced protection. *Vaccine* **38**, 2250–2257 (2020).

96. Labo, N. *et al.* Heterogeneity and Breadth of Host Antibody Response to KSHV Infection Demonstrated by Systematic Analysis of the KSHV Proteome. *PLoS Pathog* **10**, e1004046 (2014).

97. Mortazavi, Y. *et al.* The Kaposi's Sarcoma-Associated Herpesvirus (KSHV) gH/gL Complex Is the Predominant Neutralizing Antigenic Determinant in KSHV-Infected Individuals. *Viruses* **12**, 256 (2020).

98. Luna, R. E. *et al.* Kaposi's Sarcoma-Associated Herpesvirus Glycoprotein K8.1 Is Dispensable for Virus Entry. *Journal of Virology* **78**, 6389–6398 (2004).

99. Wright, D. E., Colaco, S., Colaco, C. & Stevenson, P. G. Antibody limits in vivo murid herpesvirus-4 replication by IgG Fc receptor-dependent functions. *Journal of General Virology* **90**, 2592–2603 (2009).

100. Glauser, D. L., Milho, R., Lawler, C. & Stevenson, P. G. Antibody arrests γ-herpesvirus olfactory super-infection independently of neutralization. *Journal of General Virology* **100**, 246–258 (2019).

101. Poppe, L. K., Kankasa, C., Wood, C. & West, J. T. Relationships Between Maternal Antibody Responses and Early Childhood Infection With Kaposi Sarcoma-Associated Herpesvirus. *The Journal of Infectious Diseases* **222**, 1723–1730 (2020).

102. Minab, R. *et al.* Maternal Epstein-Barr Virus-Specific Antibodies and Risk of Infection in Ugandan Infants. *The Journal of Infectious Diseases* jiaa654 (2020) doi:10.1093/infdis/jiaa654.

103. Semmes, E. C. *et al.* Maternal Fc-mediated non-neutralizing antibody responses correlate with protection against congenital human cytomegalovirus infection. *Journal of Clinical Investigation* (2022) doi:10.1172/JCI156827.

104. Poppe, L. K., Wood, C. & West, J. T. The Presence of Antibody-Dependent Cell Cytotoxicity–Mediating Antibodies in Kaposi Sarcoma–Associated Herpesvirus–Seropositive Individuals Does Not Correlate with Disease Pathogenesis or Progression. *J.I.* **205**, 2742–2749 (2020).

105. Spiller, O. B. *et al.* Complement Regulation by Kaposi's Sarcoma-Associated Herpesvirus ORF4 Protein. *J Virol* **77**, 592–599 (2003).

106. Okroj, M. *et al.* Antibodies against Kaposi sarcoma-associated herpes virus (KSHV) complement control protein (KCP) in infected individuals. *Vaccine* **25**, 8102–8109 (2007).

107. Okroj, M. *et al.* Prevalence of antibodies against Kaposi's sarcoma associated herpes virus (KSHV) complement inhibitory protein (KCP) in KSHV-related diseases and their correlation with clinical parameters. *Vaccine* **29**, 1129–1134 (2011).

108. Roshan, R. *et al.* T-cell responses to KSHV infection: a systematic approach. *Oncotarget* **8**, 109402–109416 (2017).

109. Bihl, F. *et al.* Lytic and Latent Antigens of the Human Gammaherpesviruses Kaposi's Sarcoma-Associated Herpesvirus and Epstein-Barr Virus Induce T-Cell Responses with Similar Functional Properties and Memory Phenotypes. *Journal of Virology* **81**, 4904–4908 (2007).

110. Long, H. M., Meckiff, B. J. & Taylor, G. S. The T-cell Response to Epstein-Barr Virus–New Tricks From an Old Dog. *Front. Immunol.* **10**, 2193 (2019).

111. Nalwoga, A. *et al.* Kaposi's sarcoma-associated herpesvirus T cell responses in HIV seronegative individuals from rural Uganda. *Nat Commun* **12**, 7323 (2021).

112. Sehrawat, S. *et al.* CD8+ T Cells from Mice Transnuclear for a TCR that Recognizes a Single H-2Kb-Restricted MHV68 Epitope Derived from gB-ORF8 Help Control Infection. *Cell Reports* **1**, 461–471 (2012).

113. Coscoy, L. & Ganem, D. Kaposi's sarcoma-associated herpesvirus encodes two proteins that block cell surface display of MHC class I chains by enhancing their endocytosis. *Proceedings of the National Academy of Sciences* **97**, 8051–8056 (2000).

114. Hewitt, E. W. Ubiquitylation of MHC class I by the K3 viral protein signals internalization and TSG101-dependent degradation. *The EMBO Journal* **21**, 2418–2429 (2002).

115. Cai, Q. *et al.* IRF-4-Mediated CIITA Transcription Is Blocked by KSHV Encoded LANA to Inhibit MHC II Presentation. *PLoS Pathog* **9**, e1003751 (2013).

116. Tomescu, C., Law, W. K. & Kedes, D. H. Surface Downregulation of Major Histocompatibility Complex Class I, PE-CAM, and ICAM-1 following De Novo Infection of Endothelial Cells with Kaposi's Sarcoma-Associated Herpesvirus. *J Virol* **77**, 9669–9684 (2003).

117. Nicol, S. M. *et al.* Primary B Lymphocytes Infected with Kaposi's Sarcoma-Associated Herpesvirus Can Be Expanded In Vitro and Are Recognized by LANA-Specific CD4+ T Cells. *J. Virol.* **90**, 3849–3859 (2016).

CHAPTER 2:

Immunization of mice with virus-like vesicles of Kaposi sarcoma-associated herpesvirus reveals a role for antibodies targeting ORF4 in activating complement-mediated neutralization

Abstract

The development of a prophylactic vaccine for Kaposi sarcoma-associated Herpesvirus (KSHV) would prevent consequences from infection such as Kaposi sarcoma and primary effusion lymphoma. Non-infectious enveloped virus-like vesicles (VLVs) that lack capsids and viral genomes hold a vaccine potential by presenting a repertoire of viral structural proteins to the immune system without the safety risk of an infectious virus. Here, we study the immunogenicity of KSHV VLVs produced from a viral mutant that is defective in capsid formation and DNA packaging. Mice immunized with adjuvanted VLVs generate KSHV-specific antibodies and T cells. VLV immune sera neutralize KSHV infection, and this neutralization is enhanced by the complement system. Complement-enhanced neutralization by VLV immune sera is dependent on antibodies targeting the short consensus repeat (SCR) region of viral open reading frame 4 (ORF4). However, complement-mediated enhancement was not detected in the sera of KSHV-infected humans which contained few neutralizing antibodies. Therefore, VLV vaccination can confer a potential improvement over infection-induced humoral immunity. Overall, our study supports the utility of KSHV VLVs as a multi-antigen vaccine platform to stimulate a diverse immune response and underscores a potential benefit of complement-mediated antibody function in a KSHV vaccine.

Introduction

Kaposi sarcoma-associated herpesvirus (KSHV) is the etiological agent for Kaposi sarcoma (KS), a malignancy that manifests as lesions that mainly consist of endothelial cells on the skin, lymph nodes, lungs, and digestive tract[1]. While the occurrence of KS is low overall in the US at a rate of 4.5 cases per million people in 2017, it could be up to 500 times higher in transplant patients and in people living with human immunodeficiency virus (HIV)[2,3]. KSHV is prevalent in endemic regions, such as sub-Saharan Africa and the Mediterranean region, where over 50% of individuals are infected[1]. KSHV also causes lymphoproliferative disorders including primary effusion lymphoma (PEL), multicentric Castleman disease (MCD), and KSHV inflammatory cytokine syndrome (KICS). Like all herpesviruses, KSHV establishes life-long persistent infections in hosts, and has two distinct phases in its life cycle, lytic replication and latency. KSHV-infected individuals usually remain healthy and display no symptoms due to the immune control of the virus and the virus's ability to enter a status of latency in host cells[4]. However, infection is associated with a lifelong risk of oncogenesis. During KSHV latent infection, the viral genome is maintained as an episome tethered to the host chromosome and expression of latency-associated genes from this episome drives the proliferation of infected cells and promotes cell survival, thereby predisposing cells to transformation[5]. In addition, expression of some lytic genes can also stimulate angiogenesis and paracrine signaling to latently-infected cells, contributing to KS pathogenesis[6]. Thus, persistent KSHV infection increases the risk of developing cancers, especially in the context of immunosuppression due to age, HIV infection, or post-transplant medication.

The clear link between KSHV infection and KSHV-associated cancers demonstrates a distinct benefit from a prophylactic vaccine: stopping KSHV infection to eliminate KSHV-associated disorders. This would be most beneficial in resource-limited sub-Saharan Africa where KSHV is endemic. It is thought that KSHV is largely spread through oral fluids, as evidenced by the

detection of KSHV DNA in saliva. This is especially true in endemic regions, where transmission occurs during childhood and is more likely within families and among those who share food and drink[7–15]. Another population that could benefit from KSHV vaccination is the community of men who have sex with men (MSM), which has a disproportionally higher level of seropositivity compared to other populations[16–18]. This group may be especially vulnerable, as members are more likely to be co-infected with HIV, the effects of which would put them at higher risk for KSHV-induced pathologies such as AIDS-KS. For both populations, there is a window of opportunity for prophylactic vaccination before infection. In endemic regions, KSHV seropositivity remains relatively low in early childhood[19,20], and spread in MSM communities is unlikely before sexual maturity. This is contrasted with the related gammaherpesvirus Epstein-Barr virus (EBV), which is highly prevalent even before age 2[21]. Thus, a window of early childhood provides a timeframe for KSHV vaccination to prevent infection later in life.

In general, the correlate of protection of prophylactic viral vaccines is the generation of neutralizing antibodies, which bind viral attachment and entry proteins to prevent infection[22]. For KSHV, neutralizing targets would include glycoprotein K8.1, glycoprotein B (gB), and the gH/gL complex[23]. K8.1 mediates attachment to host cells by binding to heparan sulfate[24,25]. gB and gH/gL bind to integrins and ephrin receptors, respectively, to mediate viral entry[26]. Once in the endosome, gB fuses the viral envelope with the endosomal membrane to allow release of the viral capsid into the cytoplasm, where it is directed to the nucleus to establish an infection. Thus, antibodies that block these glycoprotein functions could prevent infection. Furthermore, antibodies also have effector functions that aid in anti-viral immunity. One such effector function is the engagement of the classical complement system, which activates an enzymatic cascade after binding to an antibody complex on the surface of a pathogen or infected cell. This leads to the development of the membrane attack complex (MAC) that forms pores in the membrane to neutralize or kill the pathogen or infected cell[27]. The importance of effector functions has also

been suggested in mother-child transmission studies for KSHV and EBV. One study of mother-child pairs found that seropositive mothers of children that did not seroconvert had on average higher serum antibody levels compared to mothers of children that were infected. However, there was no difference in neutralizing antibodies between groups, implicating a role by effector functions[28]. This is supported by a study of EBV acquisition in infants, which found no evidence for protection from neutralizing maternal antibodies against EBV infection, indicating a role of non-neutralizing antibody functions in protection[29]. Thus, the induction of antibodies that possess effector functions in addition to neutralizing antibodies could be beneficial in a potential KSHV vaccine for the prevention of transmission.

Virus-like particles (VLPs) are a type of vaccine platform that is formed through self-assembly of proteins into particles that resembles virions. VLPs generated from the structural proteins of hepatitis B virus (HBV) and human papillomavirus (HPV) have been successfully used for vaccination to elicit high levels of neutralizing antibodies[30,31]. VLPs can also be generated by fusing a viral antigen of interest with a protein that is known to form particles by self-assembly or by interacting with other structural proteins. For example, a ferritin-based platform has been used to generate EBV glycoprotein VLPs by fusing the viral glycoproteins to the N-terminus of ferritin to mediate self-assembly into particles[32]. For KSHV, VLPs have been generated through the Newcastle Disease Virus (NDV) platform, which uses the NDV fusion (F) protein to display KSHV glycoproteins on the surface of VLPs that are formed when F is co-expressed with NDV matrix and nucleoprotein[33]. Unlike conventional whole inactivated viral vaccines, VLPs do not contain viral genomes but require selection of viral antigens to be displayed, risking the possibility of missing important targets. This is particularly the case for herpesviruses that have a complex profile of envelope glycoproteins. To allow for presentation of an entire repertoire of glycoproteins, another approach has been developed to generate VLPs based on mutant viruses that make only non-infectious particles without viral genomes inside. For EBV, these noninfectious particles are

generated from EBV mutants deficient in viral genome packaging or viral maturation[34,35]. We have also used KSHV capsid-deficient mutants to generate analogous non-infectious KSHV particles that we referred to as virus-like vesicles (VLVs)[36]. These KSHV VLVs contain the same set of envelope proteins as virions but lack capsid and capsid-associated proteins. Importantly, these VLVs do not contain viral genomes and are noninfectious, eliminating the oncogenic risk of latent infection. We hypothesized that these VLVs are immunogenic and hold the potential as a KSHV vaccine to present a broad spectrum of structural proteins to the immune system.

Immunization with protein preparations faces the challenge of poor immunogenicity, and these formulations require adjuvants to obtain substantial immune responses[37]. Adjuvants can promote delivery of vaccine antigens and/or modulate the immune system to better trigger adaptive responses. For example, traditional adjuvants such as aluminum salts and oil-in-water emulsions induce “danger” signals and recruit innate immune cells to improve antigen presentation[38]. Newer adjuvants trigger innate immune responses by signaling through toll-like receptors (TLRs) such as monophosphoryl lipid A (MPLA) binding to TLR4 or single-stranded RNA binding to TLR7 and TLR8[39,40]. Recently, lipid nanoparticles (LNP) have emerged as a contributor of adjuvant activity to mRNA-based vaccines, potentially through interleukin 1 beta (IL-1β) and IL-6 signaling[41,42]. Furthermore, both empty LNP and LNP encapsulating a TLR ligand have been shown to be potent adjuvants for protein-based vaccines[43,44]. Thus, the multitude of adjuvants that have been developed provides a wide base for improving responses to protein-based KSHV vaccines.

In this study, we have investigated the immunogenicity of KSHV VLVs in mice. Using a KSHV mutant deficient in capsid formation, we generated noninfectious VLVs to present KSHV antigens. We show that immunization of KSHV VLVs with an LNP-based adjuvant elicits virus-specific T cells and antibody responses in mice. Importantly, vaccine-induced antibody targets include viral open reading frame 4 (ORF4), a known complement control protein[45]. These anti-ORF4

antibodies largely target the short consensus repeat (SCR) domain and mediate complement-enhanced neutralization of KSHV infection by the VLV immune sera. Interestingly, we did not detect this enhancement in the neutralization by the sera of humans infected with KSHV, suggesting a potential benefit conferred by vaccination over infection-generated immunity. Our study demonstrates that this KSHV VLV platform can prime both humoral and cellular immune responses to multiple viral antigens. In addition, our results reveal a complement-mediated antiviral role of VLV vaccine-induced antibodies and highlights a potential advantage of engaging the complement system in a future KSHV vaccine.

Results

Production of VLVs with a KSHV mutant deficient in capsid formation

To produce VLVs without virions, we utilized a previously described KSHV mutant deficient in capsid formation due to a 60 amino acid deletion in the major capsid protein (ORF25Δ60)[46]. The iSLK cell line harboring the latent 25Δ60 viral genome was treated with sodium butyrate and doxycycline to induce the expression of a viral replication and transcription activator (RTA) to reactivate the viral lytic cycle, resulting in the production of VLVs that can be isolated from the culture supernatant by ultracentrifugation. We characterized these VLVs and compared them to KSHV virions produced in a similar manner using iSLK cells harboring wildtype (WT) latent KSHV[47]. Under cryo-electron microscopy, we observed vesicles around 200nm in diameter in samples from iSLK-25Δ60 (Fig. 2-1a), and these vesicles were referred to as VLVs. In the WT sample, we observed virions that contain capsids indicated by dense cores in addition to VLVs. To demonstrate the presence of KSHV antigens, we performed immunogold staining for viral glycoprotein K8.1. Both samples contained vesicles that were labeled with gold particles (indicated by red arrows, Fig. 2-1b) and labeled virions were detected in the WT sample (indicated by a black arrow, Fig. 2-1b). We further characterized the viral protein contents using mass

spectrometry. As expected, the 25Δ60 sample contained comparable levels of viral envelope proteins such as ORF8 (gB) and K8.1 to the WT sample (Fig. 2-1c, blue dots) and much lower levels of capsid associated proteins such as ORF25 and ORF65 (Fig. 2-1c, red dots). We also identified other viral proteins including tegument proteins and cellular proteins that were previously reported in VLVs (Tables 2-1 and 2-2). These results demonstrate the potential of VLVs generated from the 25Δ60 virus as a vaccine platform to present diverse KSHV antigens.

To confirm that VLVs from iSLK-25Δ60 are non-infectious, we incubated them with HEK293 cells. KSHV derived from BAC16 contains expression cassettes for green fluorescence protein (GFP) and hygromycin resistance in the genome[47]. Thus, cells infected with BAC16-derived viruses express GFP and are resistant to hygromycin. Using flow cytometry, we detected few to no GFP-expressing cells when incubated with VLV, similar to what was observed for cells incubated without KSHV and KSHV virions inactivated with beta-propiolactone (BPL) (KSHV+BPL) (Fig. 2-1d). On the other hand, when incubated with an equal protein amount of WT KSHV, ~8,000 GFP-positive cells were detected per μg of protein. In addition, we also performed hygromycin selection. While cells continued to proliferate after incubation with WT KSHV, we found no surviving cells after incubation with VLVs prepared from the 25Δ60 virus, confirming the lack of infectivity (data not shown). Lastly, we isolated DNA from 25Δ60-derived VLVs and WT KSHV virions to assess the levels of viral DNA. We found that VLVs had much less DNA compared to KSHV virions, which was expected due to the predicted inability of the 25Δ60 virus to encapsidate the viral genome (Fig. 2-1e). Overall, we concluded that 25Δ60-derived VLVs are a safe vaccine candidate that possess a repertoire of KSHV envelope proteins similar to KSHV virions without the risk of latent infection.

VLV immunization generates virus-specific antibodies and T cells in mice

We first examined the immunogenicity of VLVs by immunizing mice intraperitoneally (i.p.) three times with 2μg VLV and a CpG-containing oligodeoxynucleotide (CpG ODN) adjuvant (Fig. 2-2a). To identify targets of antibody responses, we utilized a bead-based multiplexed assay that included 62 KSHV proteins. We found that K8.1 is a major target of antibody responses after VLV immunization and that CpG adjuvant increased K8.1 antibody levels (Fig. 2-2b). In addition, coadministration with adjuvant also resulted in minor induction of antibodies against ORF4 and tegument protein ORF38. We next compared VLVs to inactivated KSHV virions. To control the effect of BPL inactivation, we treated VLVs with BPL employing the same protocol used to inactivate KSHV virions. Mice were immunized i.p. with 2μg of BPL-treated VLV (VLV+BPL) or BPL-treated KSHV virions (KSHV+BPL) three times in the absence of adjuvants at an interval of 3 weeks. Immune sera collected at 14 days after the third immunization was assessed for KSHV-specific antibodies (Fig. 2-3a). As K8.1 is one of the most immunogenic viral antigens in immunized mice and in human serum[48], we ran enzyme-linked immunosorbent assay (ELISA) using purified K8.1 protein. VLV immunization elicited a lower level of K8.1 antibodies compared to inactivated KSHV virions (Fig. 2-3b). To identify other targets of antibody responses, we again utilized the bead-based multiplexed assay and identified ORF4, in addition to K8.1, as targets of antibodies generated by VLV immunization (Fig. S1c). Immunization of KSHV+BPL generated a broader antibody response to multiple proteins besides K8.1 and ORF4, such as ORF38 and the small capsid protein ORF65.

We next assessed the immune responses after immunizing mice via a clinically relevant route, intramuscular administration. Unlike inactivated KSHV virions, VLVs do not contain viral DNA, a major class of pathogen-associated molecular patterns (PAMPs). Upon binding to PAMPs, pattern recognition receptors (PPRs) initiate downstream signaling to activate a variety of innate immune responses, which play an essential role in instructing adaptive immunity. Therefore, to increase the immunogenicity of VLVs, we co-administered them with one of three types of

adjuvants: (1) CpG ODN, an agonist of toll-like receptor 9 (TLR9)[49]; (2) empty lipid nanoparticles (LNP); (3) lipid nanoparticles encapsulating phosphothioate-linked polyuridlyic acid (polyUs), an agonist of TLR7[50]. Mice were immunized twice with 2μg of VLVs alone or in combination with 10μg of one type of adjuvant at a 3-week interval (Fig. 2-4a). We then examined serum antibody responses at 8 days after the second immunization. By immunofluorescence assay (IFA), we confirmed that serum from immunized mice recognized reactivated KSHV-infected iSLK cells and not uninduced cells, suggesting that it contained antibodies that recognized antigens expressed on the cell surface during the lytic viral cycle (Fig. 2-4b). By K8.1 ELISA, we found that immunization of VLVs alone was unable to generate detectable K8.1-specific IgG, and all three types of adjuvants enhanced the immunogenicity of VLVs to elicit K8.1-specific antibody responses (Fig. 2-4c). Using the multiplexed antibody assay, we found that all three adjuvants resulted in increased levels of ORF4-specific and that LNP adjuvants increased levels of ORF38-specific antibodies (Fig. 2-5). In a separate intramuscular immunization, we compared the immunogenicity of VLV+BPL with KSHV+BPL adjuvanted with polyUs-LNP (Fig. 2-4d). Using a small panel of expression plasmids for viral envelope proteins, we showed that the VLV+BPL immune sera contained antibodies that recognized surface expression of K8.1, ORF4 and gB (Fig. 2-4e), but not gH/gL, gM/gN, or ORF28 (Fig. 2-6a). VLVs elicited a similar level of K8.1-binding antibodies to inactivated virions (Fig. 2-6b). In addition, we also examined the antibody profiles using the ORFeome-wide assay. Other than the two envelope proteins, K8.1 and ORF4, VLV+BPL adjuvanted with polyUs-LNP could also induce significant antibodies against ORF38 (Fig. 2-4f), which were only weakly detected when VLVs were administered intraperitoneally without adjuvants (Fig. 2-3c). The antibody responses to these three proteins were comparable between immunization of VLVs and inactivated virions. Expectedly, VLVs did not generate antibodies against the small capsid protein, ORF65, as inactivated virions did (Fig. 2-4f). Thus,

when co-delivered with adjuvants via an intramuscular route, VLVs and inactivated virions share a similar capacity of inducing antibodies against envelope proteins.

To measure T cell responses after immunization, we performed interferon gamma (IFNγ) enzyme-linked immunosorbent spot (ELISpot) assays with splenocytes isolated from mice immunized as shown in Fig. 2-4a. Cells were stimulated with VLVs or inactivated KSHV virions and responding IFNγ-producing cells were quantified. VLVs without adjuvant did not elicit any responding T cells. However, significant numbers of IFNγ-producing cells were observed in mice that received adjuvanted immunizations, with the strongest response coming from mice immunized with VLVs adjuvanted with polyUs-LNP (Fig. 2-7a). We also used an activation induced marker (AIM) assay to examine T cell responses. The AIM assay measures the activation of T cells based on the upregulation of the markers CD69 and 4-1BB for CD8 T cells and OX40 and 4-1BB for CD4 T cells. They have been used to detect T cells generated by both infection and vaccination[51–53]. Splenocytes from mice immunized from Fig. 2-4d were stimulated with VLV+BPL or KSHV+BPL and analyzed by flow cytometry for the expression of activation markers (Fig. 2-8). AIM+ CD4 and CD8 T cells were detected in mice immunized with VLVs or inactivated KSHV virions (Figs. 2-7b & 2-7c). Moreover, both types of vaccines induced similar levels of AIM+ T cells in mice, supporting the use of VLVs over inactivated virions for generating T cell responses.

To determine which viral proteins were targets for T cell responses, we conducted a proteome-wide ELISpot assay using overlapping peptide libraries derived from viral antigens. In general, T cell responses were heterogeneous among individual mice (Fig. 2-7d). However, ORF33, a viral tegument protein, was most frequently recognized by T cells in VLV-immunized mice and was also one of the two frequent targets in mice immunized with inactivated KSHV virions. Another commonly recognized T cell target from inactivated virion immunization is ORF25, the major capsid protein. (Fig. 2-7d). We tested whether these responses could be impacted by the major

histocompatibility complex (MHC) molecules that present viral antigens by immunizing Balb/c mice in a similar manner. While we still found frequent responses to ORF33 in immunized Balb/c mice, we also saw much stronger responses towards another tegument protein ORF52 (Fig. 2-9). There were also more frequent responses to ORF35, a protein important for viral reactivation, but decreased responses to ORF25 in KSHV+BPL immunized mice. Overall, these data indicate that adjuvanted VLVs can generate KSHV-specific T cell responses, but these responses may be dependent on MHC presentation of packaged antigens.

VLV immune serum neutralizes KSHV infection

The major correlate of protection for most commercial vaccines is generally thought to be neutralizing antibodies, because these antibodies can block viral attachment or entry to stop initiation of infection. K8.1 mediates viral attachment by binding heparan sulfate moieties[24,25], and is a major target for the VLV immune sera. Notably, we also saw a strong antibody response to ORF4, a complement control protein that also possesses heparan sulfate binding activity[45,54]. In addition, we detected a weak response to gB, which mediates fusion between the viral envelope and the host's cellular membrane[26]. To determine whether vaccine-induced antibodies block attachment and entry, we conducted a neutralization assay based on GFP-expression in infected cells. Serial dilutions of the serum samples from mice immunized from Fig. 2-4a were mixed with a fixed amount of KSHV virions that lead to ~5% GFP-positive cells. The 50% neutralization titer (NT50) was determined by the last dilution of immune serum that gave more than a 50% reduction in GFP-positive cells compared to the serum samples from mock immunized mice. While neutralizing activity was undetectable when VLVs alone were used for immunization, co-administration of adjuvants enabled VLVs to induce significant amounts of neutralizing antibodies (Fig. 2-10a). When spin infection was used in the neutralization assay to facilitate viral attachment by centrifugation, the NT50 values dropped but were still detectable (Fig. 2-10b). This result is

consistent with our observation that strong antibody responses were detected against viral attachment proteins while the responses to fusion proteins were much weaker.

Complement-enhanced neutralization by VLV immune serum depends on ORF4-SCR targeting antibodies

ORF4 is one major target of VLV immune serum. Serum containing anti-ORF4 antibodies has been demonstrated to antagonize its complement inhibition function[55]. Thus, we hypothesized that the anti-ORF4 antibodies elicited by VLVs could enhance complement-mediated neutralization. To test this, we performed spin infection neutralization assays using sera from mice immunized with VLV+BPL as shown in Fig. 2-4d and guinea pig serum (GPS) as a source of complement. Complement activation can be antibody-dependent (classical) or -independent (lectin and alternative pathways)[56,57]. All three pathways converge on the cleavage of complement component 3 (C3), leading to the assembly of a “membrane attack complex” on virions and infected cells. Incubating KSHV virions with GPS without the immune serum did not result in any reduction in GFP-positive cells (data not shown). However, when the VLV immune sera were included with GPS, we observed a significant increase in neutralization (Fig. 2-11a). We also confirmed this using normal human serum (NHS) as a source of complement (Fig. 2-12). To determine the role of ORF4-specific antibodies in this complement-enhanced neutralization, we developed an adsorption procedure to deplete ORF4-specific antibodies by incubating the immune serum samples with ORF4-expressing cells. A similar adsorption by incubating with K8.1-expressing cells was carried out to deplete K8.1-specific antibodies. Antibody depletions were confirmed by IFA (Fig. 2-13a). Depletion of anti-ORF4 antibodies caused a significant loss of complement-enhanced neutralization, while depletion of K8.1 antibodies had little impact until higher serum dilutions were used (Fig. 2-11b). Therefore, ORF4-specific antibodies are critical for complement-enhanced neutralization by VLV immune serum.

To determine whether ORF4-specific antibodies counteract the complement inhibitory function of ORF4 on viral envelope to enhance complement-mediated neutralization, we generated a viral mutant with a deletion in the short consensus repeat (SCR) region of ORF4 that is responsible for its complement inhibition activity[45]. This mutant virus, referred to as KSHV ORF4-dSCR, was expected to be unable to inhibit complement, leading to an increased sensitivity to complement even in the absence of anti-ORF4 antibodies. However, the ORF4-dSCR virus remained resistant to complement, indicating that KSHV virions likely do not activate the complement system in an antibody-independent manner. In the spin infection neutralization assay with the VLV immune sera, the ORF4-dSCR virus was less susceptible to complement-enhanced neutralization compared to the WT virus (Fig. 2-11c). This result does not support the idea that anti-ORF4 antibodies enhance complement activity on KSHV virions in the neutralization assay. Instead, it suggests that the SCR region of ORF4 is needed for the formation of the antibody complex to activate the complement system.

To confirm the importance of SCR-binding antibodies in complement-dependent neutralization, we generated plasmids to express the SCR region only (ORF4-SCRonly) or the rest of ORF4 protein (ORF4-dSCR) for antibody depletion. By IFA, we found that ORF4-specific antibodies of the VLV immune serum mainly targeted the SCR region (Fig. 2-13b). When SCR-specific antibodies were depleted by adsorption on SCR-expressing cells, complement-enhanced neutralization was abolished, whereas the depletion of antibodies binding to the other non-SCR part of ORF4 had no impact (Fig. 2-11d). Thus, the antibodies binding to the SCR region of ORF4 are key to recruit and activate the complement system to facilitate neutralization of KSHV virions.

ORF4-specific antibodies mediate complement deposition on KSHV-infected B cells

One route of herpesvirus spread is through cell-to-cell transmission, which is capable of evading neutralizing antibodies[58]. One method to prevent this is by eliminating infected cells before viral

egress. The classical complement system, in addition to neutralizing viruses, can deposit complement on infected cells to activate phagocytosis by innate immune cells or initiate complement-dependent cytotoxicity[59]. We tested the ability of VLV immune serum to initiate complement deposition with a KSHV-infected B cell line, BC-3-G[60]. BC-3-G cells were reactivated to express lytic viral genes, incubated with VLV immune serum and NHS, and analyzed for the binding of complement components C1q and C3b (Fig. 2-14a). We found that VLV immune serum could cause C1q and C3b binding to reactivated BC-3-G cells, but the presence of both components was not present on uninduced BC-3-G or when using mock-immune serum (Fig. 2-14b). This deposition was lost when ORF4-specific antibodies were removed from the serum, but not when K8.1-specific antibodies were removed (Fig. 2-14c). Thus, complement deposition on infected B cells depends on ORF4-targeting antibodies.

ORF4 antibodies in KSHV-seropositive patients lack complement activity

The contribution of ORF4-specific antibodies in the sera of KSHV-infected individuals to complement activity has not yet been studied[55,61]. K8.1-specific antibodies are the predominant antibodies in infected individuals, while ORF4-specific antibodies are much rarer and lower in quantity[48,61]. We obtained serum samples from patients with and without KS from the multicenter AIDS cohort study (MACS). These serum samples were stratified for the presence of K8.1- and ORF4-specific antibodies by ELISA. Out of 35 KS+ patients, 25 were positive for K8.1 antibodies, but only 3 were positive for ORF4 antibodies (Figs. 2-15a & 2-15b). All 3 samples positive for ORF4 antibodies were also positive for K8.1 antibodies. We performed neutralization assays on all 35 serum samples at a 1:100 dilution with and without NHS as the source for complement. Only 3 samples reduced the percentage of GFP+ cells after spin infection by more than 50% without complement and 2 of these samples displayed a moderate increase in neutralization when complement was included. While enhanced neutralization by complement was observed for most

samples, only a few achieved over 50% neutralization. When samples were separated by K8.1 or ORF4 antibody status (Figs. 2-15c & 2-15d), anti-ORF4 antibody positive samples were significantly different from anti-ORF4 antibody negative samples when looking at the change in neutralization induced by adding complement (Fig. 2-15d, right). There was also very little induction of complement deposition on reactivated BC-3-G cells by these serum samples, and there was no significant difference when samples were separated by K8.1 or ORF4 antibody status (Figs. 2-15e & 2-15f). Overall, the sera of KSHV-infected human patients in the UCLA MACS repository have little neutralizing activity and do not display significant levels of complement-enhanced neutralization or complement deposition.

Discussion

Kaposi Sarcoma and other KSHV-induced diseases represent a clear need for a prophylactic KSHV vaccine. However, without known correlates of immunity, it is difficult to predict the efficacy of a vaccine candidate. The current preclinical vaccine candidate based on the NDV VLP platform is designed to generate neutralizing antibodies against viral attachment and fusion proteins, K8.1, gB, and gH/gL, to prevent viral infection[33,62]. However, it is possible that effector functions of antibodies mediated by their Fc region also contribute to protection. In addition, an effective KSHV vaccine should also elicit cellular immunity to eliminate infected cells, because herpesviruses are capable of cell-to-cell transmission that evades neutralization by antibodies[58].

Here, we present our results on the immunogenicity of a novel KSHV VLV-based platform, which incorporates a repertoire of non-capsid viral structural proteins. This provides an alternative to whole inactivated virions (WIV), which rely on chemical inactivation to abolish viral infectivity. We demonstrated that co-administration of VLVs with adjuvants elicits comparable cellular and humoral responses to WIV against antigens shared between WIV and VLVs, such as tegument and envelope proteins (Figs. 2-4 and 2-7). In addition to a conventional CpG DNA-based adjuvant,

we also employed novel LNP-based adjuvants. LNP have recently been shown to be potent adjuvants for protein based vaccines and our data supports this finding[43,44,63]. Particularly, the incorporation of 21-mer uridine-containing single-stranded RNA, a TLR7 ligand, further enhanced the ability of VLVs to elicit T cell responses after intramuscular immunizations (Fig. 2-7). In C57Bl/6 mice, we showed that ORF33, a tegument protein, is the major target for T cell responses after VLV immunization while K8.1- and ORF38-specific antibodies dominate humoral immunity. In addition, we also observed a strong antibody response toward ORF4, a complement regulatory protein. These data support the utility of VLVs as a safe vaccine to generate a diverse KSHV-specific immunity.

While T cell and antibody responses in KSHV-infected individuals are broad and heterogeneous[20,48,64], some viral proteins are more frequently targeted than others. Heterogeneity is not unique to KSHV and is also found for other herpesviruses, such as HSV-1 and HSV-2[65,66]. This is likely because large viruses like herpesviruses encode many proteins and variations in processing and presentation of this repertoire among individual hosts results in a spectrum of immune responses. Among the structural proteins shared between VLV and virions, K8.1 and ORF38 are common targets for antibodies in KSHV-infected individuals. Antibody reactivity to these proteins is detected in over 50% of patients, although it may be under 20% in recently infected children[48,67]. Interestingly, K8.1 and ORF38 reactivity was also observed for the mouse sera following immunization of adjuvanted VLVs and virions (Fig. 2-4f). Another common target in the immune sera from inactivated virions but not VLVs is ORF65, a capsid protein that is not present in VLVs. ORF65 is also among the three virion-associated proteins identified as common targets for human KS patient serum in addition to K8.1 and ORF38[48]. Therefore, viral lytic replication or differences between human and mouse B cell repertoires do not seem to play a role in determining which viral proteins are commonly targeted by antibodies. While K8.1 functions in attachment, it is unclear whether anti-ORF38 or anti-ORF65 antibodies have any antiviral

function. In contrast, we observed robust anti-ORF4 antibody response in the mouse sera from both VLV and inactivated virion immunization but not in the sera of KS patients (Fig. 2-15). It has been shown by others that the antibody response to ORF4 was rarely detected in KSHV patients[48,61]. In general, the presence of anti-ORF4 antibodies is associated with higher levels of anti-KSHV antibody responses, which is more common in KS patients. This may be due to the opportunity for less immunogenic viral proteins to stimulate the host immune system during viral reactivation in KS. However, our observation could also be due to a species-specific difference in immunogenicity for ORF4 but not for K8.1, ORF38 or ORF65. In contrast to humoral immunity, we did not observe the same shared T cell targets between mice following immunization and humans following infection. For instance, K8.1 is the most frequently recognized T cell target, with K8.1-specific T cells found in up to 30% of KSHV-infected individuals[68], but K8.1-specific cellular responses were undetectable in the immunized mice (Fig. 2-7). Instead, we identified consistent T cell responses to ORF33 in VLV-immunized C57Bl/6 mice while virion-immunized mice possessed T cells that respond to ORF33 and ORF25. Interestingly, we also saw responses to ORF33 in Balb/c mice, but they were overshadowed by responses to ORF52. The reasons for these differences could be due to different peptide presentation between MHC complexes in different mouse strains or species, but could also indicate the power of immunization to generate more focused and uniform T cell responses versus natural infection for certain antigens[69,70]. Interestingly, immunization also generated heterogeneous T cell responses to other viral proteins, which reflects the heterogeneity found in infected individuals[64,68]. The enhancement of these diverse responses could be beneficial to optimizing immunity against KSHV, since it is currently unknown which T cell targets would be protective against disease.

One salient finding is a potential role for complement in stopping KSHV infection. The complement cascade is activated by classical (antibody-dependent), lectin, and alternative pathways, converging on C3 cleavage to C3a and C3b[71]. C3b interacts with other complement proteins to

proceed with the cascade, culminating in the formation of the MAC, resulting lysis of enveloped viruses and infected cells. In addition to virolysis, complement can neutralize viruses by other mechanisms, such as C3b opsonization of virions to block receptor binding and target virions for phagocytosis[71]. C3 on the cell surface can also signal through complement receptors to initiate phagocytosis by macrophages and granulocytes[72,73]. KSHV's ORF4 antagonizes the complement system by reducing C3 cleavage and inactivating C3b[74]. Complement inhibition of ORF4 can be blocked by anti-ORF4 monoclonal antibodies or by serum containing anti-ORF4 antibodies[55,75]. Therefore, the induction of robust ORF4-specific antibodies following VLV immunization prompted us to examine complement-mediated neutralization. First, we found no evidence that the WT virus or ORF4-dSCR virus is neutralized by complement in the absence of antibodies. Second, in the presence of the VLV immune sera, complement enhances neutralization (Fig. 2-11a). Third, depletion of ORF4-specific antibodies markedly reduced complement-mediated enhancement of neutralization (Fig. 2-11b). Fourth, use of the ORF4-dSCR virus for neutralization did not enhance but diminished complement-enhanced neutralization (Fig. 2-11c). Last, ORF4-specific antibodies are able to mediate complement deposition on infected cells (Fig. 2-14c). Therefore, rather than negating the ability of ORF4 to inhibit complement, ORF4-specific antibodies of the VLV immune sera engage the complement system to neutralize KSHV virions. Notably, anti-K8.1 antibodies of the VLV immune sera, while abundant, did not seem to play any significant role in complement activity (Figs. 2-11b & 2-14c). The classical pathway is initiated by the binding of C1q to the Fc region of antibodies. C1q is a heterotrimer of C1q-A, -B, and –C that forms a stalk of six collagen-like helices connected to six globular domains that bind to antibodies[71]. Because C1q has a weak affinity to a single antibody molecule, it is thought that clustering of antigen-antibody complexes on the surface of cells or virions is necessary for the formation of a multivalent structure for C1q binding and activation. At this moment, it is unclear why K8.1 antibodies cannot afford complement-mediated effector functions and whether a different vaccine platform will be able to

induce K8.1 antibodies that can engage complement. It is possible that the K8.1 antigen-antibody complex is unable to form a high avidity C1q-binding structure. This could be due to the relatively smaller size of K8.1 compared to ORF4 or a difference in arrangement on the viral envelope. It is also unclear whether antibodies against other glycoproteins in addition to ORF4 will be able to stimulate complement-enhanced neutralization. Although it is important to consider complement as a protective immune mechanism for KSHV vaccine development, this will still need to be tested in preclinical models.

ORF4-targeting antibodies are not commonly detected in the sera of KSHV infected individuals[48,61]. Two studies have examined the function of anti-ORF4 antibodies in the context of complement. In one study, the patient sera that contained ORF4-specific antibodies increased C3b deposition on ORF4-expressing cells compared to mock-transfected cells and this increase was not seen with normal human serum[61]. However, this study did not distinguish whether this increase is because anti-ORF4 antibodies blocked ORF4 function or because these antibodies activated complement through the classic pathway. In a follow-up study, ORF4-mediated C3b degradation was inhibited by the patient serum sample that contained the highest level of ORF4 antibodies[55]. Neither of these two studies examined complement-mediated anti-viral effects on KSHV. In the current study, we attempted to characterize the role of human ORF4-specific antibodies in complement activity. Among 35 human serum samples obtained from the UCLA MACS repository, only three were categorized by us as positive for ORF4-specific antibodies based on ELISA results. These three samples at 1:100 dilution have very little neutralization activity in the absence of complement and the addition of human complement only moderately enhanced neutralization to 20%. 26 out of 35 samples were considered positive for K8.1 based on our ELISA, consistent with the previous report that K8.1 is an frequent target for antibody responses in KSHV-infected individuals[48]. Only 2 out of 35 samples could neutralize KSHV infectivity by more than 50% at 1:100 dilution and both were positive for K8.1-specific antibodies.

Neutralization of most of patent serum samples could be modestly increased by complement but only two were increased from below to above 50%. We also did not see complement deposition on BC-3-G cells expressing KSHV lytic antigens. Considering that humoral responses to KSHV infection focused on anti-K8.1 antibodies, it was not surprising to see poor complement-mediated enhancement of neutralization or complement deposition from these samples, which is consistent with our data that anti-K8.1 antibodies in VLV immune sera also do not contribute to complement-mediated neutralization. However, it is imperative to be mindful that these samples were obtained from KS+ patients, who may have immune systems that are weaker than those found in healthy humans. Therefore, additional studies will be required to confirm these findings, as other studies have reported higher levels of KSHV neutralization in other populations compared to what we observed[76,77].

Complement is an important part of host innate immune defense against pathogens and naturally, viruses have evolved multiple strategies to counteract the complement system. Gammaherpesviruses, like KSHV and murine gammaherpesvirus-68 (MHV-68) encode homologues of host regulators of complement activation (RCAs), ORF4. Alphaherpesviruses, like Herpes Simplex Virus 1 (HSV-1) and HSV-2 encodes viral unique RCA, glycoprotein C (gC). The lack of functional gC makes HSV-1 highly sensitive to complement-mediated neutralization in the absence as well as in the presence of anti-HSV antibodies[78]. Immunization with gC is capable of eliciting antibodies that block the complement inhibition function of gC, and anti-gC antibodies significantly increased the neutralization effectiveness of antibodies against gD, the receptor binding protein of HSV, in the presence of complement[79]. Therefore, adding gC to gD for immunization enhances efficacy or protection afforded by multiple vaccine formulations[79–82]**.** This supports the role of complement in vaccine-mediated protection for HSV-1 and HSV-2. Another herpesvirus where complement may play a significant role in vaccine responses is human cytomegalovirus (hCMV). gB is the fusion protein and immunodominant target in hCMV-infected

individuals[83]. In clinical trials, a gB vaccine can confer 50% efficacy against hCMV acquisition in young women, and yet their immune sera have low neutralizing titers without complement[84,85]. It has been suggested that Fc-mediated effector functions of antibodies are critical for the observed efficacy[86]. For instance, complement-enhanced neutralization was detected in the sera from people who received gB vaccine, suggesting that complement may be one of the protective mechanisms[85,87]. Notably, unlike HSV-1 and -2, our ORF4-dSCR KSHV virus with the deleted complement inhibitory region remains resistant to complement. This is consistent with previous work showing that the complement inhibition of ORF4 is highly specific for the classical pathway[74]. However, contrary to expectations, we observed a loss in complement-mediated neutralization when the ORF4-dSCR virus was used in the assay. Importantly, ORF4 has been demonstrated to be a virulence factor in the MHV-68 model during acute replication, but not necessary for latency establishment[88]. However, the impact on long term latency is unclear, as ORF4 may be needed during reactivation, which maintains the pool of latently infected cells. Immunity against ORF4 reduced MHV-68 latency in B cell deficient mice, where persistent lytic viral replication takes place[89]. Thus, the complement system is important for controlling herpesvirus pathogenesis, and targeting viral inhibitors of complement will likely play a key part in effective vaccines.

Several new classes of adjuvants have been developed to enhance vaccine-induced immune responses[37]. Some of these adjuvants stimulate type I interferons (IFN-Is) and proinflammatory cytokines by triggering endosome-located Toll-like receptors activated by nucleic acids, such as TLR3, TLR7/8, and TLR9[37,90]. IFN-Is play an important role in the induction of cellular immunity. TLR7 recognizes GU-rich single-stranded RNA (ssRNA) while TLR9 is activated by unmethylated CpG motifs prevalent in microbial DNA. A CpG-based adjuvant is used in an FDA approved Hepatitis B vaccine (Heplisav-B) and the ssRNA component in the influenza A WIV vaccine is critical for its intrinsic adjuvant activity via TLR7 activation[91]. It is worth noting that in the absence

of adjuvants BPL-inactivated KSHV virions are more immunogenic than VLV following intraperitoneal administration (Fig. 2-3), presumably due to viral DNA in virions serving as a potential TLR ligand. One major challenge of using RNA as an adjuvant is its instability. The COVID-19 pandemic has brought LNP technology to the forefront of public and scientific thought. *In vivo* delivery of immunostimulatory nucleic acids, such as ssRNA or polyUs as TLR7 ligand, can be facilitated by LNP. Moreover, LNP themselves have adjuvant activity from ionizable lipids[44]. It is clear from our study that polyUs-LNP more potently stimulate cellular immunity than empty LNP (Fig. 2-7a), though the underlying mechanism remains to be determined. CpG alone did not induce the same extent of cellular immunity as polyUs-LNP. Further studies will be required to assess the differences between these adjuvants and whether CpG-LNP can reach the same level of adjuvant activity as polyUs-LNP.

While providing a safe platform to present a spectrum of viral antigens to the host immune system, VLVs have several limitations and areas for improvement. First, VLVs do not induce strong antibody responses to gB, gH, or gL, resulting in a low level of neutralization activity of the immune sera in the absence of complement-mediated enhancement (Figs. 2-6a and 2-10b). One approach to improve the immunogenicity of gB is to stabilize it in a prefusion conformation to improve the induction of neutralizing antibodies. Prefusion conformations for gB from HSV and hCMV have been determined[92,93], and the modifications to stabilize these structures could be incorporated into the genomes of VLV-producing cells. This prefusion locking strategy has been incorporated into vaccines against pandemic coronaviruses[94,95], suggesting that it may improve herpesviral vaccines as well. In addition, we can further engineer our VLV producing mutant by fusing tegument proteins in VLVs with epitopes from other viral genes, such as latent genes, to broaden T cell responses. This has been studied in EBV VLPs, where a fragment of the immunogenic EBNA3C was linked to BNRF1 found in the VLPs, leading to improved T cell responses and control of infected cells[96]. These improvements could be tested against original

VLVs in either humanized mouse models of KSHV infection or in non-human primates to assess protection against infection[97–99]. Overall, our VLV immunogenicity study supports the notion of eliciting antibodies that possess effector functions by a KSHV vaccine.

Data Availability

The mass spectrometry proteomics data has been deposited to the ProteomeXchange Consortium via the PRIDE partner repository[100] with the dataset identifier PXD035478. All other reagents used in this manuscript are available from the corresponding author upon reasonable request.

Acknowledgements

We thank Jodi Hanson (CTL) for assistance in analysis of ELISpot plates. We thank Hong Jiang (Ren Sun lab, UCLA) for assistance with animal experiments.

This work was supported by grants from the National Institutes of Health (R01DE028774 to T.W. and R01DE025567 to Z.H.Z. and T.W.), with federal funds from the National Cancer Institute (Contract No. 75N91019D00024/HHSN261201500003I to D.W.), and by a COVID-19 Research Award from the W.M. Keck Foundation (OCRC#20-12 to C.G.R. and T.W.). A.K.L. and J.Z. were supported by the NIH Ruth L. Kirschstein Institutional Research Award for Interdisciplinary Training in Virology and Gene Therapy T32AI060567. A.K.L. was also supported by a Graduate Student Fellowship from the UCLA Jonsson Comprehensive Cancer Center. Flow cytometry was performed in the UCLA Jonsson Comprehensive Cancer Center and Center for AIDS Research Flow Cytometry Core Facility that is supported by National Institutes of Health awards P30CA016042 and P30AI028697, and by the JCCC, the UCLA AIDS Institute, the David Geffen School of Medicine at UCLA, the UCLA Chancellor's Office, and the UCLA Vice Chancellor's Office of Research.

We thank Najib Aziz and Rey Soto for assistance in obtaining KS+ serum samples. Human serum samples were collected by the MACS/WIHS Combined Cohort Study (MWCCS) and obtained from the UCLA MWCCS site. The contents of this publication are solely the responsibility of the authors and do not represent the official views of the National Institutes of Health (NIH). The MWCCS is funded primarily by the National Heart, Lung, and Blood Institute (NHLBI), with additional co-funding from the Eunice Kennedy Shriver National Institute Of Child Health & Human Development (NICHD), National Institute On Aging (NIA), National Institute Of Dental & Craniofacial Research (NIDCR), National Institute Of Allergy And Infectious Diseases (NIAID), National Institute Of Neurological Disorders And Stroke (NINDS), National Institute Of Mental Health (NIMH), National Institute On Drug Abuse (NIDA), National Institute Of Nursing Research (NINR), National Cancer Institute (NCI), National Institute on Alcohol Abuse and Alcoholism (NIAAA), National Institute on Deafness and Other Communication Disorders (NIDCD), National Institute of Diabetes and Digestive and Kidney Diseases (NIDDK), National Institute on Minority Health and Health Disparities (NIMHD), and in coordination and alignment with the research priorities of the National Institutes of Health, Office of AIDS Research (OAR). The UCLA MWCCS site is supported by U01-HL146333 (to Roger Detels and Matthew Mimiaga) and UL1-TR001881 (UCLA CTSI). The authors gratefully acknowledge the contributions of the study participants and dedication of the staff at the MWCCS sites.

Author Contributions

A.K.L and T.W. conceptualized the project and wrote the manuscript. A.K.L. generated VLVs, performed mouse immunizations, and conducted antibody and T cell studies. R.R. developed and performed the whole proteome ELISpot assay and W.M. developed and performed the multiplex antibody assay, both under the guidance of N.L. and D.W.. J.Z. performed cryoEM studies. C.C. performed serum adsorption and IFA experiments. H.H. generated KSHV ORF4-dSCR. P.T. and

C.H. generated expression plasmids and conducted IFA studies. A.P.K. and J.R.J. performed mass spectrometry analysis. D.G., Y.K.T., and C.G.R. provided valuable reagents. M.E., Z.H.Z., J.R.J., D.W., and T.W. supervised the work. All authors edited the manuscript and approved its submission.

Conflicts of Interest

Y.K.T. is an employee of and holds equity in Acuitas Therapeutics, a producer of lipid nanoparticle technology. All other authors declare no conflicts of interest.

Figures and Figure Legends

Figure 2-1

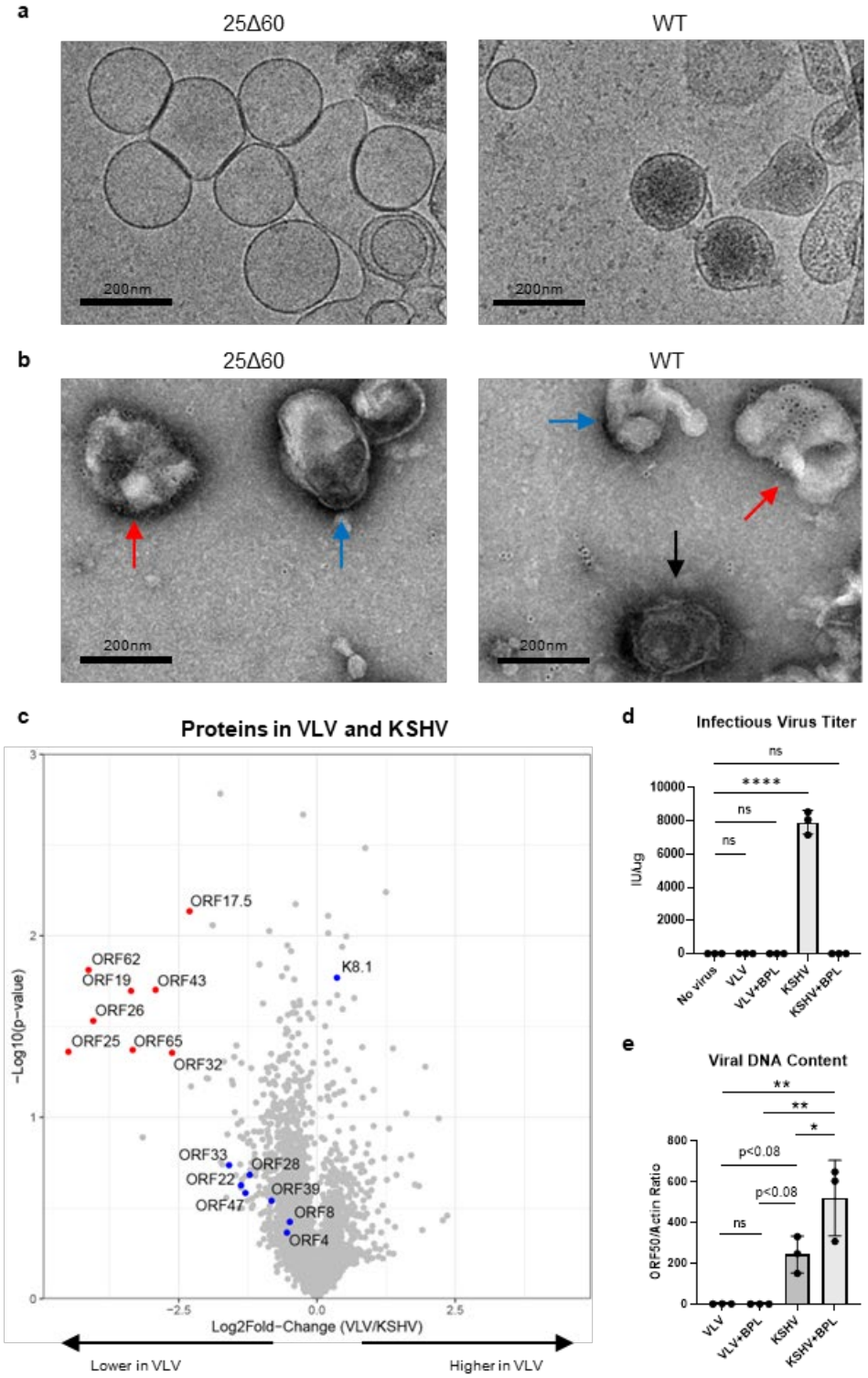

Figure 2-1: VLVs generated from a KSHV mutant defective in capsid formation present KSHV antigens without viral DNA or infectivity

(a) Cryo-electron micrographs of VLVs and KSHV virions obtained from reactivated iSLK 25Δ60 or WT cells

(b) Negative stain micrographs of VLVs and KSHV virions labeled with K8.1 antibodies and immunogold beads. Red arrows indicate labeled VLVs, blue arrows indicate unlabeled vesicles, and black arrows indicate labeled virions. Vesicles were considered positively labeled if they were over 100nm in diameter and were labeled with more than five gold beads.

(c) A volcano plot showing proteins found in VLV and KSHV virion preparations. Differentially present (log_2 fold-change <-2 and $p<0.05$) proteins are highlighted in red and other viral proteins of interest are highlighted in blue.

(d) Infectious virus titer from VLV and KSHV preparations or preparations inactivated with betapropiolactone (BPL)

(e) Ratio of viral ORF50 DNA in VLV and KSHV preparations to actin from carrier DNA used during isolation

Statistical analysis: Ordinary one way ANOVA with Dunnett's (c) or Tukey's (d) test for multiple comparisons. *$p<0.05$, **$p<0.01$, ****$p<0.0001$. Mean and standard deviation shown. N=3 independent infection assays (d) or DNA extractions (e)

Figure 2-2

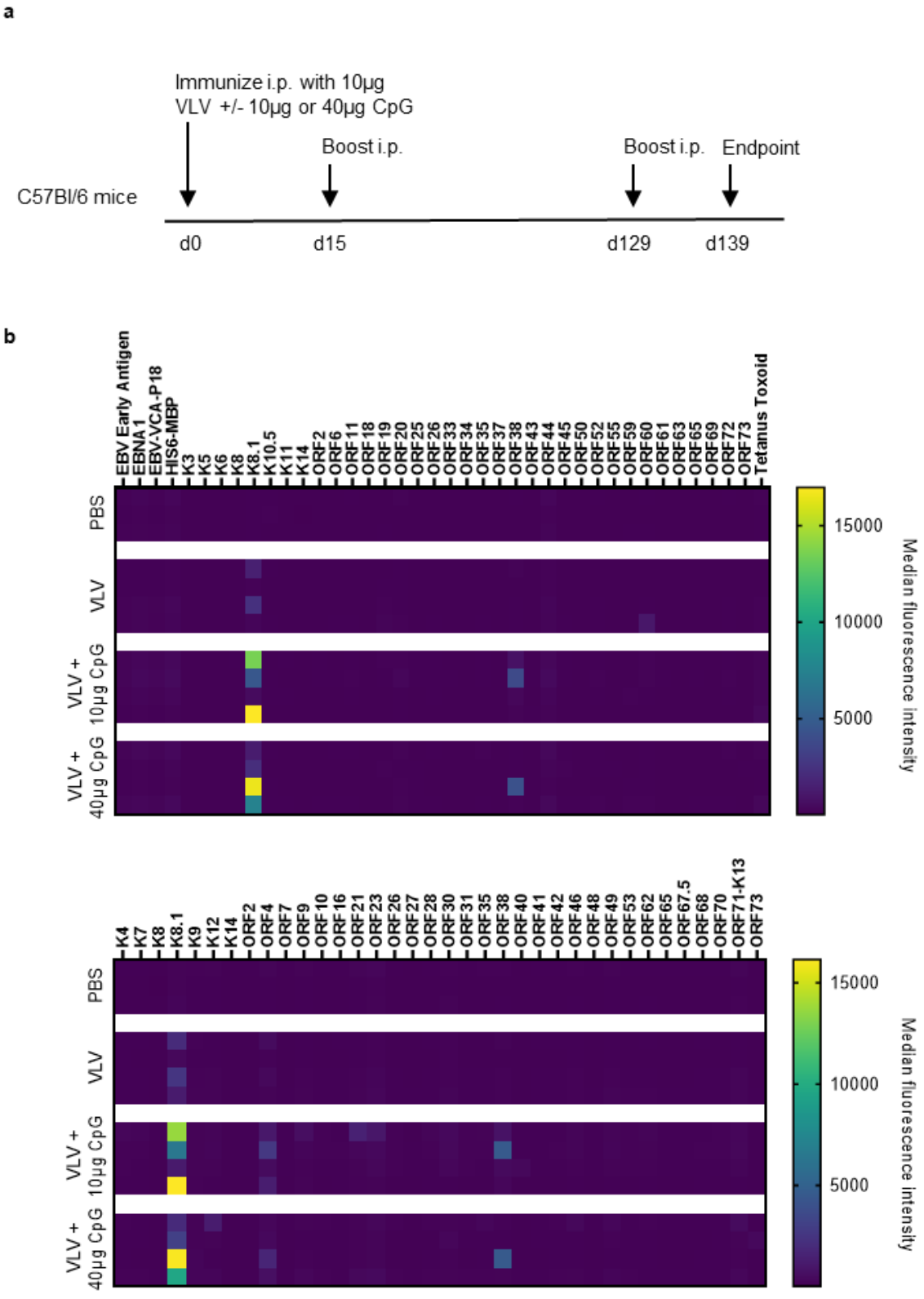
a
Immunize i.p. with 10µg
VLV +/- 10µg or 40µg CpG
Boost i.p.
Boost i.p.
Endpoint
C57Bl/6 mice
d0
d15
d129
d139
b
EBV Early Antigen
EBNA1
EBV-VCA-P18
HIS6-MBP
K3
K5
K6
K8
K8.1
K10.5
K11
K14
ORF2
ORF6
ORF11
ORF18
ORF19
ORF20
ORF25
ORF26
ORF33
ORF34
ORF35
ORF37
ORF38
ORF43
ORF44
ORF45
ORF50
ORF52
ORF55
ORF59
ORF60
ORF61
ORF63
ORF65
ORF69
ORF72
ORF73
Tetanus Toxoid
PBS
VLV
VLV + 10µg CpG
VLV + 40µg CpG
15000
10000
5000
Median fluorescence intensity
K4
K7
K8
K8.1
K9
K12
K14
ORF2
ORF4
ORF7
ORF9
ORF10
ORF16
ORF21
ORF23
ORF26
ORF27
ORF28
ORF30
ORF31
ORF35
ORF38
ORF40
ORF41
ORF42
ORF46
ORF48
ORF49
ORF53
ORF62
ORF65
ORF67.5
ORF68
ORF70
ORF71-K13
ORF73
PBS
VLV
VLV + 10µg CpG
VLV + 40µg CpG
15000
10000
5000
Median fluorescence intensity

Figure 2-2: Antibody responses to VLV with CpG adjuvant administered intraperitoneally

(a) Immunization scheme for intraperitoneal administration of VLV with CpG used in (b)

(b) Heatmaps showing antibody binding to KSHV antigens in a multiplexed bead assay. Each heatmap represents a different set of beads with some overlapping antigens.

Figure 2-3

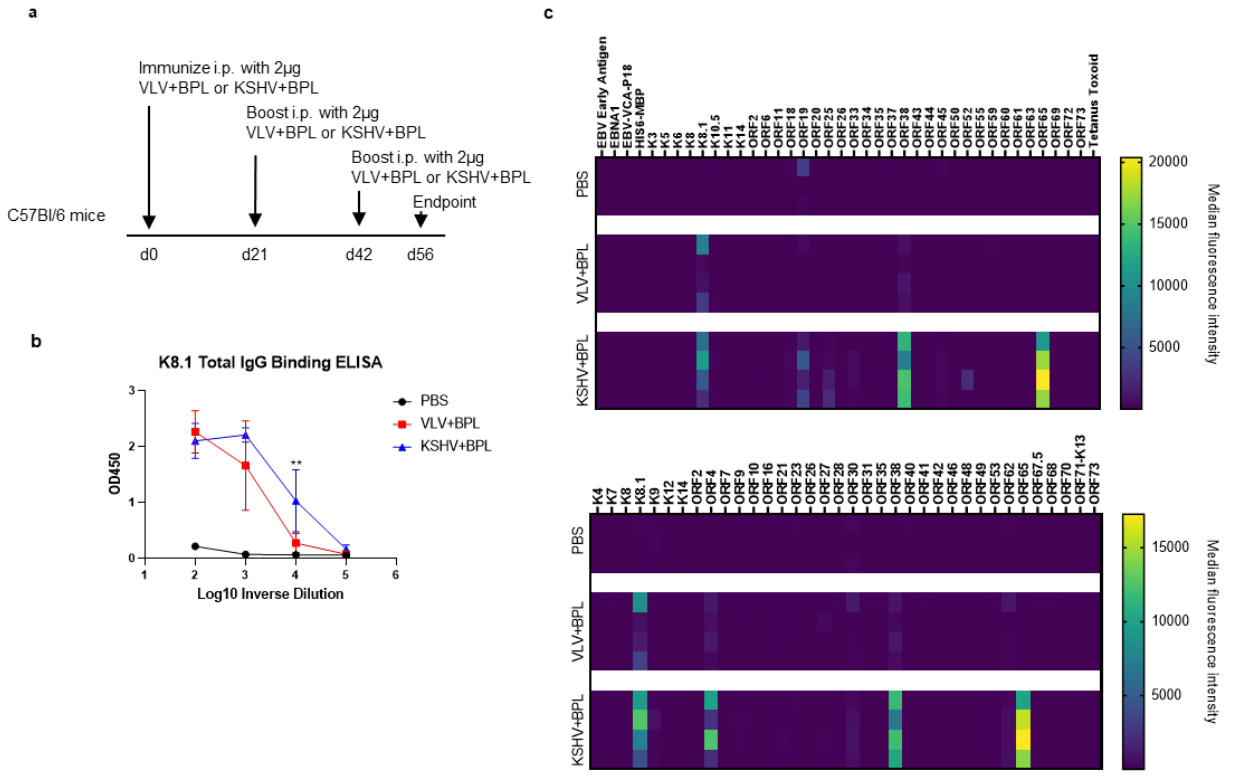

Figure 2-3: Antibody responses after intraperitoneal immunization of inactivated VLV and KSHV

(a) Immunization scheme for (b) and (c)

(b) K8.1 ELISA signals from mice immunized with VLV+BPL or KSHV+BPL

(c) Heatmaps showing antibody binding by VLV+BPL or KSHV+BPL immune serum in a bead-based multiplex KSHV antigen assay. Each heatmap represents a different set of beads with some overlapping antigens.

Statistical analysis: (b) Two-way ANOVA with Tukey's multiple comparisons. Difference between VLV+BPL and KSHV+BPL is shown. **p<0.01. Mean and standard deviation are shown. N=3-4 mice per group

Figure 2-4

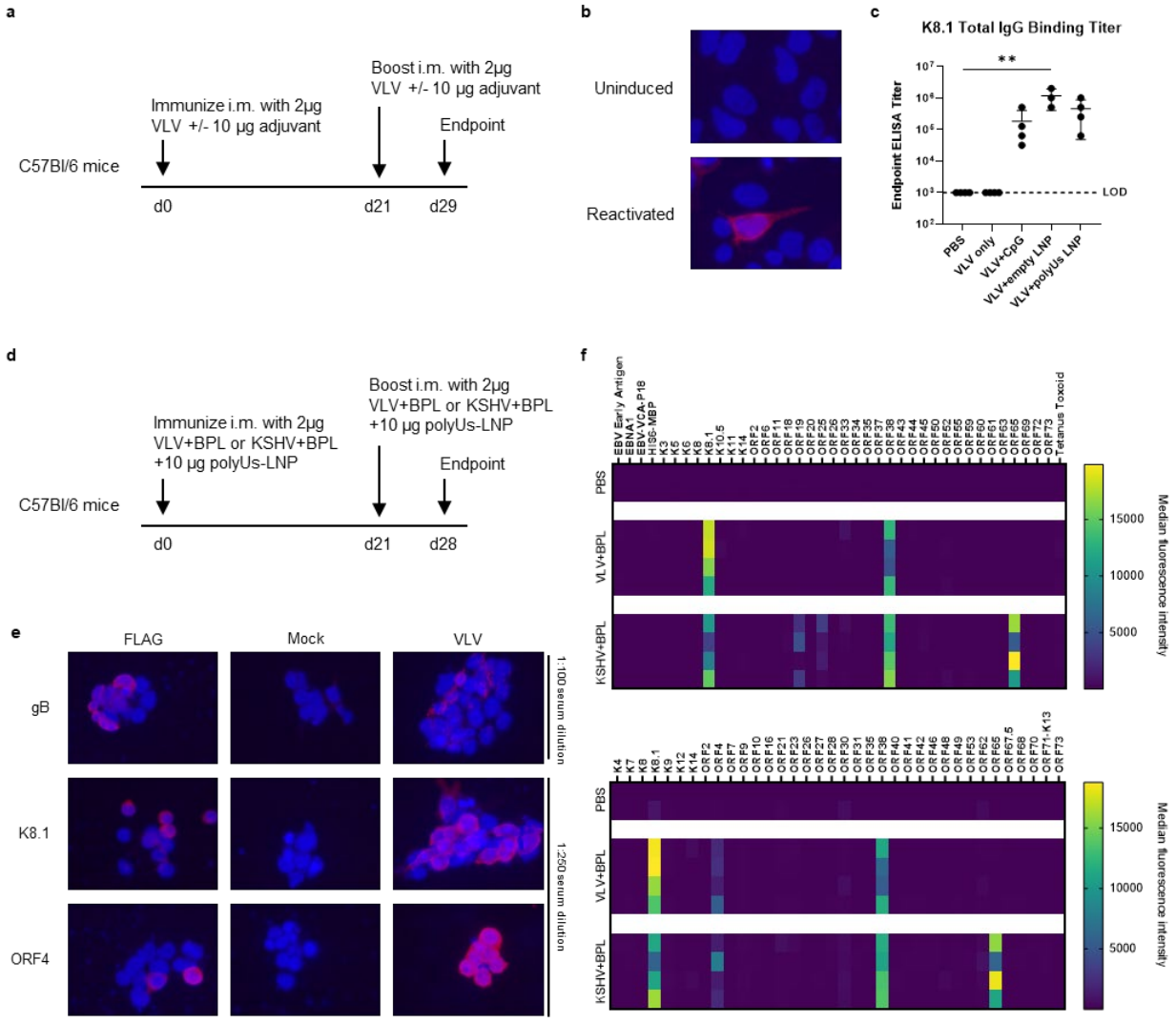

Figure 2-4: Mice immunized intramuscularly with adjuvanted VLVs generate virus-specific antibody responses

(a) Immunization scheme to study immunogenicity of VLV with adjuvant used in (b) and (c)

(b) Immunofluorescence images of pooled VLV+polyUs-LNP immune serum at a 1:250 dilution binding to uninduced or reactivated iSLK WT cells

(c) Endpoint K8.1 ELISA titers of VLV immune sera. LOD = limit of detection

(d) Immunization scheme to compare VLV+BPL and KSHV+BPL with polyUs-LNP adjuvant used in (e) and (f)

(e) Immunofluorescence images of pooled mock or VLV+BPL immune serum at the indicated dilutions binding to 293T cells expressing KSHV glycoproteins

(f) Heatmaps showing antibody binding from immune sera at a 1:200 dilution in a bead-based multiplex KSHV antigen assay. Each heatmap represents a different set of beads with some overlapping antigens.

Statistical analysis: (c) Ordinary one-way ANOVA with Dunnett's test for multiple comparisons. **$p<0.01$. Mean with standard deviation shown. N=3-4 per group

Figure 2-5

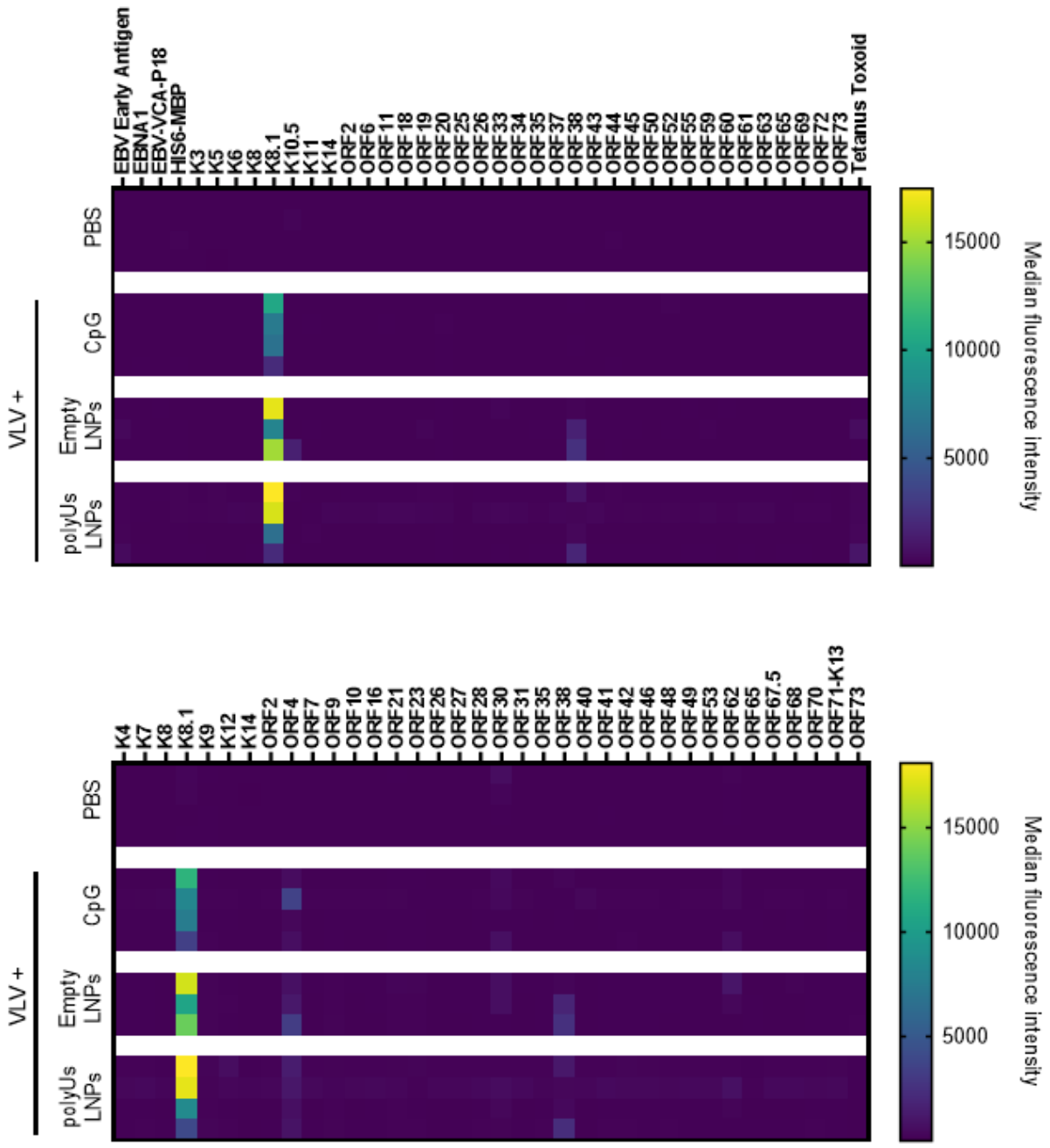

Figure 2-5: Antibody responses to adjuvanted VLV administered intramuscularly

Mice were immunized as in Fig. 2-4a and serum was analyzed for antibody binding to KSHV antigens in a multiplexed bead assay. Each heatmap represents a different set of beads with some overlapping antigens.

Figure 2-6

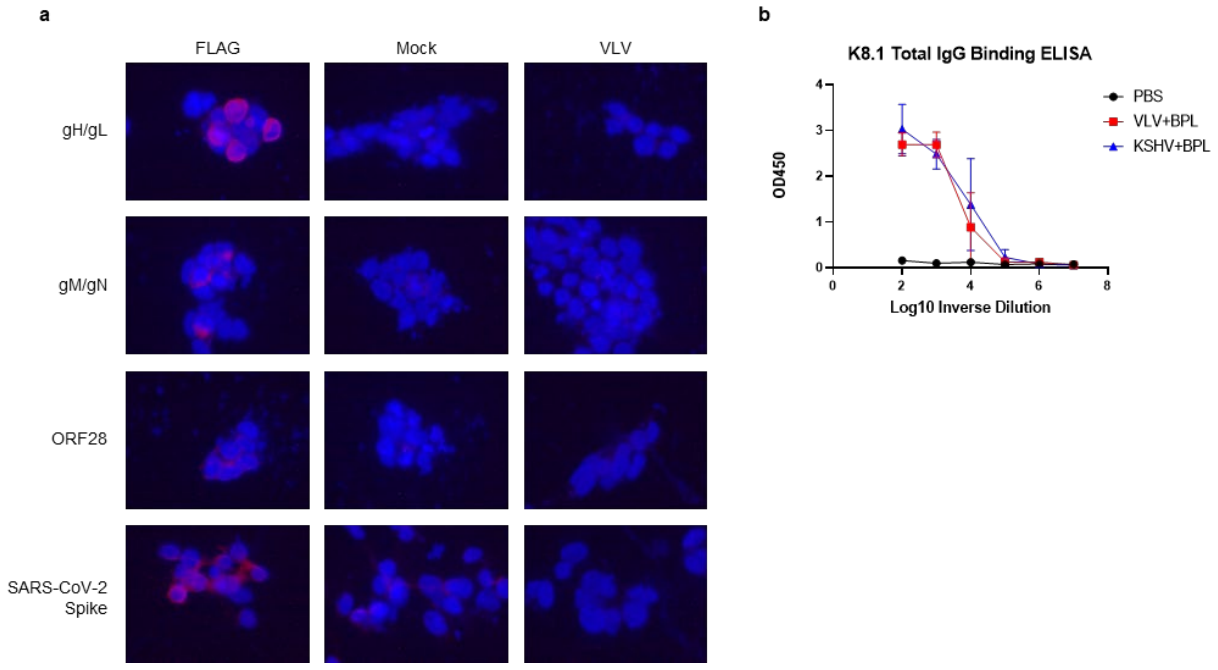

Figure 2-6: Antibody responses after intramuscular immunization of polyUs-LNP adjuvanted VLV and KSHV virions

(a-b) Mice were immunized as shown in Figure 2-4d

(a) Immunofluorescence images of 293T cells expressing KSHV glycoproteins or SARS-CoV-2 Spike stained with pooled mock or VLV+BPL + polyUs-LNP immune serum at a 1:100 dilution

(b) K8.1 ELISA signals from mice immunized with VLV+BPL and KSHV+BPL. Mean and standard deviation are shown. N=3-4 mice per group

Figure 2-7

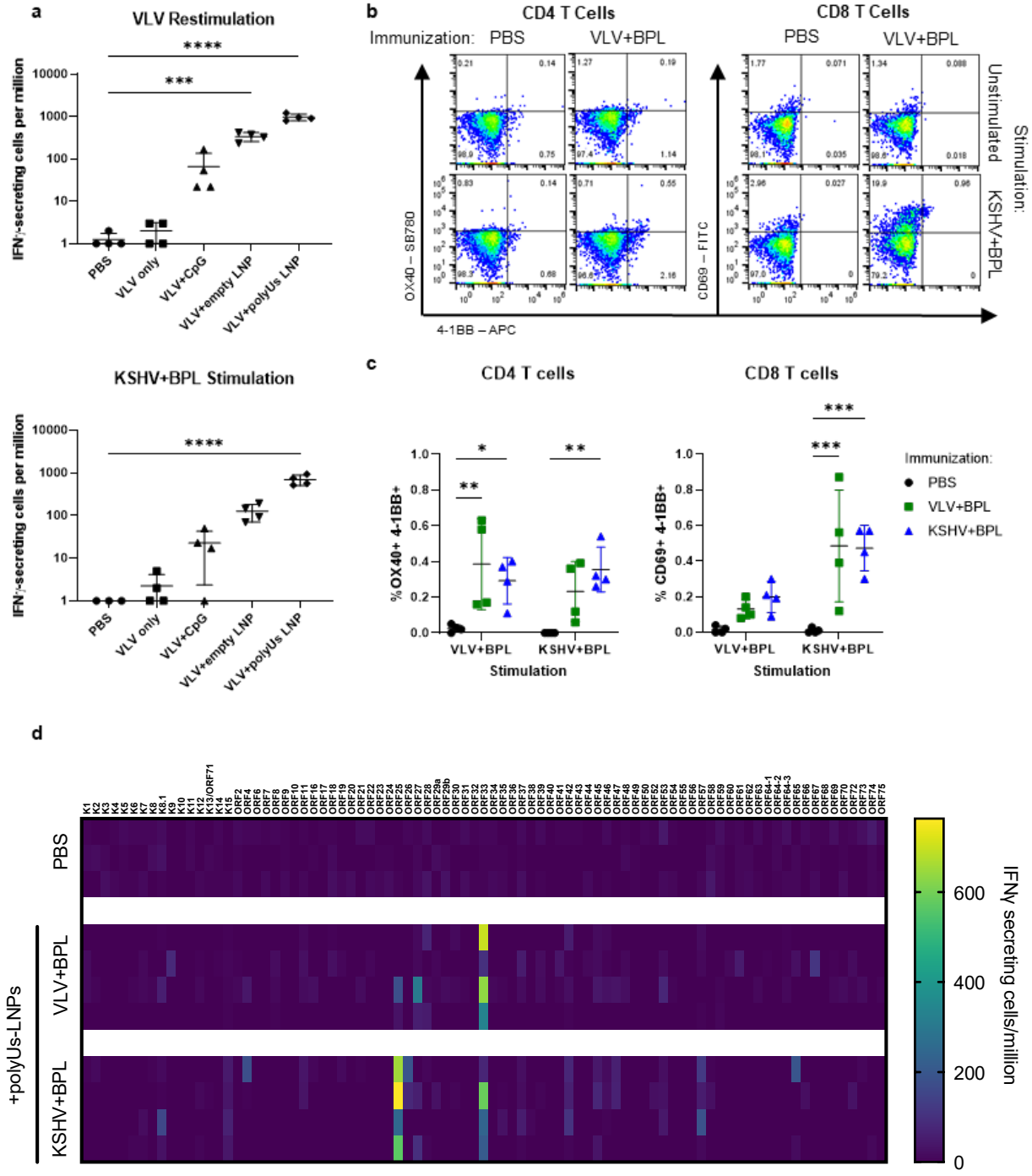
a
VLV Restimulation
IFNγ-secreting cells per million
PBS
VLV only
VLV+CpG
VLV+empty LNP
VLV+polyUs LNP
KSHV+BPL Stimulation
b
CD4 T Cells
CD8 T Cells
Immunization: PBS VLV+BPL
Stimulation: Unstimulated KSHV+BPL
OX40 – SB780
4-1BB – APC
CD69 – FITC
c
CD4 T cells
CD8 T cells
%OX40+ 4-1BB+
% CD69+ 4-1BB+
VLV+BPL
KSHV+BPL
Stimulation
Immunization:
PBS
VLV+BPL
KSHV+BPL
d
+polyUs-LNPs
PBS
VLV+BPL
KSHV+BPL
IFNγ secreting cells/million

Figure 2-7: Adjuvanted VLV immunization generates virus-specific T cells

(a) Mice were immunized as shown in Figure 2-4a. IFNγ secreting cell frequencies from VLV-immunized mouse splenocytes restimulated with VLV or KSHV+BPL

(b-d) Mice were immunized as shown in Figure 2-4d.

(b) Representative flow cytometry plots of CD4 and CD8 T cells used in an AIM assay

(c) Percentages of AIM-positive CD4 and CD8 cells after subtracting background from unstimulated cells

(d) Heatmap showing IFNγ secreting cell frequencies from VLV-immunized mouse splenocytes stimulated with overlapping peptide libraries of KSHV ORFs

Statistical analysis: (a) Ordinary one-way ANOVA with Dunnett's test for multiple comparisons. (c) Two-way ANOVA with Tukey's test for multiple comparisons. *p<0.05, ** p<0.01, ***p<0.001, ****p<0.0001. Mean and standard deviation are shown. N=4 mice per group

APC – allophycocyanin; FITC – fluorescein isothiocyanate; SB780 – Super Bright 780

Figure 2-8

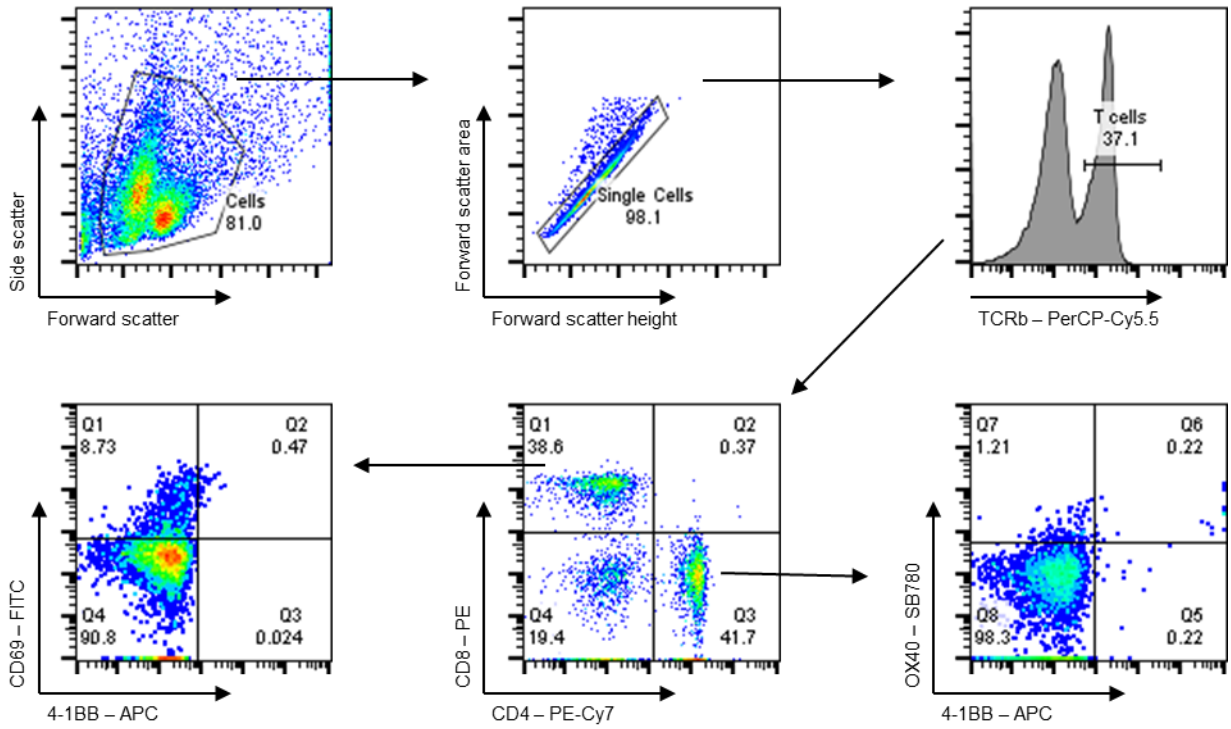

Figure 2-8: Representative gating strategy for AIM assay

Splenocytes were gated for single T cells, separated by CD4 and CD8 expression, and analyzed for AIM markers OX40 and 4-1BB (CD4 cells) or CD69 and 4-1BB (CD8 cells).

APC – allophycocyanin; FITC – fluorescein isothiocyanate; PE – R-phycoerythrin; PE-Cy7 – PE-Cyanine7; PerCP-Cy5.5 – Peridinin chlorophyll protein-Cyanine5.5; SB780 – Super Bright 780; TCRb – T cell receptor beta chain

Figure 2-9

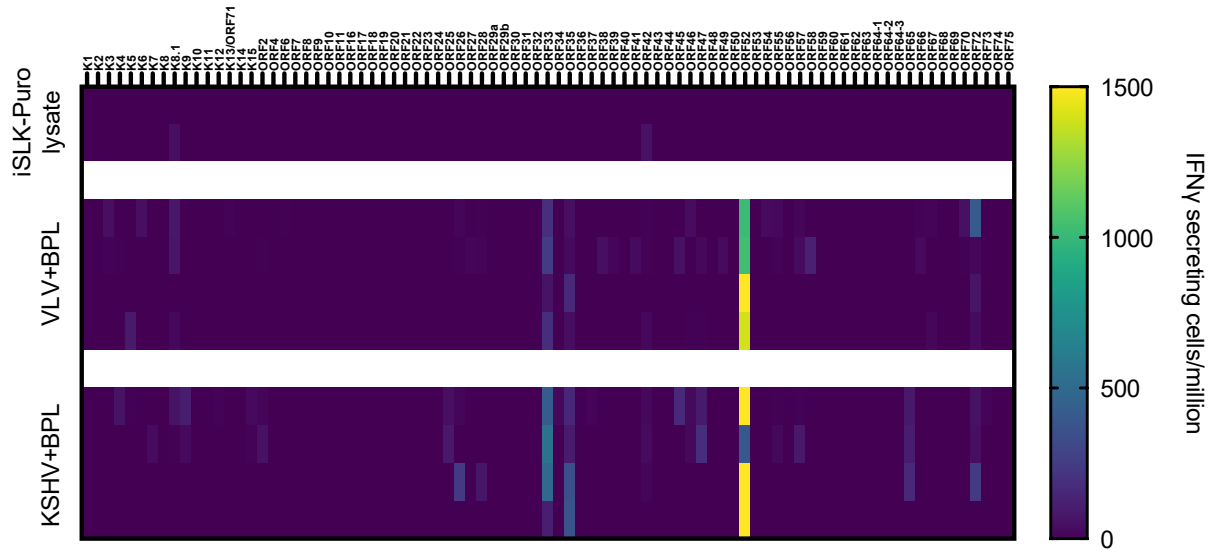

Figure 2-9: T cell responses to adjuvanted VLV+BPL and KSHV+BPL immunization in Balb/c mice

Balb/c mice were immunized with iSLK-Puro cell lysates, VLV+BPL, or KSHV+BPL adjuvanted with polyUs-LNP adjuvant as shown in Fig. 2-4d and splenocytes were stimulated with overlapping peptide libraries for IFNγ ELISpot. Wells with too many spots to count were set to 1500 spots per million.

Figure 2-10

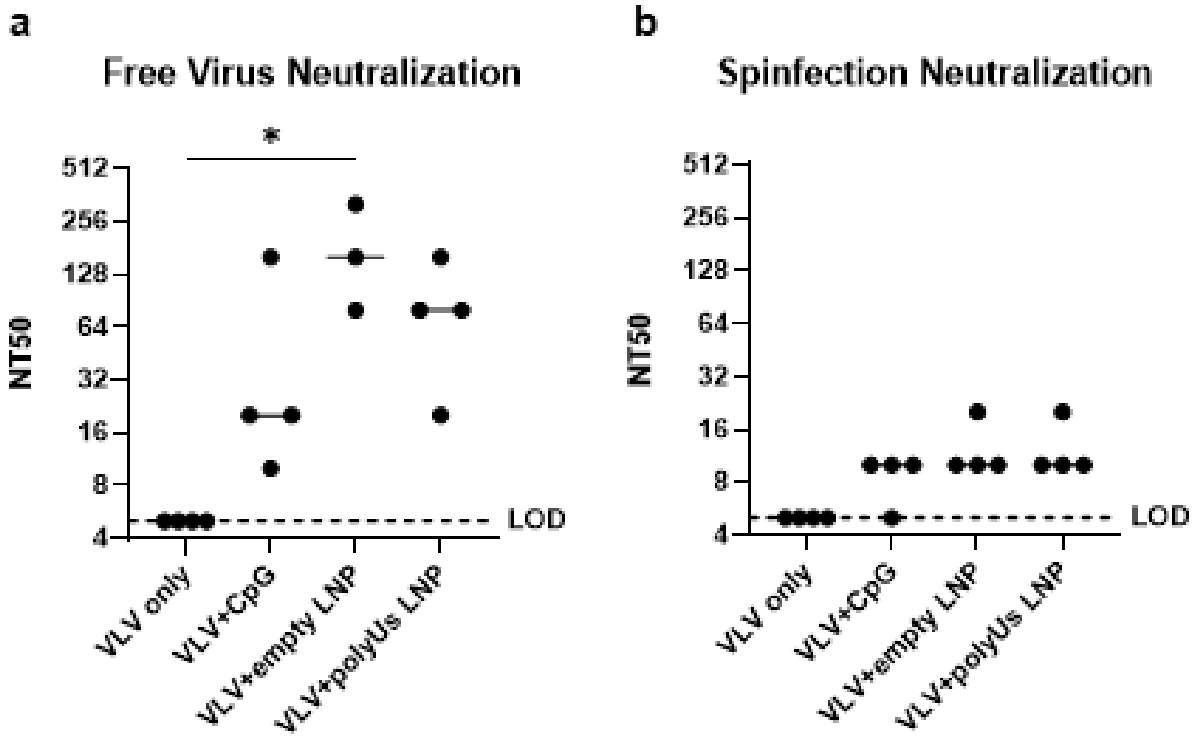

Figure 2-10: Serum from VLV-immunized mice neutralize KSHV infection

(a and b) 50% neutralization titers of serum from mice immunized as shown in Figure 2-4a. Infection was performed using soluble virus (a) or spin infection (b). LOD = limit of detection

Statistical analysis: Ordinary one-way ANOVA with Tukey's test for multiple comparisons. *p<0.05. Median is shown. N=3-4 mouse serum samples per group

Figure 2-11

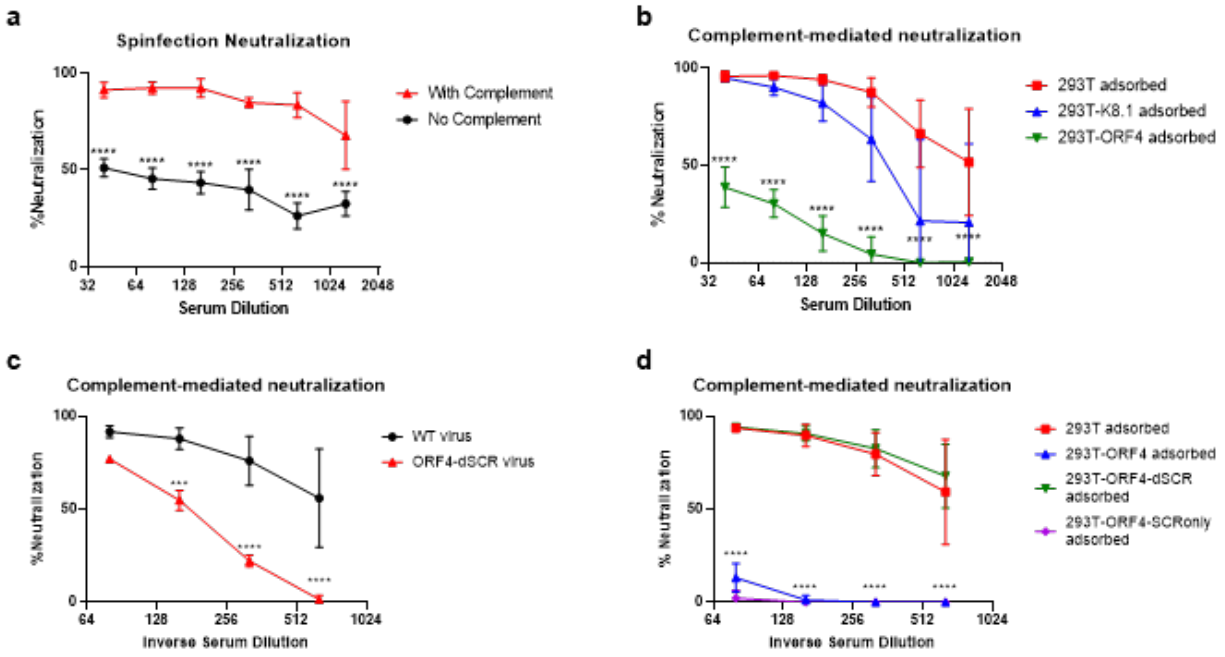

Figure 2-11: Complement-mediated enhancement of neutralization by VLV-immune serum depends on antibodies targeting ORF4

(a-d) Mice were immunized according to the scheme in Figure 2-4d and serum from the VLV+BPL group were serially diluted for neutralization.

(a) Spin infection neutralization by VLV-immune serum in the presence or absence of complement.

(b) Complement-mediated spin infection neutralization by VLV-immune serum adsorbed on 293T cells or 293T cells expressing K8.1 or ORF4

(c) Complement-mediated spin infection neutralization by VLV-immune serum on WT KSHV or KSHV ORF4-dSCR

(d) Complement-mediated spin infection neutralization by VLV-immune serum adsorbed on 293T cells or 293T cells expressing ORF4, ORF4-dSCR, or ORF4-SCRonly

Statistical analysis: Two-way ANOVA with Tukey's multiple comparisons test. Differences between VLV with and without complement (a), between 293T-adsorbed and 293T-ORF4 adsorbed (b), between VLV immune sera neutralization of WT and ORF4-dSCR virus (c), or between 293T-adsorbed and 293T-ORF4-SCRonly adsorbed (d) are shown. Mean and standard deviation are shown. N=3-4 mice per group

Figure 2-12

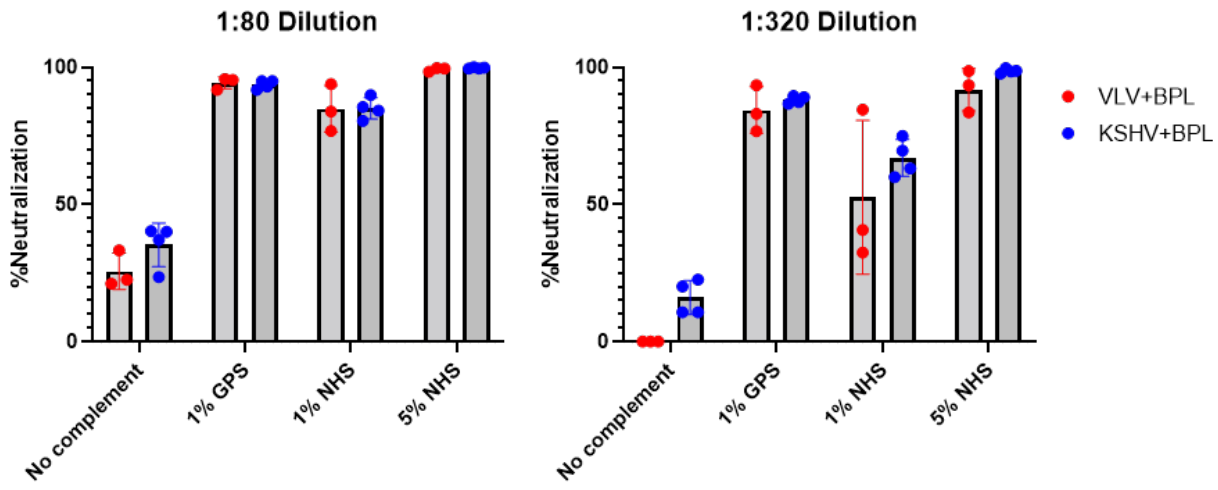

Figure 2-12: Complement mediated neutralization with two sources of complement

Serum from mice immunized as shown in Fig. 2-4d were used for complement-mediated spin infection neutralization at the indicated dilutions with the indicated sources of complement.

Figure 2-13

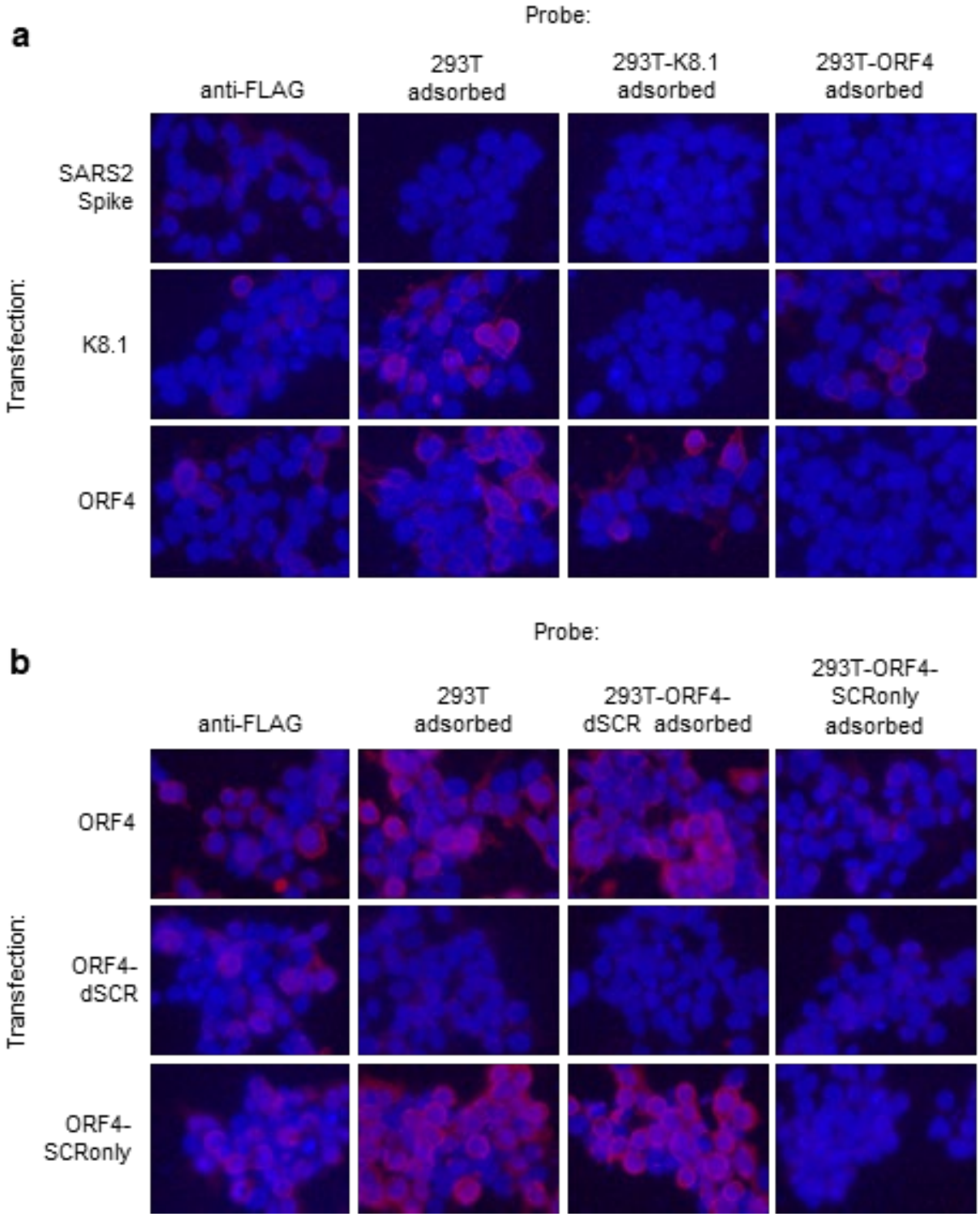
a
Probe:
anti-FLAG
293T adsorbed
293T-K8.1 adsorbed
293T-ORF4 adsorbed
Transfection:
SARS2 Spike
K8.1
ORF4
b
Probe:
anti-FLAG
293T adsorbed
293T-ORF4-dSCR adsorbed
293T-ORF4-SCRonly adsorbed
Transfection:
ORF4
ORF4-dSCR
ORF4-SCRonly

Figure 2-13: Adsorption of VLV-immune serum removes antigen-specific antibodies

(a and b) Mice were immunized as shown in Figure 2-4d. Representative immunofluorescence images of 293T cells expressing the indicated KSHV glycoprotein and stained with serum from the VLV+BPL group adsorbed on 293T cells or 293T cells expressing K8.1 (a), ORF4 (a), ORF4-dSCR (b), or ORF4-SCRonly (b).

Figure 2-14

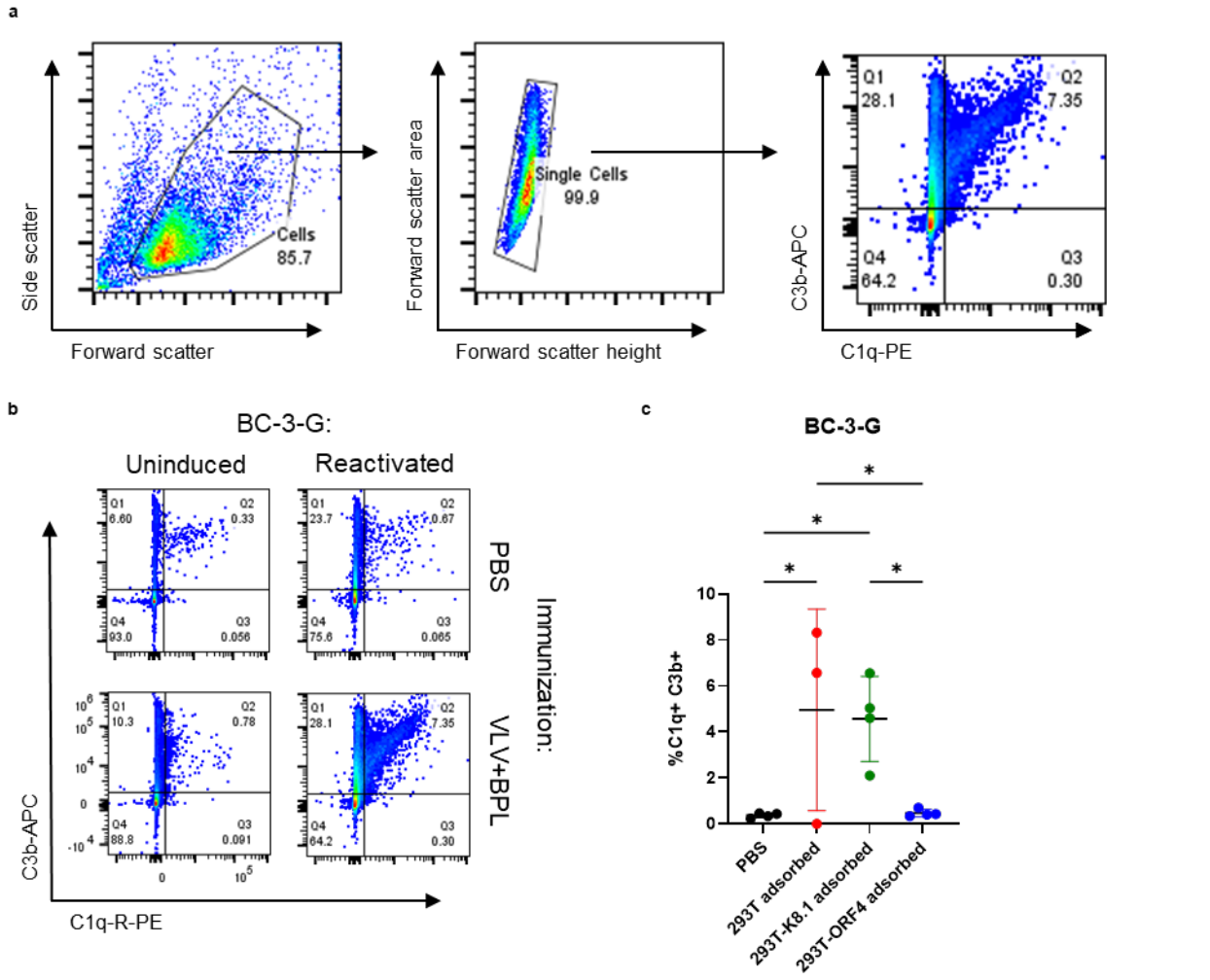

Figure 2-14: VLV immune serum induces complement deposition on KSHV-infected B cells

(a) Gating strategy to investigate complement deposition on BC-3G cells. Cells were gated for single cells then analyzed for C1q and C3b binding.

(b) Representative flow cytometry plots of BC-3G cells incubated with VLV immune serum and stained for complement deposition.

(c) Percentages of C1q and C3b double positive reactivated BC-3G cells after subtracting background from uninduced BC-3G cells

Statistical analysis: One way ANOVA with Tukey's test for multiple comparisons. *$p<0.05$. Mean and standard deviation are shown. N=3-4 mice per group

APC – allophycocyanin; PE – R-phycoerythrin

Figure 2-15

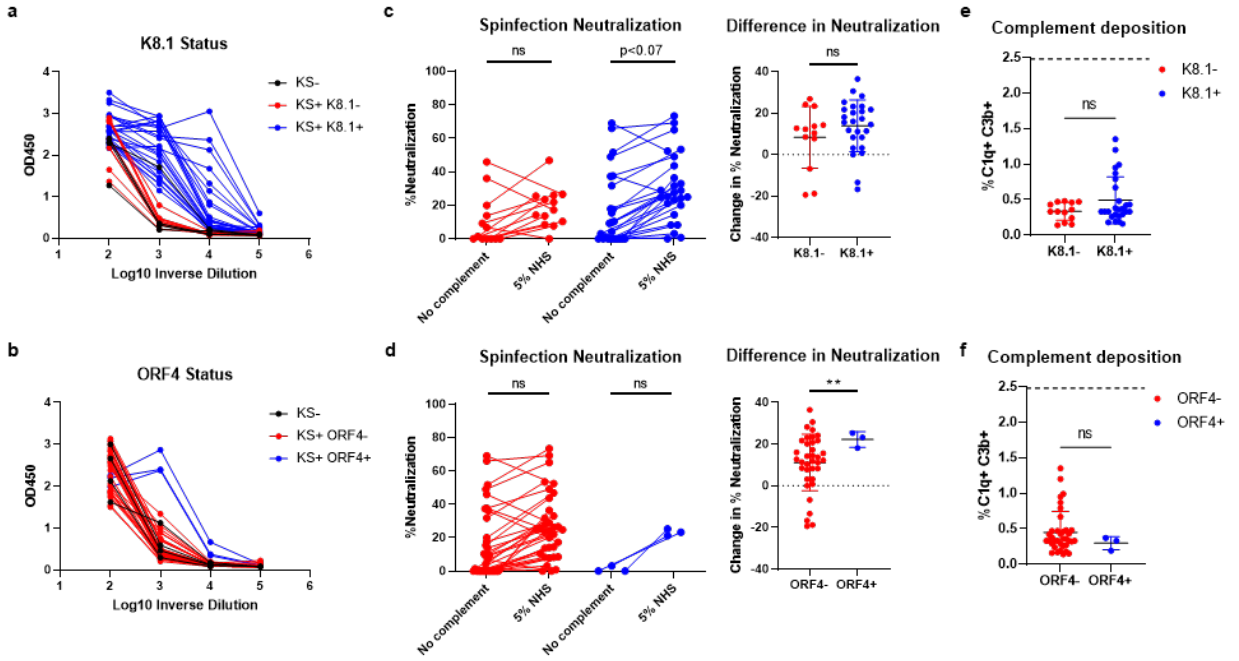

Figure 2-15: Serum from KS+ human patients does not possess complement activity

(a and b) K8.1 (a) and ORF4 (b) ELISA signals from serially diluted KS+ human serum

(c and d) Neutralization of WT KSHV by serum diluted 1:100 in the presence and absence of normal human serum (NHS) as a source of complement (left) and difference in neutralization upon addition of complement (right). Samples are separated by K8.1 (c) or ORF4 (d) serostatus as determined by ELISA

(e and f) Deposition of C1q and C3b on reactivated BC-3-G cells separated by K8.1 (e) or ORF4 (f) serostatus as determined by ELISA. Dotted line indicates staining level by VLV-immunized mouse serum samples

Statistical analysis: 2-way ANOVA with Sidak's multiple comparison's test (%neutralization), Welch's t test (change in neutralization), or unpaired t test (complement deposition). **p<0.05. Mean and standard deviation shown. N=13 (K8.1-), 26 (K8.1+), 35 (ORF4-), or 3 (ORF4+) human serum samples

Table 2-1

Protein	VLV/KSHV Intensity Ratio	Function
Capsid and capsid-associated proteins		
ORF25	0.051	Major capsid protein
ORF26	0.038	Triplex protein
ORF17.5	0.202	Capsid protein
ORF65	0.051	Small capsid protein
ORF62	0.029	Triplex protein
ORF32	0.088	Binds capsid
Envelope proteins		
ORF8	0.647	Glycoprotein B
ORF4	0.603	Complement control
ORF28	0.419	EBV gp150 homolog
ORF22	0.396	Glycoprotein H
ORF39	0.394	Glycoprotein M
ORF47	0.354	Glycoprotein L
K8.1	1.044	Glycoprotein K8.1
Tegument proteins		
ORF75	0.311	Tegument protein, inhibition of ND10 innate immunity
ORF52	0.419	Tegument protein, viral egress, inhibition of cGAS
ORF64	0.423	Tegument protein, inhibition of RIG-I
ORF21	0.395	Thymidine kinase
ORF63	0.399	Tegument protein, inhibition of inflammasome
ORF42	0.587	Tegument protein, viral egress
ORF55	0.684	Tegument protein
ORF67	0.539	Tegument protein
Other detected proteins		
ORF45	0.423	Viral egress, inhibition of IRF7
ORF33	0.372	Viral egress
ORF38	0.385	Viral egress
ORF27	0.640	Cell to cell spread
ORF11	0.337	EBV LF2 homolog
ORF59	0.733	Viral processivity factor
ORF68	0.703	Genome packaging
ORF23	0.397	RNA polymerase pre-initiation complex
ORF60	0.720	Viral ribonucleotide reductase subunit
ORF61	0.481	Viral ribonucleotide reductase subunit
K5	0.517	MHC-I downregulation
ORF6	0.706	ssDNA binding protein

Table 2-1: Viral proteins found in VLV and KSHV preparations

The viral proteins found in the top 1200 proteins identified by average intensity in VLV preparations, organized by function.

Table 2-2

UniprotKB Accession No.	Protein Symbol	Protein Description
P63261	ACTG	Actin, cytoplasmic 2
P07355	ANXA2	Annexin A2
Q09666	AHNK	Neuroblast differentiation-associated protein
P08195	4F2	4F2 cell-surface antigen heavy chain
P08238	HS90B	Heat shock protein HSP 90-beta
P68104	EF1A1	Elongation factor 1-alpha 1
P21333	FLNA	Filamin-A
P14618	KPYM	Pyruvate kinase
P04406	G3P	Glyceraldehyde-3-phosphate dehydrogenase
P11142	HSP7C	Heat shock cognate 71 kDa protein
P0DMV8	HSP1A	Heat shock 70 kDa protein 1A
P68363	TBA1B	Tubulin alpha-1B chain
P23528	COF1	Cofilin-1
P68371	TBB4B	Tubulin beta-4B chain
Q06830	PRDX1	Peroxiredoxin-1
P08133	ANXA6	Annexin A6
P08670	VIME	Vimentin
P08758	ANXA5	Annexin A5
P05023	AT1A1	Sodium/potassium-transporting ATPase subunit alpha-1
P21980	TGM2	Protein-glutamine gamma-glutamyltransferase 2
P13639	EF2	Elongation factor 2
P00338	LDHA	L-lactate dehydrogenase A chain
P35579	MYH9	Myosin-9
Q562R1	ACTBL	Beta-actin-like protein 2
O75369	FLNB	Filamin-B
P05556	ITB1	Integrin beta-1
P49327	FAS	Fatty acid synthase
P02751	FINC	Fibronectin
P69905	HBA	Hemoglobin subunit alpha
P62937	PPIA	Peptidyl-prolyl cis-trans isomerase A

Table 2-2: Cellular proteins found in VLV and KSHV preparations

The top 30 cellular proteins as determined by average intensity in VLV preparations.

Materials and Methods

Plasmids and Cell Lines

KSHV glycoprotein sequences were amplified from KSHV BAC16 derived from rKSHV.219 (a gift from Jae Jung)[47]. Sequences were cloned into the pCAG-GFPd2 overexpression vector (a gift from Connie Cepko, Addgene, Watertown, MA #14760) using the EcoRI and BglII cut sites to replace the GFP coding region or into the pcDNA3-OVA vector (a gift from Sandra Diebold and Martin Zenke, Addgene #64599) replacing the OVA coding region. SARS-CoV-2 Spike was expressed from pCMV14-3X-FLAG-SARS-CoV-2 S (a gift from Zhaohui Qian, Addgene #145780) as a negative control. K8.1 and ORF4 were cloned with FLAG tags on the extracellular domain right after the signal sequence (after amino acid 28 for K8.1 and after amino acid 20 for ORF4). ORF4 without the SCR region was cloned by removing amino acids 24-314 from the original protein sequence. The SCRonly version of ORF4 was cloned by removing amino acids 315-519 and connecting the SCR region to the transmembrane domain of ORF4 with a GGGGS linker. gB was cloned with a FLAG tag on the C terminal end. C terminal FLAG-tagged gL was connected to C terminal HA-tagged gH with a P2A sequence for stoichiometric coexpression and proper association of the gH/gL complex[101]. Signal peptides were determined using SignalP version 4.1[102,103] and transmembrane regions were determined using TMHMM-2.0[104]. Cloning primers were synthesized by Integrated DNA Technologies (IDT, Coralville, IA) and plasmids were confirmed via Sanger sequencing by Laragen, Inc (Culver City, CA).

293T and HEK293 cells were cultured in Dulbecco's Modification of Eagle's Medium (DMEM) (Corning, Corning, NY #10017CV) supplemented with 10% fetal bovine serum (FBS) (Corning #35010CV) and 1X Penicillin/Streptomycin (Corning #35010CV). iSLK cells containing latent KSHV were cultured in DMEM supplemented with 10% FBS and 1X Penicillin/Streptomycin with 1μg/mL puromycin, 250μg/mL G418, and 1200μg/mL hygromycin (all from Invivogen, San Diego,

CA #ant-pr-1, ant-gn-2, and ant-hg-5) for selection. iSLK-WT cells harboring BAC-16 that produced GFP-expressing KSHV were a gift from Jae Jung[47]. iSLK-25Δ60 cells were generated as previously described[46]. BC-3-G cells were a gift from Ren Sun[60] and cultured in (Corning #10040CV) containing 10% FBS and 1X PenStrep (complete RPMI).

KSHV ORF4-dSCR was generated with *en passant* mutagenesis to replace amino acids 24-314 of ORF4 with the HA tag using GS1783 *E. coli* in accordance with previously described protocols[105]. BAC DNA containing the KSHV ORF4-dSCR genome was transfected into 293T cells using Lipofectamine (Thermo Fisher Scientific, Waltham, MA #11668027). 293T stably harboring the viral genome were selected with 100µg hygromycin. 293T cells were cocultured with iSLK cells in the presence of 20ng/mL 12-O-tetradecanoyl-phorbol-13-acetate (TPA, Fisher Scientific, Waltham, MA #AAJ63916MCR) and 1mM sodium butyrate (Fisher Scientific #AC263191000) to induce infection of iSLK cells. Infected iSLK cells were selected with iSLK cell media described above to establish iSLK-ORF4-dSCR.

Virus Production, Isolation, and Inactivation

Wildtype KSHV, KSHV-ORF4dSCR, and VLV were produced by reactivating the latent KSHV virus in iSLK-WT, iSLK-ORF4dSCR, or iSLK-25Δ60 cells, respectively, with DMEM containing 10% FBS, 1X Penicillin/Streptomycin, 5µg/mL doxycycline, and 1mM sodium butyrate. Supernatants were harvested after 4-5 days of reactivation, when over 90% of cells exhibited cytopathic effect.

For virus used for neutralization assays, supernatants collected from 4-6 10cm dishes of reactivated iSLK cells were clarified at 2000g for 10 minutes, and the virus was concentrated at 21000g for 90 minutes. Pellets were washed gently with serum-free DMEM before resuspension

in serum-free DMEM. The virus suspension was clarified to remove debris by centrifugation at 7000rpm for 3 minutes in a microcentrifuge.

For VLVs and virions used for immunization studies and T cell stimulation, supernatants collected from 20-30 15cm dishes of reactivated iSLK cells were clarified at 8000g for 10 minutes. Virions were pelleted by ultracentrifugation at 80,000g for 1 hour in sterile ultracentrifuge tubes (Beckman Coulter, Indianapolis, IN #C14292), and the pellets were incubated in Dulbecco's phosphate-buffered saline (DPBS) (Thermo Fisher Scientific #14190250) overnight. The resuspended viral pellets were then loaded on top of a sucrose cushion consisting of 25% sucrose in DPBS over 50% sucrose in DPBS and centrifuged at 100,000g for 1 hour in sterile ultracentrifuge tubes (Beckman Coulter #C14297). The band at the sucrose interface was collected, diluted in DPBS, and centrifuged at 80,000g for 1 hour. The final pellet was incubated in DPBS overnight before resuspension. Preparations were separated into single-use aliquots immediately after resuspension and stored at -80ºC. Viral protein concentration was determined by standard Bradford assay with bovine serum albumin (BSA) as standards (Fisher Scientific #BP9703100).

For chemical inactivation, KSHV or VLV were resuspended in 1mL DPBS containing 100mM sodium phosphate (Fisher Scientific #S374-500). 1µL beta-propiolactone (Alfa Aesar, Haverhill, MA #AAB2319703) was added for a final concentration of 0.1% (v/v). This solution was inverted at room temperature overnight to inactivate virus. BPL was removed by dialysis against DPBS at 4ºC overnight using 15kDa molecular weight cut-off TUBE-O-DIALYZER (G-Biosciences, St. Louis, MO #786618). Dialyzed preparations were collected, separated into single-use aliquots, and stored at -80ºC.

Cryo-electron Microscopy

2.5μL aliquots of VLV and virion preparations were applied to glow-discharged Quantifoil 200 mesh Cu R2/1 grids (Electron Microscopy Sciences, Hatfield, PA #Q250CR1). Grids were plunge-frozen in liquid ethane using an FEI Vitrobot Mark IV at 22°C and 100% humidity. Images were acquired at 25,000 × and 50,000 × on an FEI Tecnai TF20 equipped with a 4k × 4k TVIPS F415MP CCD detector.

Immunogold Staining

2.5μL aliquots of VLV or virion preparations were incubated on glow-discharged homemade 200 mesh formvar/carbon-coated copper grids for 5 minutes at room temperature. After sample incubation, the grids were passed through two drops of blocking buffer (PBS + 0.4% BSA, filtered) on Parafilm and floated on a third drop for 30 min in a homemade moisture chamber. Excess blocking buffer was removed by lightly blotting with filter paper prior to incubation with primary antibody against K8.1 (Santa Cruz Biotechnology, Dallas, TX #sc-65446) diluted 1:50 in blocking buffer for 1 hour. Negative controls substituted primary anti-K8.1 with anti-FLAG M2 (Sigma-Aldrich, St. Louis, MO #F1804) or blocking buffer. After primary antibody incubation, the grids were washed by passing through two drops of blocking buffer and floating on a third drop for 10 minutes. The washed grids were lightly blotted before incubation with 6 nm gold-conjugated Fabs of goat anti-mouse IgG (Electron Microscopy Sciences #25374) diluted 1:20 in blocking buffer for 1 hour. The grids were washed with three drops of PBS and kept floating on a drop of PBS for at most 1 hour until ready for negative staining. For negative stain, grids were washed with three drops of distilled water and stained with 2% uranyl acetate (Electron Microscopy Sciences #22400-2) for 1 minute. Particles that were greater than 100 nm in diameter and had five or more gold beads were considered positively labeled.

Mass Spectrometry

20μL of each VLV or KSHV preparation was diluted with 80μL of a master mix consisting of 43μL HPLC water, 25μL 8M urea, 10μL 100mM ammonium bicarbonate, and 1μL 100 mM Dithiothreitol (DTT). Samples were then incubated at 60°C to reduce disulfide linkages for 30 minutes. Iodoacetamide (IAA) was then added to a 10mM final concentration to alkylate free cysteines and lysates were incubated in the dark at room temperature for 30 minutes. Lysates were next digested with Trypsin Gold (Promega Corporation, Madison, WI #V5280). 0.4μg of trypsin was added to each sample, and lysates were then incubated for 16 hours at 37°C while being vortexed at 1000rpm. Trypsin activity was quenched by adding 10% v/v trifluoroacetic acid (TFA) to a final concentration of 0.1% TFA. Samples were then desalted on a C18 minispin column (The Nest Group, Inc., Ipswich, MA #HUM S18V) per the manufacturer's protocol. Samples were eluted from these columns with 200μL 40% acetonitrile (ACN)/0.1% TFA. Samples were dried by vacuum centrifugation and stored at -80°C until analysis.

All samples were analyzed on an Orbitrap Eclipse mass spectrometry system equipped with an Easy nLC 1200 ultra-high pressure liquid chromatography system (Thermo Fisher Scientific) interfaced via a Nanospray Flex nanoelectrospray source. Immediately prior to analysis, lyophilized samples were resuspended in 0.1% formic acid (FA). Samples were injected on a C18 reverse phase column (30cm x 75μm (ID)) packed with ReprosilPur 1.9μm particles. Mobile phase A consisted of 0.1% FA, and mobile phase B consisted of 0.1% FA/80% ACN. Peptides were separated by an organic gradient from 5% to 35% mobile phase B over 120 minutes followed by an increase to 100% B over 10 minutes at a flow rate of 300 nL/minute. Analytical columns were equilibrated with 3μL of mobile phase A. To build a spectral library individual samples were analyzed by a data-dependent acquisition (DDA) method. DDA data was collected by acquiring a full scan over a m/z range of 375-1025 in the Orbitrap at 120,000 resolution resolving power (@200m/z) with a normalized AGC target of 100%, an RF lens setting of 30%, and an instrument-controlled ion injection time. Dynamic exclusion was set to 30 seconds, with a 10-ppm exclusion

width setting. Peptides with charge states 2-6 were selected for MS/MS interrogation using higher energy collisional dissociation (HCD) with a normalized HCD collision energy of 28%, with three seconds of MS/MS scans per cycle. All individual samples were analyzed by a data-independent acquisition (DIA) method. DIA was performed on all individual samples. An MS scan was performed at 60,000 resolution (@200m/z) over a scan range of 390-1010 m/z, an instrument controlled AGC target, an RF lens setting of 30%, and an instrument controlled maximum injection time, followed by DIA scans using 8 m/z isolation windows over 400-1000 m/z at a normalized HCD collision energy of 28%.

Spectral libraries were built with Spectronaut factory settings from DDA pools and from DDA runs from a previous SARS-CoV-2 study[106]. Individual samples run with DIA methods were then analyzed against the before mentioned library with Spectronaut as previously described[107]. False discovery rates were estimated using a decoy database strategy[108]. All data were filtered to achieve a false discovery rate of 0.01 for peptide-spectrum matches, peptide identifications, and protein identifications. Search parameters included a fixed modification for carbamidomethyl cysteine and variable modifications for N-terminal protein acetylation and methionine oxidation. All other search parameters were defaults for the respective algorithms. Analysis of protein expression was conducted utilizing the MSstats statistical package in R. Output data from Spectronaut was annotated based on the human reference (SwissProt human reviewed sequences downloaded on 10/10/2019) and the Human herpesvirus-8 (HHV8) BAC16 strain (sequences were extracted from NCBI GenBank accession: GQ994935.1 on 03/15/2022). Technical and biological replicates were integrated to estimate $\log_2$fold-changes, p-values, and adjusted p-values. All data were normalized by equalizing median intensities, the summary method was Tukey's median polish, and the maximum quantile for deciding censored missing values was 0.999. Significantly dysregulated proteins were defined as those which had a fold change value >2 or <-2, with a p-value <0.05.

Viral DNA Extraction and RT-PCR

DNA extraction was performed using the DNeasy Blood and Tissue Kit (Qiagen, Germantown, MD #69504). 1µg of protein from VLV or KSHV preparations was mixed with 10µg salmon sperm DNA (Thermo Fisher Scientific #15632011) as a carrier. Eluted DNA was adjusted to 100ng/µL and 1µL was used for RT-PCR. RT-PCR was performed using a 10µL reaction of the iTaq Universal SYBR Green Supermix (BioRad, Hercules, CA #1725120) with primers specific for the ORF50 gene (F: 5'-CGCAATGCGTTACGTTGTTG-3', R: 5'-GCCCGGACTGTTGAATCG-3')[109] on a 96-well CFX Connect Real-Time PCR system (BioRad). Cycle threshold (Ct) was compared to the threshold obtained using primers for the actin gene (F: 5'-CATGTACGTTGCTATCCAGGC-3', R: 5'-CTCCTTAATGTCACGCACGAT-3') to normalize to the amount of carrier DNA isolated. ORF50/Actin ratio was calculated using 2^ΔCt.

KSHV Titer and Neutralization Assay

KSHV viral titer was obtained by infecting 10,000 HEK293 cells seeded overnight in a 96-well plate. 50µL of virus diluted in serum-free DMEM was added to each well and incubated at 37°C for 2 hours. For spin infection, an additional 50µL of serum-free DMEM was added to each well and the plate was spun at 400g for 20 minutes before the 2 hour incubation. The inoculum was removed, replaced with growth medium, and incubated for an additional 2 days. Infection was measured by flow cytometry for GFP+ cells on an Attune NxT with a plate autosampler (Thermo Fisher Scientific). Flow cytometry data was analyzed with FlowJo (BD, Ashland, OR).

KSHV neutralization was performed by infection of 10,000 HEK293 cells seeded overnight in a 96-well plate. The amount of virus used was calculated to give ~5% GFP+ cells for samples without neutralization. This amount differed between free virus and spin infection, as spin infected resulted in ~3x more infected cells from the same volume of virus. All assays comparing

complement-enhanced neutralization were performed using spin infection. Immune serum was diluted in DMEM containing 2% normal mouse serum (Abcam, Cambridge, UK #ab7486) and KSHV was diluted in serum-free DMEM. For complement-dependent neutralization, KSHV was diluted with DMEM containing 2% guinea pig serum or 10% normal human serum (Complement Technology Inc., Tyler, TX #GPS and #NHS). Diluted serum was mixed with diluted virus at a 1:1 ratio and incubated at 37^{o}C for 1 hour. 50µL of the serum/virus mixture was used to infect cells as described for the viral titer above. Neutralization was calculated as (%GFP_{PBS}-%GFP_{immune})/%GFP_{PBS}*100, where %GFP_{PBS} is the percentage of cells expressing GFP from wells infected with virus mixed with control serum from mock-immunized mice and %GFP_{immune} is from experimental wells infected with virus mixed with serum from immunized mice. If %GFP_{immune} was greater than %GFP_{PBS}, neutralization was defined to be zero. NT50 was defined as the last serum dilution before neutralization drops below 50%.

Mice and Immunizations

All animal experiments were conducted with the approval of the UCLA Institutional Animal Care and Use Committee and the Chancellor's Animal Research Committee. 6-10 week old female C57Bl/6J and Balb/cJ mice (The Jackson Laboratory, Bar Harbor, ME #000664 and #000651) were immunized with PBS, VLV, or KSHV virions in a 50µL volume intramuscularly or a 200µL volume intraperitoneally using insulin syringes (Becton, Dickinson, and Company (BD), Franklin Lakes, NJ #329461) at the described time points. Immunogens were premixed with adjuvants and injected in the same volume described above. ODN2395 CpG adjuvant was purchased from Invivogen (#vac-2395-1). 21-mer polyU with phosphothioate linkages (polyUs) was custom synthesized by IDT. Lipid nanoparticles were prepared using a self-assembly process as previously described[110]; the ionizable cationic lipid and LNP composition are described in the patent application WO 2017/004143. At the experimental endpoint, mice were euthanized and

blood was collected by cardiac puncture with tuberculin syringes (BD #309623). Serum was collected by centrifugation in serum gel tubes (Sarstedt, Numbrecht, Germany #41.1378.005) and heat inactivated at 56C for 30 minutes before storage at -80C. Splenocytes were harvested in complete RPMI. Single cell suspensions were prepared by pushing spleens through 70um cell strainers (Fisher Scientific #22-363-548). Red blood cells were removed with ACK lysing buffer (Thermo Fisher Scientific #A1049201). Splenocytes were resuspended in complete RPMI and stored at 4°C for no longer than overnight until stimulation.

Bead-based Multiplexed KSHV Antibody Assay

The assay was adapted to murine antibodies from a previously described protocol[48]. Briefly, 68 recombinant KSHV antigens were each covalently attached to Bio-Plex Pro Magnetic COOH beads (Bio-Rad #MC10026 to #MC10065) via a sulfo-N-hydroxysulfosuccinimide mediated ester according to the manufacturer's protocol. enAntigens were split into two sets, with K8.1, ORF38, and ORF73 present in both sets to ensure consistency. 2500 beads in 50µL assay buffer were added to each well and 50µL of serum diluted 1:200 was added. Beads were incubated with serum for 1 hour at room temperature and washed with assay buffer. Beads were then incubated with an R-PE-labeled goat anti-mouse IgG secondary antibody (Jackson ImmunoResearch Laboratories, Inc., West Grove, PA #115-116-146) for 30 minutes. Samples were washed, resuspended in 100µL assay buffer and analyzed on the Bio-Plex 200 system (Bio-Rad #171000201). The median fluorescence intensity (MFI) across all counted beads was computed for each sample and recorded after subtracting the background fluorescence.

Enzyme –linked immunospot (ELISpot) Assay

ELISpot using VLV and KSHV+BPL stimulation was performed using a murine TNFα/IFNγ ELISpot kit (Cellular Technology Limited (CTL), Shaker Heights, OH #mIFNgTNFa-1M/10)

following the manufacturer's instructions. Negative control wells contained unstimulated splenocytes and positive control wells were stimulated with a cocktail of phorbol 12-myristate 13-acetate (PMA) and ionomycin (Thermo Fisher Scientific #00-4970-03). Experimental wells were stimulated with 1µg/mL VLV, VLV+BPL, or KSHV+BPL as indicated. 500,000 cells were used per well and plates were incubated for 20-22 hours at 37°C before development. Plates were scanned and spot counts were analyzed by CTL. The number of spots in negative control wells was subtracted from experimental wells to determine the number of antigen-specific spot-forming cells.

Activation Induced Marker Assay

250,000 splenocytes were plated in 100µL complete RPMI in a 96-well U-bottom plate (Fisher Scientific #FB012932) and stimulated with the same conditions as for ELISpot. After 18-20 hours, cells were transferred to a 96-well V-bottom plate (Corning #3897) and washed with FACS buffer (DPBS containing 2% FBS and 0.05% sodium azide). All wash steps were followed by centrifugation at 500g for 5 minutes to pellet cells. Cells were resuspended in 50µL DPBS containing a 1:25 dilution of Fc block (anti-CD16/CD32 clone 93, Thermo Fisher Scientific #14-0161-86) and incubated at 4°C for 10 minutes. 50µL of cell surface antibodies were added to a final dilution of 1:200 and cells were further incubated for 30-60 minutes at 4°C. Cells were stained with the following antibody cocktail: anti-TCR beta-PerCP-Cy5.5 clone H57-597, CD4-PE-Cy7 clone RM4-5, CD8a-PE clone 53-6.7, CD69-FITC clone H1.2F3, OX40-Super Bright 780 clone OX-86, and 4-1BB-APC clone 17B5 (Thermo Fisher Scientific #50-158-64, 50-154-37, 50-112-9416, 50-965-3, 78-134-182, and 50-112-9043, respectively). After staining, cells were washed twice with FACS buffer, then fixed in 1% paraformaldehyde with incubation at 4°C for 20 minutes. After fixation, cells were washed twice in FACS buffer then resuspended in FACS buffer. Cells were analyzed on an Attune NxT with a plate autosampler and data was analyzed using FlowJo.

AIM+ cells were defined as OX40+ 4-1BB+ for CD4 T cells and CD69+ 4-1BB+ for CD8 T cells. Antigen-specific AIM+ cells were calculated by subtracting AIM+ cells in unstimulated samples from stimulated samples.

KSHV ORFeome ELISpot

The ORFeome assay was adapted to murine cells from a previously described protocol[64]. KSHV 15mer peptides overlapping by 10 amino acids spanning the entire KSHV genome and totaling to over 7500 were synthesized as previously described (Mimotopes, Victoria, Australia). Peptide sequences were based on the sequence of BC-1 cell line derived virus. Eighty-five peptide pools were prepared, each corresponding to a single KSHV ORF except ORF64 which was represented by 3 pools. A total of 83 ORFs were represented. The individual lyophilized peptides were reconstituted using 50% acetonitrile. Peptide pools representing each ORF were prepared by combining the reconstituted peptides corresponding to that ORF. The pools were frozen and re-lyophilized. The lyophilized pools were reconstituted in DMSO (<20%) and PBS. A concentration of 5μg/ml/peptide was used in the assay.

A single 96 well precoated mouse IFN-γ ELISpot plate (Mabtech, Cincinnati, OH #3321-4AST-2) was used per mouse to map responses to the 83 KSHV ORFs. Two positive controls, concanavalin A and cell stimulation Cocktail (Thermo Fisher Scientific) and one negative control, SIV Gag CM9 peptide (New England Peptide, Gardner, MA) were used. VLV was used as a positive control for VLV and KSHV vaccinated mice and a negative control for mock vaccinated mice. A medium only control was used to monitor background activity. All controls excluding the medium only well were plated in duplicate, the KSHV ORFs were plated in single wells and medium only controls were plated in triplicates. Each well of the ELISpot plate was seeded with 160,000-500,000 freshly processed splenocytes and incubated for 18 hours at 37°C, 5% CO2.

Two step detection with R4-6A2-biotin and Streptavidin-ALP, developed with BCIP/NBT-plus substrate was used and plates were read using the CTL ImmunoSpot Analyzer (CTL).

K8.1 and ORF4 ELISA

ELISA plates were prepared by coating with recombinant K8.1 or ORF4 protein as previously described[48]. Coated 96-well plates were blocked with assay buffer consisting of DPBS with 2.5% BSA (%w/v), 2.5% normal goat serum (%v/v) (Equitech-Bio, Kerrville, TX #SG-0500), 0.005% Tween-20 (%v/v) (Fisher Scientific #BP337-500), and 0.005% Triton X-100 (%v/v) (Fisher Scientific #BP151-500) and stored at -80°C until use. All serum samples and secondary antibodies were diluted in assay buffer. Coated plates were thawed at room temperature on an orbital shaker and washed with DPBS containing 0.1% Tween-20 (%v/v) (PBS-T) twice for 3 minutes. Plates were then washed twice quickly with PBS-T before the addition of 50µL serially diluted immune serum. 6-8 wells per plate were incubated with assay buffer containing no primary antibody as a background control. Plates were incubated for 1-2 hours at room temperature on an orbital shaker. Plates were washed with PBS-T twice for 3 minutes, then twice quickly before the addition of 50µL 1:4000 goat anti-mouse HRP secondary antibody (Thermo Fisher Scientific #62-6520) or 1:5000 KPL peroxidase-labeled goat anti-human IgG (gamma) (LGC Clinical Diagnostics #474-1002). Secondary antibody was incubated for 1 hour at room temperature with shaking. Plates were then washed once with PBS-T for 3 minutes, then four times quickly. After one final wash with PBS (no Tween-20), 100µL 1-Step Ultra TMB ELISA Substrate (Thermo Fisher Scientific #34028) was added to each well. Plates were covered to protect them from light and incubated at room temperature for 30 minutes with shaking. Signal development was stopped by the addition of 100µL 1M sulfuric acid (Sigma-Aldrich #1603131000) and the optical density at 450nm (OD450) was measured with a ClarioStar plate reader (BMG Labtech, Cary, NC). Endpoint

ELISA titer was defined as the first dilution before the OD450 dropped below the average signal from PBS-immunized serum at a 1:1000 dilution.

Immunofluorescence Assay (IFA)

iSLK cells were analyzed 2 days post reactivation with 1-5μg/mL doxycycline and 1mM sodium butyrate and 293T cells were analyzed 1-2 days post transfection with plasmid of interest using BioT transfection reagent (Bioland Scientific LLC, Paramount, CA #B01). Cells were fixed with 4% paraformaldehyde (Electron Microscopy Sciences #15710) in DPBS for 15 minutes at room temperature without shaking. Cells were washed 3 times with PBS for 5 minutes and blocked with IFA buffer consisting of DPBS with 10% heat inactivated FBS (%v/v) and 3% BSA (%w/v) for 1 hour at room temperature with orbital shaking. For intracellular IFA, IFA buffer contained 0.3% Triton X-100 (%v/v). Cells were probed with primary antibody diluted in IFA buffer overnight at 4^{o}C on a rocker. After primary incubation, cells were washed 3 times with PBS for 5 minutes before the addition of 1:2000 goat anti-mouse IgG(H+L)-Alexa Fluor 594 secondary antibody (Thermo Fisher Scientific #A11032) diluted in IFA buffer. Cells were covered to protect them from light and incubated with secondary antibody for 2 hours at room temperature on an orbital shaker. Secondary antibody was removed, and nuclei were stained with 1:10000 aqueous Hoescht 33342 solution (Thermo Fisher Scientific #H3570) diluted in IFA buffer for 10 minutes at room temperature protected from light with orbital shaking. Cells were washed three times for 5 minutes with PBS before being visualized by fluorescence microscopy.

Serum antibody removal by cell adsorption

293T cells were seeded in 10cm tissue culture dishes (VWR #10062-880) at a density of 4x10^{6} cells. One day after seeding, cells were transfected using BioT with 10μg of plasmid for the glycoprotein of interest per dish. One day after transfection, cells were washed gently with DPBS,

pushed into suspension with DPBS, and split into 3 tubes. Cells were pelleted and kept at 4°C for no longer than 1-2 days before use. Serum of interest was diluted 1:2 with DPBS and 50μL of the diluted serum was used to resuspend the cell pellet. The mixture was inverted at room temperature for 4 hours before the cells were removed by centrifugation at 500g for 5 minutes. This was repeated twice for a total of 3 adsorptions per serum sample per cell line. The removal of glycoprotein-specific antibodies was verified by immunofluorescence.

Complement deposition assay

Lytic replication of KSHV in BC-3-G cells was reactivated with 20ng/mL TPA in complete RPMI for 2 days. 100,000 cells were placed in a 96-well V-bottom plate and washed twice with FACS buffer. Cells were then incubated in 50μL PBS containing experimental serum diluted 1:50 and 10% normal human serum for 30 minutes at 37°C. Cells were washed twice with FACS buffer then stained with the following antibodies at a 1:100 dilution in PBS for at least 30 minutes at 4°C: C1q-PE clone 1A4 (Santa Cruz Biotechnology #sc-53544 PE) and C3b-APC clone 3E7 (Biolegend, San Diego, CA #846106). Cells were washed twice, then analyzed on an Attune NxT flow cytometer equipped with a plate reader.

Statistical analysis

Statistical analysis was performed using the tests described in the figure legends using Prism (Graphpad Software, San Diego, CA).

References

1. Cesarman, E. *et al.* Kaposi sarcoma. *Nat Rev Dis Primers* **5**, 9 (2019).

2. Howlander, N. *et al.* SEER Cancer Statistics Review, 1975-2017. (2020).

3. Woodle, E. S. *et al.* Kaposi sarcoma: an analysis of the US and international experiences from the Israel Penn international transplant tumor registry. *Transplantation Proceedings* **33**, 3660–3661 (2001).

4. Uppal, T., Banerjee, S., Sun, Z., Verma, S. C. & Robertson, E. S. KSHV LANA--the master regulator of KSHV latency. *Viruses* **6**, 4961–4998 (2014).

5. Dittmer, D. P. & Damania, B. Kaposi sarcoma–associated herpesvirus: immunobiology, oncogenesis, and therapy. *Journal of Clinical Investigation* **126**, 3165–3175 (2016).

6. Ganem, D. KSHV and the pathogenesis of Kaposi sarcoma: listening to human biology and medicine. *J. Clin. Invest.* **120**, 939–949 (2010).

7. Minhas, V. & Wood, C. Epidemiology and Transmission of Kaposi's Sarcoma-Associated Herpesvirus. *Viruses* **6**, 4178–4194 (2014).

8. Boldogh, I. *et al.* Kaposi's Sarcoma Herpesvirus-Like DNA Sequences in the Saliva of Individuals Infected with Human Immunodeficiency Virus. *Clinical Infectious Diseases* **23**, 406–407 (1996).

9. Koelle, D. M. *et al.* Frequent Detection of Kaposi's Sarcoma—Associated Herpesvirus (Human Herpesvirus 8) DNA in Saliva of Human Immunodeficiency Virus-Infected Men: Clinical and Immunologic Correlates. *J INFECT DIS* **176**, 94–102 (1997).

10. Webster-Cyriaque, J. *et al.* Epstein-Barr Virus and Human Herpesvirus 8 Prevalence in Human Immunodeficiency Virus-Associated Oral Mucosal Lesions. *J INFECT DIS* **175**, 1324–1332 (1997).

11. Olp, L. N. *et al.* Early childhood infection of Kaposi's sarcoma-associated herpesvirus in Zambian households: A molecular analysis. *Int. J. Cancer* **132**, 1182–1190 (2013).

12. Labo, N. *et al.* Mutual detection of Kaposi's sarcoma-associated herpesvirus and Epstein–Barr virus in blood and saliva of Cameroonians with and without Kaposi's sarcoma. *Int. J. Cancer* **145**, 2468–2477 (2019).

13. Dedicoat, M. *et al.* Mother-to-Child Transmission of Human Herpesvirus–8 in South Africa. *J INFECT DIS* **190**, 1068–1075 (2004).

14. Brayfield, B. P. *et al.* Distribution of Kaposi Sarcoma–Associated Herpesvirus/Human Herpesvirus 8 in Maternal Saliva and Breast Milk in Zambia: Implications for Transmission. *J INFECT DIS* **189**, 2260–2270 (2004).

15. Crabtree, K. L. *et al.* Association of Household Food- and Drink-Sharing Practices With Human Herpesvirus 8 Seroconversion in a Cohort of Zambian Children. *The Journal of Infectious Diseases* **216**, 842–849 (2017).

16. Kedes, D. H. *et al.* The seroepidemiology of human herpesvirus 8 (Kaposi's sarcoma-associated herpesvirus): distribution of infection in KS risk groups and evidence for sexual transmission. *Nat. Med.* **2**, 918–924 (1996).

17. Martin, J. N. *et al.* Sexual Transmission and the Natural History of Human Herpesvirus 8 Infection. *N Engl J Med* **338**, 948–954 (1998).

18. Liu, Z. *et al.* Global epidemiology of human herpesvirus 8 in men who have sex with men: A systematic review and meta-analysis. *J Med Virol* **90**, 582–591 (2018).

19. Butler, L. M. *et al.* Kaposi Sarcoma–Associated Herpesvirus (KSHV) Seroprevalence in Population-Based Samples of African Children: Evidence for At Least 2 Patterns of KSHV Transmission. *J INFECT DIS* **200**, 430–438 (2009).

20. Nalwoga, A. *et al.* Variation in KSHV prevalence between geographically proximate locations in Uganda. *Infect Agents Cancer* **15**, 49 (2020).

21. Hjalgrim, H., Friborg, J. & Melbye, M. The epidemiology of EBV and its association with malignant disease. in *Human Herpesviruses: Biology, Therapy, and Immunoprophylaxis* (eds. Arvin, A. et al.) (Cambridge University Press, 2007).

22. Plotkin, S. A. Correlates of protection induced by vaccination. *Clin. Vaccine Immunol.* **17**, 1055–1065 (2010).

23. Dollery, S. J. Towards Understanding KSHV Fusion and Entry. *Viruses* **11**, 1073 (2019).

24. Birkmann, A. *et al.* Cell surface heparan sulfate is a receptor for human herpesvirus 8 and interacts with envelope glycoprotein K8.1. *J Virol* **75**, 11583–11593 (2001).

25. Wang, F. Z., Akula, S. M., Pramod, N. P., Zeng, L. & Chandran, B. Human herpesvirus 8 envelope glycoprotein K8.1A interaction with the target cells involves heparan sulfate. *J. Virol.* **75**, 7517–7527 (2001).

26. Pertel, P. E. Human Herpesvirus 8 Glycoprotein B (gB), gH, and gL Can Mediate Cell Fusion. *Journal of Virology* **76**, 4390–4400 (2002).

27. Janeway, C., Travers, P. & Walport, M. *Immunobiology: The Immune System in Health and Disease*. (Garland Science, 2001).

28. Poppe, L. K., Kankasa, C., Wood, C. & West, J. T. Relationships Between Maternal Antibody Responses and Early Childhood Infection With Kaposi Sarcoma-Associated Herpesvirus. *The Journal of Infectious Diseases* **222**, 1723–1730 (2020).

29. Minab, R. *et al.* Maternal Epstein-Barr Virus-Specific Antibodies and Risk of Infection in Ugandan Infants. *The Journal of Infectious Diseases* jiaa654 (2020) doi:10.1093/infdis/jiaa654.

30. Moradi Vahdat, M. *et al.* Hepatitis B core-based virus-like particles: A platform for vaccine development in plants. *Biotechnology Reports* **29**, e00605 (2021).

31. Wang, J. W. & Roden, R. B. Virus-like particles for the prevention of human papillomavirus-associated malignancies. *Expert Review of Vaccines* **12**, 129–141 (2013).

32. Bu, W. *et al.* Immunization with Components of the Viral Fusion Apparatus Elicits Antibodies That Neutralize Epstein-Barr Virus in B Cells and Epithelial Cells. *Immunity* **50**, 1305-1316.e6 (2019).

33. Barasa, A. K. *et al.* BALB/c mice immunized with a combination of virus-like particles incorporating Kaposi sarcoma-associated herpesvirus (KSHV) envelope glycoproteins gpK8.1, gB, and gH/gL induced comparable serum neutralizing antibody activity to UV-inactivated KSHV. *Oncotarget* **8**, 34481–34497 (2017).

34. Ruiss, R. *et al.* A virus-like particle-based Epstein-Barr virus vaccine. *J. Virol.* **85**, 13105–13113 (2011).

35. Pavlova, S. *et al.* An Epstein-Barr virus mutant produces immunogenic defective particles devoid of viral DNA. *J Virol* **87**, 2011–2022 (2013).

36. Gong, D. *et al.* Virus-Like Vesicles of Kaposi's Sarcoma-Associated Herpesvirus Activate Lytic Replication by Triggering Differentiation Signaling. *Journal of Virology* **91**, (2017).

37. Reed, S. G., Orr, M. T. & Fox, C. B. Key roles of adjuvants in modern vaccines. *Nat Med* **19**, 1597–1608 (2013).

38. HogenEsch, H. Mechanism of Immunopotentiation and Safety of Aluminum Adjuvants. *Front. Immun.* **3**, (2013).

39. Casella, C. R. & Mitchell, T. C. Putting endotoxin to work for us: Monophosphoryl lipid A as a safe and effective vaccine adjuvant. *Cell. Mol. Life Sci.* **65**, 3231–3240 (2008).

40. Dowling, D. J. Recent Advances in the Discovery and Delivery of TLR7/8 Agonists as Vaccine Adjuvants. *IH* **2**, 185–197 (2018).

41. Ndeupen, S. *et al.* The mRNA-LNP platform's lipid nanoparticle component used in preclinical vaccine studies is highly inflammatory. *iScience* **24**, 103479 (2021).

42. Tahtinen, S. *et al.* IL-1 and IL-1ra are key regulators of the inflammatory response to RNA vaccines. *Nat Immunol* (2022) doi:10.1038/s41590-022-01160-y.

43. Shirai, S. *et al.* Lipid Nanoparticle Acts as a Potential Adjuvant for Influenza Split Vaccine without Inducing Inflammatory Responses. *Vaccines* **8**, 433 (2020).

44. Alameh, M.-G. *et al.* Lipid nanoparticles enhance the efficacy of mRNA and protein subunit vaccines by inducing robust T follicular helper cell and humoral responses. *Immunity* **54**, 2877-2892.e7 (2021).

45. Spiller, O. B. *et al.* Complement Regulation by Kaposi's Sarcoma-Associated Herpesvirus ORF4 Protein. *J Virol* **77**, 592–599 (2003).

46. Dai, X. *et al.* Structure and mutagenesis reveal essential capsid protein interactions for KSHV replication. *Nature* **553**, 521–525 (2018).

47. Brulois, K. F. *et al.* Construction and Manipulation of a New Kaposi's Sarcoma-Associated Herpesvirus Bacterial Artificial Chromosome Clone. *Journal of Virology* **86**, 9708–9720 (2012).

48. Labo, N. *et al.* Heterogeneity and Breadth of Host Antibody Response to KSHV Infection Demonstrated by Systematic Analysis of the KSHV Proteome. *PLoS Pathog* **10**, e1004046 (2014).

49. Bauer, S. *et al.* Human TLR9 confers responsiveness to bacterial DNA via species-specific CpG motif recognition. *Proc. Natl. Acad. Sci. U.S.A.* **98**, 9237–9242 (2001).

50. Diebold, S. S. *et al.* Nucleic acid agonists for Toll-like receptor 7 are defined by the presence of uridine ribonucleotides. *Eur. J. Immunol.* **36**, 3256–3267 (2006).

51. Reiss, S. *et al.* Comparative analysis of activation induced marker (AIM) assays for sensitive identification of antigen-specific CD4 T cells. *PLoS ONE* **12**, e0186998 (2017).

52. Bowyer, G. *et al.* Activation-induced Markers Detect Vaccine-Specific CD4+ T Cell Responses Not Measured by Assays Conventionally Used in Clinical Trials. *Vaccines* **6**, 50 (2018).

53. Grifoni, A. *et al.* Targets of T Cell Responses to SARS-CoV-2 Coronavirus in Humans with COVID-19 Disease and Unexposed Individuals. *Cell* **181**, 1489-1501.e15 (2020).

54. Mark, L., Lee, W. H., Spiller, O. B., Villoutreix, B. O. & Blom, A. M. The Kaposi's sarcoma-associated herpesvirus complement control protein (KCP) binds to heparin and cell surfaces via positively charged amino acids in CCP1-2. *Mol Immunol* **43**, 1665–1675 (2006).

55. Okroj, M. *et al.* Prevalence of antibodies against Kaposi's sarcoma associated herpes virus (KSHV) complement inhibitory protein (KCP) in KSHV-related diseases and their correlation with clinical parameters. *Vaccine* **29**, 1129–1134 (2011).

56. Mellors, J., Tipton, T., Longet, S. & Carroll, M. Viral Evasion of the Complement System and Its Importance for Vaccines and Therapeutics. *Front. Immunol.* **11**, 1450 (2020).

57. Agrawal, P., Nawadkar, R., Ojha, H., Kumar, J. & Sahu, A. Complement Evasion Strategies of Viruses: An Overview. *Front. Microbiol.* **8**, 1117 (2017).

58. Johnson, D. C. & Huber, M. T. Directed Egress of Animal Viruses Promotes Cell-to-Cell Spread. *J Virol* **76**, 1–8 (2002).

59. Oldstone, M. B. A. & Lampert, P. W. Antibody mediated complement dependent lysis of virus infected cells. *Springer Semin Immunopathol* **2**, 261–283 (1979).

60. Yu, F. *et al.* Systematic Identification of Cellular Signals Reactivating Kaposi Sarcoma–Associated Herpesvirus. *PLoS Pathog* **3**, e44 (2007).

61. Okroj, M. *et al.* Antibodies against Kaposi sarcoma-associated herpes virus (KSHV) complement control protein (KCP) in infected individuals. *Vaccine* **25**, 8102–8109 (2007).

62. Mulama, D. H. *et al.* A multivalent Kaposi sarcoma-associated herpesvirus-like particle vaccine capable of eliciting high titers of neutralizing antibodies in immunized rabbits. *Vaccine* **37**, 4184–4194 (2019).

63. Swaminathan, G. *et al.* A novel lipid nanoparticle adjuvant significantly enhances B cell and T cell responses to sub-unit vaccine antigens. *Vaccine* **34**, 110–119 (2016).

64. Roshan, R. *et al.* T-cell responses to KSHV infection: a systematic approach. *Oncotarget* **8**, 109402–109416 (2017).

65. Kalantari-Dehaghi, M. *et al.* Discovery of Potential Diagnostic and Vaccine Antigens in Herpes Simplex Virus 1 and 2 by Proteome-Wide Antibody Profiling. *J Virol* **86**, 4328–4339 (2012).

66. Jing, L. *et al.* Cross-presentation and genome-wide screening reveal candidate T cells antigens for a herpes simplex virus type 1 vaccine. *J. Clin. Invest.* **122**, 654–673 (2012).

67. Sabourin, K. R. *et al.* Malaria Is Associated With Kaposi Sarcoma-Associated Herpesvirus Seroconversion in a Cohort of Western Kenyan Children. *The Journal of Infectious Diseases* **224**, 303–311 (2021).

68. Nalwoga, A. *et al.* Kaposi's sarcoma-associated herpesvirus T cell responses in HIV seronegative individuals from rural Uganda. *Nat Commun* **12**, 7323 (2021).

69. Man, S., Ridge, J. P. & Engelhard, V. H. Diversity and dominance among TCR recognizing HLA-A2.1+ influenza matrix peptide in human MHC class I transgenic mice. *J Immunol* **153**, 4458–4467 (1994).

70. Kotturi, M. F. *et al.* Of mice and humans: how good are HLA transgenic mice as a model of human immune responses? *Immunome Res* **5**, 3 (2009).

71. Dunkelberger, J. R. & Song, W.-C. Complement and its role in innate and adaptive immune responses. *Cell Res* **20**, 34–50 (2010).

72. van Strijp, J. A., van Kessel, K. P., Miltenburg, L. A., Fluit, A. C. & Verhoef, J. Attachment of human polymorphonuclear leukocytes to herpes simplex virus-infected fibroblasts mediated by antibody-independent complement activation. *J Virol* **62**, 847–850 (1988).

73. Van Strijp, J. A., Van Kessel, K. P., van der Tol, M. E. & Verhoef, J. Complement-mediated phagocytosis of herpes simplex virus by granulocytes. Binding or ingestion. *J. Clin. Invest.* **84**, 107–112 (1989).

74. Spiller, O. B., Blackbourn, D. J., Mark, L., Proctor, D. G. & Blom, A. M. Functional Activity of the Complement Regulator Encoded by Kaposi's Sarcoma-associated Herpesvirus. *Journal of Biological Chemistry* **278**, 9283–9289 (2003).

75. Mark, L., Proctor, D. G., Blackbourn, D. J., Blom, A. M. & Spiller, O. B. Separation of decay-accelerating and cofactor functional activities of Kaposi's sarcoma-associated herpesvirus complement control protein using monoclonal antibodies. *Immunology* **0**, 070903002036001-??? (2007).

76. Kumar, P. *et al.* Higher Levels of Neutralizing Antibodies against KSHV in KS Patients Compared to Asymptomatic Individuals from Zambia. *PLoS ONE* **8**, e71254 (2013).

77. Mortazavi, Y. *et al.* The Kaposi's Sarcoma-Associated Herpesvirus (KSHV) gH/gL Complex Is the Predominant Neutralizing Antigenic Determinant in KSHV-Infected Individuals. *Viruses* **12**, 256 (2020).

78. Friedman, H. M. *et al.* Immune evasion properties of herpes simplex virus type 1 glycoprotein gC. *J Virol* **70**, 4253–4260 (1996).

79. Awasthi, S., Lubinski, J. M. & Friedman, H. M. Immunization with HSV-1 glycoprotein C prevents immune evasion from complement and enhances the efficacy of an HSV-1 glycoprotein D subunit vaccine. *Vaccine* **27**, 6845–6853 (2009).

80. Awasthi, S. *et al.* Immunization with a Vaccine Combining Herpes Simplex Virus 2 (HSV-2) Glycoprotein C (gC) and gD Subunits Improves the Protection of Dorsal Root Ganglia in Mice and Reduces the Frequency of Recurrent Vaginal Shedding of HSV-2 DNA in Guinea Pigs Compared to Immunization with gD Alone. *Journal of Virology* **85**, 10472–10486 (2011).

81. Awasthi, S. *et al.* Nucleoside-modified mRNA encoding HSV-2 glycoproteins C, D, and E prevents clinical and subclinical genital herpes. *Sci Immunol* **4**, (2019).

82. Egan, K. P. *et al.* An HSV-2 nucleoside-modified mRNA genital herpes vaccine containing glycoproteins gC, gD, and gE protects mice against HSV-1 genital lesions and latent infection. *PLoS Pathog* **16**, e1008795 (2020).

83. Britt, W. J., Vugler, L., Butfiloski, E. J. & Stephens, E. B. Cell surface expression of human cytomegalovirus (HCMV) gp55-116 (gB): use of HCMV-recombinant vaccinia virus-infected cells in analysis of the human neutralizing antibody response. *J Virol* **64**, 1079–1085 (1990).

84. Bernstein, D. I. *et al.* Safety and efficacy of a cytomegalovirus glycoprotein B (gB) vaccine in adolescent girls: A randomized clinical trial. *Vaccine* **34**, 313–319 (2016).

85. Li, F. *et al.* Complement enhances in vitro neutralizing potency of antibodies to human cytomegalovirus glycoprotein B (gB) and immune sera induced by gB/MF59 vaccination. *npj Vaccines* **2**, 36 (2017).

86. Nelson, C. S. *et al.* HCMV glycoprotein B subunit vaccine efficacy mediated by nonneutralizing antibody effector functions. *Proc Natl Acad Sci USA* **115**, 6267–6272 (2018).

87. Li, L. *et al.* A conditionally replication-defective cytomegalovirus vaccine elicits potent and diverse functional monoclonal antibodies in a phase I clinical trial. *npj Vaccines* **6**, 79 (2021).

88. Kapadia, S. B., Levine, B., Speck, S. H. & Virgin, H. W. Critical Role of Complement and Viral Evasion of Complement in Acute, Persistent, and Latent γ-Herpesvirus Infection. *Immunity* **17**, 143–155 (2002).

89. Gangappa, S., Kapadia, S. B., Speck, S. H. & Virgin, H. W. Antibody to a Lytic Cycle Viral Protein Decreases Gammaherpesvirus Latency in B-Cell-Deficient Mice. *J Virol* **76**, 11460–11468 (2002).

90. Pulendran, B., S. Arunachalam, P. & O'Hagan, D. T. Emerging concepts in the science of vaccine adjuvants. *Nat Rev Drug Discov* (2021) doi:10.1038/s41573-021-00163-y.

91. Geeraedts, F. *et al.* Superior Immunogenicity of Inactivated Whole Virus H5N1 Influenza Vaccine is Primarily Controlled by Toll-like Receptor Signalling. *PLoS Pathog* **4**, e1000138 (2008).

92. Vollmer, B. *et al.* The prefusion structure of herpes simplex virus glycoprotein B. *Sci. Adv.* **6**, eabc1726 (2020).

93. Liu, Y. *et al.* Prefusion structure of human cytomegalovirus glycoprotein B and structural basis for membrane fusion. *Sci. Adv.* **7**, eabf3178 (2021).

94. Pallesen, J. *et al.* Immunogenicity and structures of a rationally designed prefusion MERS-CoV spike antigen. *Proc. Natl. Acad. Sci. U.S.A.* **114**, (2017).

95. Corbett, K. S. *et al.* SARS-CoV-2 mRNA vaccine design enabled by prototype pathogen preparedness. *Nature* **586**, 567–571 (2020).

96. van Zyl, D. G. *et al.* Immunogenic particles with a broad antigenic spectrum stimulate cytolytic T cells and offer increased protection against EBV infection ex vivo and in mice. *PLoS Pathog* **14**, e1007464 (2018).

97. Wang, L.-X. *et al.* Humanized-BLT mouse model of Kaposi's sarcoma-associated herpesvirus infection. *Proceedings of the National Academy of Sciences* **111**, 3146–3151 (2014).

98. McHugh, D. *et al.* Persistent KSHV Infection Increases EBV-Associated Tumor Formation In Vivo via Enhanced EBV Lytic Gene Expression. *Cell Host Microbe* **22**, 61-73.e7 (2017).

99. Chang, H. *et al.* Non-Human Primate Model of Kaposi's Sarcoma-Associated Herpesvirus Infection. *PLoS Pathog* **5**, e1000606 (2009).

100. Perez-Riverol, Y. *et al.* The PRIDE database resources in 2022: a hub for mass spectrometry-based proteomics evidences. *Nucleic Acids Res* **50**, D543–D552 (2022).

101. Hahn, A. *et al.* Kaposi's Sarcoma-Associated Herpesvirus gH/gL: Glycoprotein Export and Interaction with Cellular Receptors. *Journal of Virology* **83**, 396–407 (2009).

102. Petersen, T. N., Brunak, S., von Heijne, G. & Nielsen, H. SignalP 4.0: discriminating signal peptides from transmembrane regions. *Nat Methods* **8**, 785–786 (2011).

103. Nielsen, H. Predicting Secretory Proteins with SignalP. in *Protein Function Prediction* (ed. Kihara, D.) vol. 1611 59–73 (Springer New York, 2017).

104. Krogh, A., Larsson, B., von Heijne, G. & Sonnhammer, E. L. L. Predicting transmembrane protein topology with a hidden markov model: application to complete genomes11Edited by F. Cohen. *Journal of Molecular Biology* **305**, 567–580 (2001).

105. Tischer, B. K., Smith, G. A. & Osterrieder, N. En passant mutagenesis: a two step markerless red recombination system. *Methods Mol. Biol.* **634**, 421–430 (2010).

106. Higgins, C. A. *et al. SARS-CoV-2 hijacks p38ß/MAPK11 to promote viral protein translation*. http://biorxiv.org/lookup/doi/10.1101/2021.08.20.457146 (2021) doi:10.1101/2021.08.20.457146.

107. Bruderer, R. *et al.* Optimization of Experimental Parameters in Data-Independent Mass Spectrometry Significantly Increases Depth and Reproducibility of Results. *Mol Cell Proteomics* **16**, 2296–2309 (2017).

108. Elias, J. E. & Gygi, S. P. Target-decoy search strategy for increased confidence in large-scale protein identifications by mass spectrometry. *Nat Methods* **4**, 207–214 (2007).

109. Krishnan, H. H. *et al.* Concurrent expression of latent and a limited number of lytic genes with immune modulation and antiapoptotic function by Kaposi's sarcoma-associated herpesvirus early during infection of primary endothelial and fibroblast cells and subsequent decline of lytic gene expression. *J Virol* **78**, 3601–3620 (2004).

110. Maier, M. A. *et al.* Biodegradable Lipids Enabling Rapidly Eliminated Lipid Nanoparticles for Systemic Delivery of RNAi Therapeutics. *Molecular Therapy* **21**, 1570–1578 (2013).

CHAPTER 3:

Antigen-specific impact of type I interferon on the immunogenicity of mRNA lipid nanoparticle vaccination

Abstract

Type I interferons (IFN-I) are a key bridge between the innate and adaptive immune systems during infection and immunization. Current generations of messenger RNA-lipid nanoparticle (mRNA-LNP) vaccines have been engineered to minimize IFN-I stimulation, but it is still unclear what levels of IFN-I signaling are needed for effective mRNA-LNP immunogenicity. In this study, we utilize genetic and antibody-mediated ablation of IFN-I responses in mice and analyze the impact on immune responses to three viral antigens. We demonstrate antigen-specific differences to antibody and T cell responses in the absence of IFN-I signaling. We also provide evidence that IFN-I sensitivity may result in negative interactions between antigens when multiple mRNA-LNP are administered together. Our work highlights the need to study the impacts of IFN-I on mRNA-LNP in an antigen-specific manner.

Introduction

The SARS-CoV-2 pandemic has brought messenger RNA lipid nanoparticle (mRNA-LNP) technology to the forefront of vaccinology. Many traditional vaccines deliver viral proteins as part of whole-inactivated viral particles or in virus-like particles. Others utilize live-attenuated viruses or viral vectors that induce expression of viral proteins by host cells as part of the viral life cycle. In contrast, mRNA-LNP deliver *in vitro*-transcribed mRNA packaged in a particle that includes cationic and ionizable lipids. These LNP can be taken up by endocytosis and low endosomal pH leads to release of the mRNA into the cytoplasm. Translation products of the mRNA can be presented by dendritic cells as whole proteins or as peptides on major histocompatibility complexes (MHC) to direct the induction of antibody and T cell responses[1].

Type I interferons (IFN-I), consisting of two main classes, interferons α and β, are an essential component of host defense against pathogens. Sensing of pathogen-associated molecular patterns (PAMPs) by host pattern recognition receptors (PRRs) leads to production of IFN-I that acts in an autocrine or paracrine manner. Binding of IFN-I to the heterodimeric interferon α/β receptor (IFNAR) composed of IFNAR1 and IFNAR2 leads to the initiation of antiviral gene programs to restrict viral replication in host cells[2]. While IFN-I are considered to be part of the innate immune system, they can act on antigen-presenting cells (APCs) to induce maturation and increase antigen presentation to the adaptive immune system[3]. IFN-I can also act as signal 3 for T cells after T cell receptor (TCR) engagement (signal 1) and costimulation by antigen presenting cells (signal 2), leading to enhanced T cell proliferation and differentiation[4]. Due to these impacts, IFN-I could play an important role in generating protective immune responses to vaccines. IFN-I has been demonstrated to be necessary for developing immune responses to viral vectored and live attenuated virus vaccination[5,6]. We and others have also taken advantage of using IFN-I for an adjuvant effect for subunit, DNA, and live-attenuated viral vaccines[7–9]. However, IFN-I can also

have detrimental effects on vaccine responses. Exposure to IFN-I before TCR ligation can inhibit T cell responses[10,11], and certain vaccine responses can be enhanced by short term blockade of IFN-I signaling[12]. Thus, IFN-I have pleotropic effects on the immunogenicity of vaccines.

RNA sensors in the endosome serve as sentries to alert for incoming viral nucleic acids, and activation of these sensors (toll-like receptor 7 (TLR7), TLR8, and TLR3) leads to production of IFN-I and inflammatory cytokines[13]. TLR7 and TLR8 require binding to both RNA degradation products and single-stranded RNA for activation[14]. In contrast, TLR3 is activated upon binding to double-stranded RNA (dsRNA)[15]. Importantly, *in vitro* transcribed RNA is capable of activating all three of these TLRs[16,17]. However, this can be avoided by nucleoside-modified RNAs that incorporate nucleosides with naturally-occurring modifications during the transcription process. For example, pseudouridine (ψ)-modified RNA does not activate TLR7 or TLR8 but maintains the ability to activate TLR3[17]. *In vitro* transcribed RNA can also be detected by several RNA sensors in the cytosol, including the dsRNA sensors retinoic acid-inducible gene I (RIG-I) and melanoma differentiation-associated protein 5 (MDA5)[18]. In general, MDA5 recognizes longer dsRNA and RIG-I recognizes uncapped 5'-triphosphate RNAs. While both of these recognition features are usually absent from cytoplasmic cellular mRNAs, they can be generated during *in vitro* transcription[19–21]. Thus, a multitude of innate immune sensors can produce IFN-I in response to synthetic mRNA.

The immunostimulatory nature of *in vitro* transcribed RNA leads to limited *in vivo* applications due to toxicity and reactogenicity associated with robust inflammation. In addition, three interferon stimulated genes (ISGs), protein kinase R (PKR), 2′-5′-oligoadenylate synthetase 1 (OAS1) and ribonuclease L (RNase L), reduce protein expression from *in vitro* transcribed RNA via translation inhibition (PKR) or RNA degradation (OAS1 and RNaseL)[22]. PKR and OAS1 also require binding to dsRNA to activate their enzymatic activities[23,24]. Therefore, toning down the immunostimulatory

ability of *in vitro* transcribed RNA may be needed to reduce inflammation and maintain antigen expression. The finding that ψ-modified RNA diminishes not only TLR7/8 sensing but also PKR and OAS1 activation is one major breakthrough for the development of mRNA-based vaccines[17,25,26]. As a result, current generations of mRNA vaccines make use of *in vitro* transcribed ψ-modified RNA, which also comes with the benefit of fewer dsRNA byproducts[25]. To further minimize the induction of IFN-I for maximal protein expression, especially in cases of protein replacement therapy, residual dsRNA can be removed by digestion with RNAse III[27,28] or reduced by purifying the transcription product with affinity chromatography to the polyA tail using oligo-deoxy-thymidine (oligo dT) resin, cellulose chromatography, or high performance liquid chromatography (HPLC)[28–30].

Despite a toned-down IFN-I induction by pseudouridine-modified RNA, conflicting results on the role of IFN-I in the immunogenicity of mRNA-LNP vaccines call for further investigations. Notably, the Pfizer/BioNTech full-length SARS-CoV2 Spike mRNA vaccine still stimulates a robust IFN-response in humans as well as in mice[31,32]. This mRNA vaccine induces IFN-I through MDA5 and abrogation of IFN-I signaling reduces vaccine-induced CD8 T cell and antibody responses in mice[32]. In contrast, a preprint on an mRNA vaccine based on the receptor binding domain (RBD) of Spike showed that both antibody and T-cell responses are negatively affected by the ability of RBD mRNA vaccine to induce IFN-I induction[33]. This response can be abolished by HPLC purification, resulting in enhanced immunogenicity. Thus, further investigations are needed to clarify the role of IFN-I in the immunogenicity of mRNA vaccines.

In this work, we study the impacts of IFN-I on the immunogenicity of nucleoside-modified mRNA-LNP. We generate mRNA constructs for 3 viral antigens: influenza hemagglutinin (HA), SARS-CoV-2 Spike RBD, and SARS-CoV-2 RNA-dependent RNA polymerase (RdRp). Using genetic knockout and antibody blockade of IFN-I responses, we demonstrate antigen-specific impacts of

IFN-I on T cell and antibody responses after mRNA-LNP immunization. While removal of IFN-I signaling negatively impacts T cells against HA and RBD, it has the opposite effect on RdRp-specific T cells. For antibodies, we found minimal impact of IFN-I signaling on HA-specific antibodies, but found that IFN-I negatively impacts RBD antibodies in C57Bl/6 mice. Finally, we provide evidence of potential negative interactions of mRNA-LNP with each other when immunized close in time. This study highlights the need to analyze the impact of IFN-I on mRNA vaccines in an antigen-specific manner during development.

Results

Induction of IFN-I by mRNA-LNP

To test the impact of IFN-I on the immunogenicity of mRNA-LNP vaccines, we generated three mRNA constructs and encapsulated them into LNP (Fig. 3-1a). The influenza HA sequence was generated based on the A/WSN/1933 H1N1 (WSN) strain with a K58I mutation in the HA2 subunit to stabilize the prefusion conformation[34]. The RBD sequence was generated using amino acids 319-541 from the Spike protein of the original Wuhan strain. It was fused with the murine IgK signal sequence at the N-terminus to improve protein secretion and the foldon trimerization domain of bacteriophage T4 at the C-terminus to improve antibody responses[35,36]. The RdRp sequence was generated using the N-terminal 611 amino acids from the Wuhan strain. It was fused with an N-terminal MHC class I signal peptide and a C-terminal MHC-I trafficking domain (MITD) to enhance presentation to T cells[37,38]. All mRNAs were *in vitro* transcribed using N1-methyl-pseudouridine (ψ) and purified using silica membrane before encapsulation into LNP. For comparison, a separate WSN HA mRNA was also generated and purified using HPLC.

We confirmed that the mRNA-LNP expressed the correct antigens *in vitro* (Fig. 3-2). To determine whether these mRNA-LNP triggered IFN-I responses *in vivo*, we immunized C57Bl/6 and Balb/c

mice intramuscularly and analyzed peripheral blood mononuclear cells (PBMCs) for expression of the interferon-stimulated gene (ISG) *IFIT1* 24 hours post immunization (Fig. 3-1b). While the inclusion of ψ in the mRNA synthesis likely reduced the amount of IFN generated, we still found that levels of *IFIT1* were higher in C57Bl/6 mice treated with LNP compared to untreated mice or mice injected with phosphate-buffered saline (PBS) (Fig. 3-1c). Surprisingly, there was a slight induction of *IFIT1* in mice injected with empty LNP, to a level comparable to HPLC-purified HA mRNA-LNP. In Balb/c mice, HPLC-purified HA mRNA-LNP induced a lower level of *IFIT1* expression in PBMCs than silica membrane-purified mRNA-LNP, and IFNAR blockade by neutralizing antibodies diminished IFIT1 induction to equivalent minuscule levels. This result also confirms that IFIT1 induction after intramuscular injection of mRNA-LNPs is mediated by IFN signaling. In addition, there was no difference in the level of *IFIT1* induction between the three silica membrane-purified constructs (Fig. 3-1d), indicating that mRNA sequences do not play a major role in determining the level of IFN-I induction. Furthermore, based on the IFIT1/Actin ratios, IFIT1 induction was similar between C57Bl/6 and Balb/c mice. These data indicate that ψ-containing mRNA-LNP still trigger IFN-I signaling that can be reduced, but not eliminated, by HPLC purification.

IFN-I, but not purification, impacts T cell responses to an influenza HA mRNA-LNP

To determine whether IFN-I signaling impacts the immunogenicity of our two HA mRNA-LNP, we immunized wildtype (WT) C57Bl/6 or age-matched IFNAR knockout (KO) mice with 2.5μg mRNA-LNP intramuscularly and gave a boosting shot three weeks later (Fig. 3-3a). One week after the boost, near the peak of the adaptive immune response, we analyzed the antibody and T cell responses in these mice. Using ELISAs against a homologous WSN H1N1 HA protein, we found only a slight decrease in binding antibodies in WT mice immunized with silica membrane-purified HA compared to HPLC-purified HA. IFNAR KO mice immunized with either HA construct showed

comparable levels of antibodies (Fig. 3-3b). We also observed no difference in cross-binding antibodies toward a heterologous HA from the A/California/7/09 (CA09) strain between the two mRNA-LNP in both WT and IFNAR KO mice (Fig. 3-3b). Interestingly, we observed slightly higher levels of neutralizing antibodies by hemagglutination inhibition (HAI) in IFNAR KO mice with both versions of the HA compared to WT mice (Fig. 3-3c). However, all groups still had HAI titers much higher than what is considered protective in humans[39]. For T cell analyses, we stimulated cells from the lungs and spleens with a commercially available overlapping 15mer peptide library from the HA of the A/PR8/1934 (PR8) strain (PR8 HA Pepmix) or with whole WSN virions inactivated with beta-propiolactone (WSN+BPL). T cells that responded to these stimulations were measured by interferon gamma (IFNγ) ELISpot. We found no difference in T cells that responded to the PR8 HA Pepmix, but found that the lungs of IFNAR KO mice had significantly fewer cells that responded to WSN+BPL from both HA mRNA-LNP (Fig. 3-3d). This trend was also found in the spleen but was not statistically significant.

In order to confirm these findings, we repeated this immunization in Balb/c mice (Fig. 3-3e), which have different HLA and T cell repertoires than C57Bl/6 mice. These mice were administered an IFNAR blocking antibody or an isotype matched control antibody 1 day before each immunization. We confirmed that IFNAR blockade was present 1 day after immunization by competitive staining of PBMCs and that this blockade was gone by two weeks (Fig. 3-4a). Two weeks after boosting, we found no significant difference in binding antibodies towards WSN HA regardless of purification or IFNAR blockade (Fig. 3-3f). However, IFNAR blockade with immunization of the silica membrane purified HA mRNA led to higher CA09 HA binding antibodies (Fig. 3-3f). The levels of HA-binding antibodies were comparable between Balb/c and C57Bl/6 mice. When we analyzed neutralizing antibodies by hemagglutinin inhibition (HAI), mice that received IFNAR blockade with the HPLC-purified HA had the highest levels of neutralization of WSN (Fig. 3-3g). In terms of cellular response, we observed an impact of IFNAR1 blocking antibody on cellular

immunity for both vaccines, resulting in fewer T cells that responded to stimulation with a known H-2K(d) restricted peptide (IYSTVASSL, HA-1), the PR8 HA Pepmix, and WSN+BPL in mice treated with the IFNAR1 blocking antibody (Fig. 3-3h). Again, this effect was more pronounced in IFNγ-secreting cells responding to WSN+BPL in the lung compared to the spleen, and there was little difference between the silica membrane and HPLC-purified HA constructs. We also checked these observations in mice at a longer timepoint, approximately four weeks after the boosting shot (Fig. 3-4b). In these mice, there was no difference in binding antibodies toward WSN or CA09 HA (Fig. 3-4c). However, there was still a consistent decrease in IFNγ-secreting cells from the lung that responded to WSN+BPL stimulation (Fig. 3-4d). Overall, although we saw minimal impacts by purification and IFNAR signaling in antibody responses to HA mRNA-LNP, we observed a consistent decrease in T cells that respond to whole inactivated virions in the lung when IFNAR signaling is removed.

Next, we asked whether these IFNγ-secreting T cells in response to WSN+BPL stimulation were CD4 or CD8 T cells. WSN+BPL is a whole inactivated virus with full-length HA proteins that need to be processed by APCs to peptides before being presented on MHC molecules. We pooled splenocytes from the mice in Fig. 3-4b and removed CD4 and CD8 T cells by positive selection. We found that the majority of T cells that responded to our overlapping peptide library were CD8 T cells, while cells that responded to WSN+BPL were largely CD4 T cells (Fig. 3-4e). Therefore, IFN signaling, even low levels generated by HPLC-purified mRNA-LNP is critical for generating CD4 T cells that can respond to the peptide-MHCII complex on lung APCs stimulated with whole inactivated virions, a context that is likely relevant during infection[40].

Opposing impacts of IFN-I on T cell and antibody responses to a SARS-CoV-2 RBD mRNA-LNP

Next, we examined the role of IFN-I in the immunogenicity of RBD mRNA-LNPs employing both IFNAR KO mice and administration of IFNAR blocking antibody to WT C57Bl/6 mice as orthogonal

methods to inhibit IFN-I responses. Two weeks after a boosting immunization, we analyzed these mice for RBD-specific antibody and T cell responses (Fig. 3-5a). Surprisingly, we found that both genetic and antibody-mediated inhibition of IFN-I signaling dramatically increased the amount of antibodies that bound to the RBD-containing Spike S1 subunit by ELISA (Fig. 3-5b). Neutralizing antibodies were absent in WT mice, but were detected in mice without IFNAR signaling (Fig. 3-5c). To detect T cells specific for RBD, we used IFNγ ELISpot after stimulating cells from the lung and spleen with overlapping peptides spanning the RBD. We found fewer cells in the lung in both IFNAR KO and IFNAR blocked C57Bl/6 mice, but neither was statistically significant compared to WT mice (Fig. 3-5d). There was no noticeable difference in T cells in the spleen between RBD LNP immunized groups.

We wanted to confirm these observations in Balb/c mice using antibody blockade of IFNAR signaling (Fig. 3-5e). Surprisingly, when we analyzed Balb/c mice 8 days after the boosting immunization, we found only slight differences in RBD-binding antibodies between mice treated with IFNAR-blocking antibody compared to isotype-matched control antibody (Fig. 3-5f). While IFNAR blockade led to 100x more antibodies in C57Bl/6 mice, it had minimal impact in the Balb/c mice, with only a slight decrease in mice without IFNAR signaling. The antibody levels in Balb/c mice were much higher than WT C57Bl/6 mice and similar to C57Bl/6 mice without IFNAR signaling (Figs. 3-5b & 3-5f). Levels of neutralizing antibodies were also comparable regardless of IFNAR blockade in Balb/c mice (Fig. 3-5g). Similar to our findings in C57Bl/6 mice, we observed fewer RBD-specific T cells in both the lungs and spleens in the Balb/c mice (Fig. 3-5h). Overall, this data indicates that there is a strain-specific difference in antibody responses for RBD, but a consistent dependence on IFN-I signaling for T cell responses.

IFN-I negatively impacts T cell responses to a SARS-CoV-2 RdRp mRNA-LNP

Immunization of HA and RBD mRNA-LNP is targeted toward the generation of antibody responses to block viral infection. However, the generation of T cells against a conserved target, such as the SARS-CoV-2 RdRp, is could be beneficial for protection against viral variants that can evade antibody immunity[41,42]. Therefore, we generated an mRNA construct encoding the N-terminal half of RdRp fused with a signal peptide and MITD domain to optimize presentation on MHC to T cells (Fig. 3-1a). We immunized WT and IFNAR KO C57Bl/6 mice with the RdRp mRNA-LNP and T cell responses were analyzed (Fig. 3-6a). In contrast to our observations with the HA and RBD mRNA-LNP, there were significantly more T cells that responded to an RdRp peptide library in IFNAR KO mice compared to WT mice in both lungs and spleens (Fig. 3-6b). As with the other mRNA-LNP, we immunized Balb/c mice in the presence of IFNAR blocking antibodies to confirm these observations (Fig. 3-6c). We found no difference between mice treated with the IFNAR blocking antibody or an isotype-matched control (Fig. 3-6d). Thus, while HA and RBD require IFN-I signaling for optimal T cell responses, this is not the case for RdRp, suggesting that the role of IFN-I cannot be generalized for all antigens delivered by mRNA-LNP.

Altered immunogenicity of mRNA-LNP administered together close in time

Ideally, our two SARS-CoV-2 mRNA constructs could be co-administered to generate neutralizing antibodies from the RBD construct and T cells from the RdRp construct. Therefore, we immunized mice with 2.5μg of both mRNA-LNP at the same time in the same location and investigated the immunogenicity 10 days after a boosting immunization (Fig. 3-7a). We found that compared to individual mRNA-LNP immunizations, RBD-specific immunity, both humoral (Fig. 3-7b) and cellular (Fig. 3-7c), was negatively impacted by co-immunization, but interestingly, not RdRp-specific T cell responses (Fig. 3-7c). This negative effect on RBD-specific T cells was seen in both the spleen (Fig. 3-7c) and the lungs (Fig. 3-8a). Overall, this data indicates that the compatibility of antigens may need to be tested empirically.

In order to avoid the negative interference we observed during coimmunization, we immunized C57Bl/6 mice with either the RBD or RdRp mRNA-LNP and injected the other mRNA-LNP in the same location after 3 days. We checked the immunogenicity 10-11 days after the final injection (Fig. 3-7d). We observed that the immune responses against the second antigen were negatively impacted compared to the first antigen. When RBD was given 3 days before RdRp, there was no impact on Spike-binding antibodies compared to single RBD injection, but there were no Spike antibodies detected when RdRp was given 3 days before RBD (Fig. 3-7e). However, RBD-specific T cell responses were still inhibited when RdRp was given 3 days after RBD. This reduction was not as strong as during coimmunization or when RdRp was given before RBD (Fig. 3-7f). T cell responses against RdRp were not affected when RdRp was given first, but were inhibited when RdRp was administered after RBD. This reduction was not to the same level as observed with RBD. Thus, both RBD and RdRp mRNA-LNP can be affected when another antigen is administered soon before them.

Lastly, we attempted to minimize co-administration interactions by immunizing mice with each mRNA-LNP at opposite hindlegs at the same time. In addition, we examined whether IFNAR blockade has any effect on the interference between immunizations of the two mRNA-LNPs (Fig. 3-7g). We found that administration of RdRp at the same time as, but at a different location than the RBD still resulted in reduced levels of Spike-specific antibodies and RBD-specific T cells compared to RBD mRNA-LNP immunization alone. However, Spike-specific antibodies were rescued with IFNAR blockade, suggesting a role of IFN-I in the interference from RdRp mRNA-LNP (Fig. 3-7h). IFNAR blockade with coimmunization did not affect RBD-specific T cells in the spleen compared to coimmunization with an isotype matched control. In contrast, RdRp-specific T cells were similar or even slightly higher than RdRp-N mRNA-LNP immunization alone and further increased by IFNAR blockade (Fig. 3-7i). Similar effects on RBD and RdRp-specific T cells were observed in the lung (Fig. 3-8b). Overall, this data indicates that interaction between mRNA-

LNP can still occur when administered from different sites, and that this interaction is partly through IFNAR signaling.

Discussion

mRNA-LNP have emerged as powerful tools not only as prophylactic vaccines for infectious disease, but also in the fields of cancer and autoimmunity. The immunostimulatory nature of the mRNA cargo has been modulated to minimize induction of IFN-I and maximize antigen expression. This can be achieved by incorporating modified nucleosides to reduce detection by TLR7 and TLR8 and confer resistance to PKR and OAS1[17,25,26,43]. IFN-I can also be reduced by purifying *in vitro* transcribed mRNA to remove dsRNA byproducts that are detected by RIG-I and MDA5[28,30]. However, IFN-I is a key activator of the adaptive immune system, acting to improve antigen presentation and stimulate both B and T cells[2]. In this manuscript, we expand on the impacts of IFN-I in the immunogenicity of nucleoside-modified mRNA vaccines. We find antigen-specific and mouse strain-specific changes to immunogenicity of mRNA-LNP after inhibition of IFN-I signaling, suggesting that the role of IFN-I may not be generalizable for all mRNA vaccines.

Preclinical studies of the Pfizer and Moderna SARS-CoV-2 Spike mRNA vaccines utilized magnetic beads and oligo-dT affinity chromatography, respectively, to purify their transcribed mRNA products[44,45]. However, it is unclear which techniques have been applied to commercial-scale production. Significant fractions of clinical trial participants reported systemic reactogenicity after immunization[46,47]. While this has been attributed interleukin 1 (IL-1) produced after mRNA-LNP immunization[48], IFN-I responses have also been linked to adverse systemic reactogenicity after administration of other vaccines[49]. Indeed, strong IFN-I gene signatures have been observed after immunization with the commercial Pfizer BNT162b2 mRNA vaccine, and inhibition of IFN-I reduced antibody and T cell responses after vaccination in mice[31,32]. MDA5 has been implicated in the IFN-I response to this vaccine, suggesting that some dsRNA byproducts trigger this IFN-I

signaling[32]. However, it is unclear the magnitude of these byproducts and how it was affected by mRNA purification. We observed stronger IFN-I induction by silica membrane-purified mRNA-LNP compared to HPLC-purified mRNA-LNP. Notably, empty LNP can induce slight levels of IFN comparable to HPLC-purified mRNA-LNP (Fig. 3-1). Thus, despite efforts to minimize IFN-I induction from mRNA-LNP, there is evidence that it has not been eliminated and in fact could be necessary for optimal adaptive immune responses for some antigens.

While ablation of IFN-I response in C57Bl/6 mice has been shown to minimally impact antibodies elicited by BNT162b2[32], which expresses a full-length prefusion-stabilized SARS-CoV-2 Spike protein, our work on RBD mRNA-LNP demonstrates a completely different result. We found that antibodies elicited by the RBD mRNA-LNP were significantly increased by 100-fold when IFNAR signaling was abolished genetically or pharmacologically in C57Bl/6 mice (Fig. 3-5). However, this enhancement was not observed in Balb/c mice where RBD mRNA-LNP already induced a 100-fold higher level of antibodies than WT C57Bl/6 mice. Our results are similar to what has been reported on an RBD mRNA-LNP in a preprint[33]. It showed that antibodies elicited by RBD mRNA-LNP were lower in C57Bl/6 mice compared to Balb/c mice and that HPLC purification of RBD mRNA reduced IFN-I induction and rescued antibody production in C57Bl/6 mice[33]. This study also indicated that dendritic cells from C57Bl/6 mice produced more IFNα than those from Balb/c mice upon treatment of RBD mRNA-LNP that was not purified by HPLC. This strain-specific difference was not as significant for Moderna's mRNA-1273[45], which expresses a full-length Spike. C57Bl/6 mice had only slightly lower levels of antibodies compared to Balb/c mice after immunization with Moderna's mRNA-1273[45], though IFN-I responses were not compared in these two strains. While both Pfizer and Moderna's mRNA-LNPs are pseudouridine-modified, it is possible that they contain different amounts of dsRNA contaminants depending on the purification methods used. Pfizer and Moderna mRNA vaccines may contain less dsRNA contaminants than our RBD mRNA-LNP and therefore may induce less IFN-I and reducing the impact of abolished

IFNAR signaling. Although we have not been able to directly compare the ability of Pfizer BNT162b2 vaccine to induce IFN-I with our RBD mRNA-LNP, it is clear from studies in humans and mice that BNT162b2 stimulates a robust IFN-I response. Hence, it is more likely that the difference in the role of IFN-I is due to the encoded antigen, full-length Spike versus RBD. Further supporting this antigen-specific effect is that the pronounced increase in antibodies by blocking IFNAR signaling was also not observed for our HA mRNA-LNP. We found minimal effects of purification methods or ablation of IFN-I responses on antibodies elicited by HA mRNA-LNP, which induced similar levels of antibody responses in Balb/c and C57Bl/6 mice (Fig. 3-3). These results are consistent with the central idea of our study: antigen-specific effects of IFN-I signaling on the immunogenicity of mRNA-LNP.

In general, magnitude and duration of antigen expression influence the resulting immune responses after vaccination. This has been shown for an adenovirus-vectored vaccine as well as for mRNA vaccines where unmodified mRNA-LNP express less antigen with a shorter duration than modified ones, resulting in lower antibody and T cell responses[50,51]. Another study using both immunization and infection models demonstrated that short-term IFN-I blockade could increase antigen expression and presentation early after vaccine or virus administration, which led to improved adaptive immune responses[12]. In these examples, IFN-I responses were thought to be detrimental by attenuating antigen expression. Moreover, antibody responses from an self-amplifying mRNA were also shown to be inhibited by IFN responses after intramuscular immunization[52]. However, the high levels of IFN generated by these vaccine platforms could be the reason for why antibody or T cell responses are inhibited. Our pseudouridine-modified HA and RBD mRNA-LNPs without HPLC purification still induced an IFN-I response after intramuscular injections. It is possible that blocking this IFN-I response increases protein expression from these mRNA-LNP in C57Bl/6 mice to an extent that enhances the ability mRNA-LNP to induce antibodies. One possible explanation as to why only RBD mRNA-LNP is improved

but not HA or full-length Spike could be due to an inherent difference in how effective each antigen activates B cell receptor (BCR) signaling. Antigens differ in their affinity for BCR and ability to induce subsequent BCR clustering for initiating B cell responses. Moreover, both HA and full-length Spike are membrane bound while our RBD is designed to be secreted, and membrane-bound antigens are more efficient at driving BCR activation[53]. It is likely that HA and full-length Spike more potently activate B cells than RBD and saturate antibody production at the dose of mRNA-LNP used in immunizations. Thus, only RBD mRNA-LNP would benefit from more antigen expression to induce antibodies in C57Bl/6 mice. However, this must be confirmed through a method where antigen levels can be more precisely controlled, such as with recombinant RBD proteins. It is also worth noting that human studies comparing Pfizer's BNT162b1 (RBD) and BNT162b2 (full-length Spike) demonstrated similar abilities to elicit antibody responses in aggregate[54], suggesting a role specifically in the MHC or BCR repertoire of C57Bl/6 mice. This phenomenon has been observed with the hepatitis B virus (HBV) vaccine, where certain HLA haplotypes can reduce responsiveness to vaccination[55]. This genetic component regarding the ability of mRNA-LNP to elicit antibody responses will require additional investigation to confirm in humans.

Although high levels of IFN-I induced by unmodified mRNA diminishes T-cell induction by curtailing antigen expression, it is critical for Pfizer's BNT162b2 modified mRNA vaccine to stimulate CD8 T cells in mice[32]. In addition to acting on APCs to enhance their functionality in activating antigen-specific T cells, IFN-I also serves as signal 3 for T cell activation along with T cell receptor (TCR) ligation as signal 1 and costimulatory molecule interactions with APCs as signal 2. Thus, for mRNA vaccines, there is a trade-off between having IFN-I for T cell activation and reduced antigen translation due to IFN-I. Regarding the role of IFN-I, several studies have been performed using unmodified mRNA packaged in lipoplexes made of cationic lipids. These studies showed that IFN signaling was generally detrimental to T cell responses after local

administration by subcutaneous, intradermal, or intranodal injection, but had conflicting results after systemic intravenous administration[56–58]. These studies utilized unmodified mRNA, which induces high levels of IFN-I. On the other hand, increasing IFN-I with nucleoside-modified mRNA-LNP can enhance T cell responses if IFN-I is kept at a moderate level[59]. The study presented here further suggests that the effect of IFN-I on T cell immunity is not generalizable for all antigens. Ablation of IFN-I signaling displayed a trend of negative effect on T-cell responses elicited by RBD and HA mRNA LNPs in both Balb/c and C57Bl/6 mice (Fig. 3-3 and Fig. 3-5). This effect was especially consistent and statistically significant on T cells that responded to inactivated influenza virions processed and presented by APCs in the lung, a population that consists largely of CD4 T cells. Although IFN-I is thought to help T cell responses, lowering IFN-I response by HPLC purification did not impact the induction of T cell responses but there was a negative effect when IFN-I signaling was completely removed (Fig. 3-3). Therefore, even a small amount of IFN-I induced by HPLC purified mRNA-LNP, possibly due to LNP itself, could be critical for an optimal T cell response. In addition, RBD and HA are not designed the same way as RdRp, which was fused with a signal peptide and MITD to enhance presentation on MHC to T cells[37]. While mRNA-encoded antigens are synthesized in APCs and presented by MHC-I, IFN-I can enhance cross presentation by DCs, which may be important for HA and RBD mRNA-LNP to activate CD8 T cells[60]. Strikingly, the opposite effect was observed for the RdRp mRNA-LNP. Lack of IFN-I signaling significantly increased the induction of T cells in C57Bl/6 mice, but no increase was observed in Balb/c mice when the IFNAR neutralizing antibodies were administered. This strain-specific increase also reflects how RBD-specific antibodies are more sensitive to IFN-I signaling in C57Bl/6 mice compared to Balb/c mice, suggesting that the responsiveness of mouse strains to IFN-I may play a role in mRNA vaccine immunogenicity. Furthermore, the only other cytokine that is known to possess the signal 3 capability is IL-12, which can serve as signal 3 in the absence of IFN-I[61,62]. Indeed, IL-12 is stimulated downstream of IL-1 signaling after mRNA lipoplex

administration in mice and in human PBMCs[48]. In addition, IL-12 production can be increased in the absence of IFN-I due to a lack of feedback inhibition[62]. This might explain why antigen-specific T cells are still induced or enhanced, in the case of RdRp, even without IFN-I as signal 3. Overall, similar to antibodies, the effects of blocking IFNAR signaling on T cells elicited by mRNA-LNP are antigen-specific.

The reason for a differential impact on antigen-specific T cell responses between RdRp and HA or RBD mRNA-LNP is unlikely due to the particular design of RdRp mRNA. In a previous study, the same signal peptide and MITD designs were used for generating unmodified mRNA to induce CD8 T cells, and IFNAR signaling was found to be required for optimal T cell responses[63]. This is contrary to our results on RdRp. TCR signaling as signal 1 for T cell activation is influenced by the affinity and quantity of peptide-MHC complexes present on APCs[64]. In general, increasing the amount of peptide-MHC complexes causes an increase in the number of responding T cells[65]. However, the dose-dependent effect is limited once very high levels of peptide-MHC complexes are reached. It's possible that at the dose of mRNA-LNP used in this study (2.5 µg), peptide-MHC complexes from HA and RBD already reached a level that induced maximal responding T cells but in the case of RdRp, blocking IFNAR signaling could be still able to further enhance T cell responses by increasing the number of peptide-MHC complexes available. For instance, RdRp might be processed less efficiently than RBD or HA, resulting in lower levels of peptide-MHC complex being displayed. In addition, peptide-MHC complexes derived from RdRp might be less capable of activating TCR than RBD or HA, saturating at higher levels for maximal induction. Another possible explanation is that the effects of IFN-I on translation from these mRNA-LNPs might differ among antigens with RdRp more significantly affected than others. Again, this effect was limited to C57Bl/6 mice, indicating a potential genetic component in IFN-I response that facilitates it.

One advantage of mRNA vaccines is the ability to simultaneously introduce multiple antigens in one immunization by combining mRNA-LNP that share similar manufacturing processes. This is in contrast with protein-based subunit vaccines, where each protein may have its own challenge for mass production, or with whole virus vaccines, which may include unimportant but immunodominant antigens. However, we have observed that administering two different mRNA-LNPs at the same time may negatively impact the immunogenicity (Fig. 3-7). When RBD and RdRp mRNA-LNPs were mixed and administered together, both RBD-specific antibodies and T cell responses were significantly reduced while RdRp-specific T cells were unaffected compared to individual administration. These two mRNA-LNPs could be individually enhanced by blocking IFNAR signaling to increase RBD-specific antibodies and RdRp-specific T cells in C57Bl/6 mice. While impacts on both mRNA-LNPs were expected due to increase IFN-I induction after co-administration, only RBD was affected, even when the two mRNA-LNP were administered at the different hindlegs. This suggests that the immunogenicity of RBD mRNA-LNP is more sensitive to IFN-I than RdRp mRNA-LNP. However, when spacing them by 3 days, the inhibition of IFN-I from the former mRNA-LNP affected the immunogenicity of the latter regardless of which mRNA-LNP was administered first. A premature IFN-I response prior to TCR signaling is detrimental for T cell responses[10,11]. We currently do not know whether our observation on co-administration of RBD and RdRp holds true for other antigens, such as HA mRNA-LNP. However, a separate study investigating a trivalent mRNA-LNP vaccine composed of glycoprotein D (gD), gC and gE of herpes simplex virus 2 (HSV-2), did not demonstrate lower antibodies toward gD compared to gD mRNA-LNP alone[66]. In addition, antibodies elicited by multivalent influenza HA mRNA vaccines do not seem reduced compared to monovalent ones[67]. Moderna is currently conducting a clinical trial for Epstein-Barr virus (EBV) which consists of multiple mRNAs encoding four different viral antigens, and it remains to be seen if interaction effects are observed[68]. Nonetheless, our work

indicate that care must be taken to avoid negative interactions between mRNA-LNPs and the causes for this should be further studied to optimize future vaccines.

Overall, our study has demonstrated that IFN-I plays an antigen-specific role in the immunogenicity of mRNA vaccines, and that this needs to be carefully considered when designing and producing future mRNA-LNP. It has been shown that removal of dsRNA from RBD enhanced its ability to induce antibodies, and this approach could be applied for the RdRp mRNA-LNP to increase RdRp-specific T cells. It is possible that the level of IFN-I response induced by LNP itself is low enough to avoid impacting antigen expression but sufficient to benefit for the generation of antigen-specific immune responses. Therefore, one avenue of future investigations is to study whether additional adjuvants can be exploited to improve the immunogenicity of highly purified mRNA. These findings will play a major role in the development of next-generation mRNA vaccines.

Acknowledgements

This work was supported by grants from the National Institutes of Health (R01DE028774 to T.W., R01EY032149 to V.A., and R01DK132735 to V.A.), by COVID-19 Research Awards from the W.M. Keck Foundation and the Broad Stem Cell Research Center (OCRC#20-12 to C.G.R. and T.W., OCRC#20-15 to V.A., and OCRC#21-100 to O.N.W.), and by a grant from the California HIV/AIDS Research Program (#H22BD4466 to T.W.). A.K.L. was supported by the NIH Ruth L. Kirschstein Institutional Research Award for Interdisciplinary Training in Virology and Gene Therapy T32AI060567 and by a graduate student fellowship from the Jonsson Comprehensive Cancer Center (JCCC). Flow cytometry was performed in the UCLA JCCC and Center for AIDS Research Flow Cytometry Core Facility that is supported by National Institutes of Health awards P30CA016042 and P30AI028697, and by the JCCC, the UCLA AIDS Institute, the David Geffen School of Medicine at UCLA, the UCLA Chancellor's Office, and the UCLA Vice Chancellor's

Office of Research. The following reagent was obtained through BEI Resources, NIAID, NIH: SARS-Related Coronavirus 2, Isolate USA-WA1/2020 (NR-52281).

We are grateful to Barbara Dillon, UCLA High Containment Program Director for supporting BSL3 work. We thank Jodi Hanson (CTL) for assistance in analysis of ELISpot plates.

Author Contributions

A.K.L. conducted animal experiments with assistance from P.T., K.R., E.R.A., and H.R.L. A.K.L. and P.T. performed ELISpot assays. A.K.L. and S.Z. performed ELISA studies. M.A.N. and P.A.N. performed ICS experiments. A.V.J. and G.G.Jr. conducted SARS-CoV-2 neutralization studies. A.L.C. designed the RdRp mRNA sequence. Y.K.T. provided LNP. V.A., O.N.W., C.G.R., and T.W. supervised the research. A.K.L. and T.W. conceptualized the study, coordinated the research, and wrote the manuscript. All authors edited the manuscript and approved its submission.

Conflicts of Interest

Y.K.T. is an employee of and holds equity in Acuitas Therapeutics, a producer of lipid nanoparticle technology.

Figures and Figure Legends

Figure 3-1

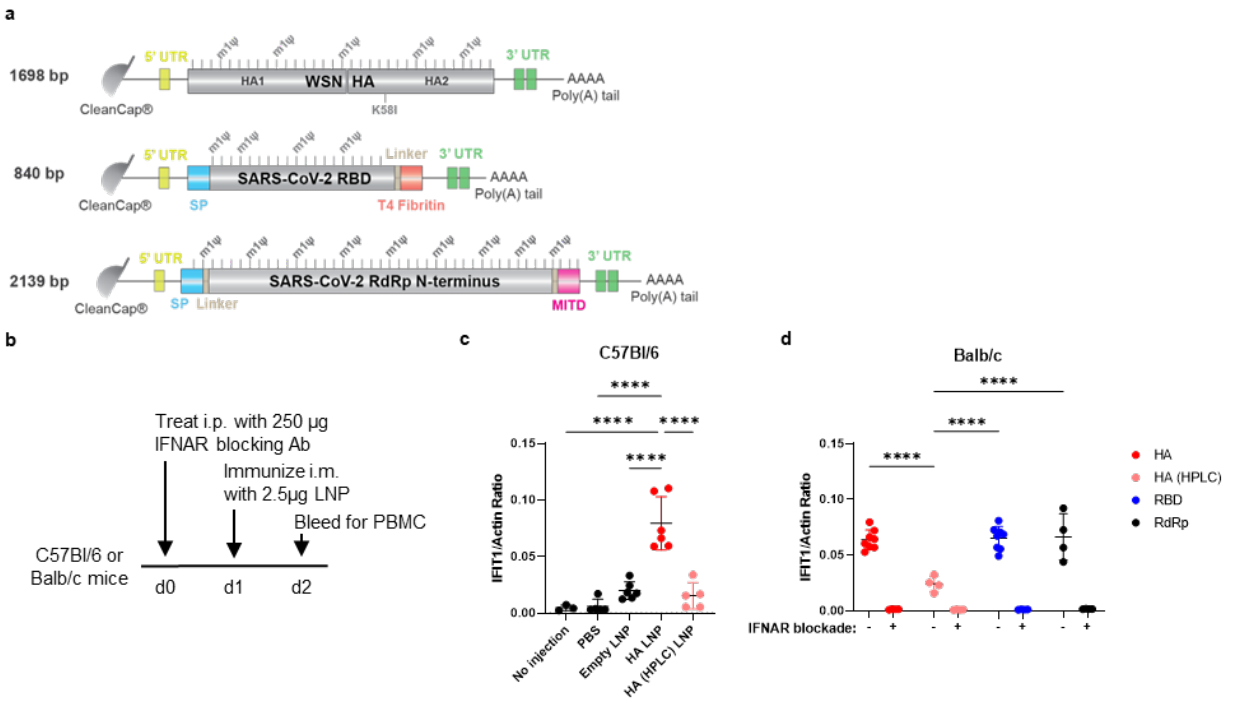

Figure 3-1: Stimulation of IFN by mRNA-LNP immunization

(a) Graphical depiction of mRNA constructs used in this study

(b) Immunization strategy for studying IFN induction after vaccination used in (c) and (d)

(c-d) Induction of IFIT1 in PBMCs from C57Bl/6 (c) and Balb/c (d) mice 24 hours after immunization

Statistical analysis: Two-way ANOVA with Tukey's multiple comparisons test. ****p<0.0001 Mean and standard deviation are displayed. N=4 or 8 mice per group

Figure 3-2

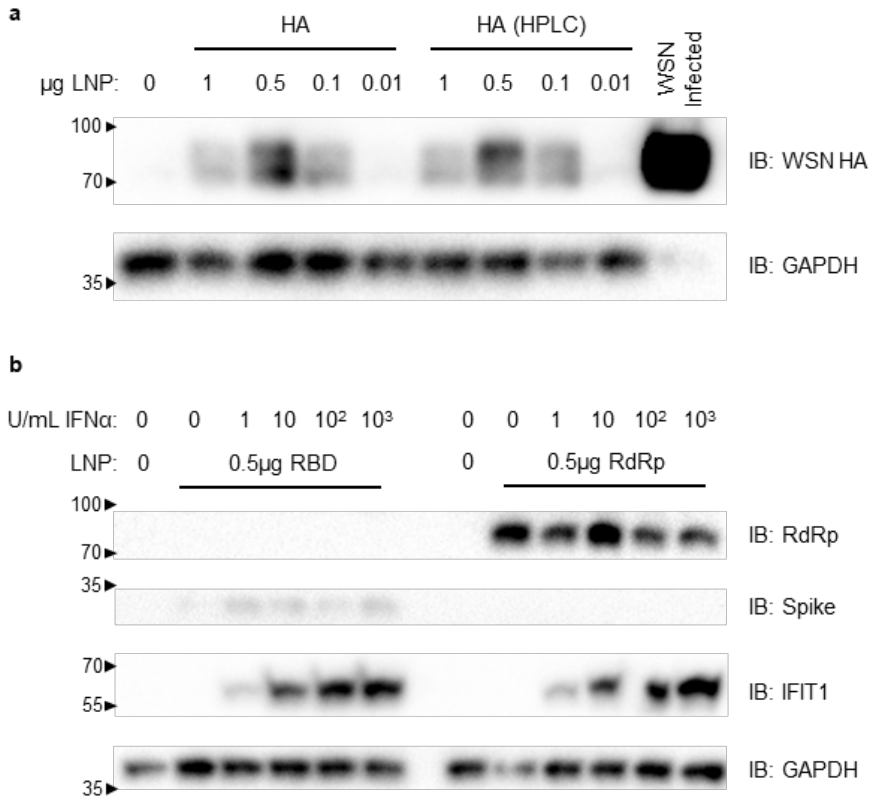

Figure 3-2: Antigen expression by mRNA-LNPs *in vitro*

(a) Western blot showing expression of HA mRNA-LNPs in 293T cells

(b) Western blot showing expression of RBD and RdRp in 293T cells with IFN treatment

Figure 3-3

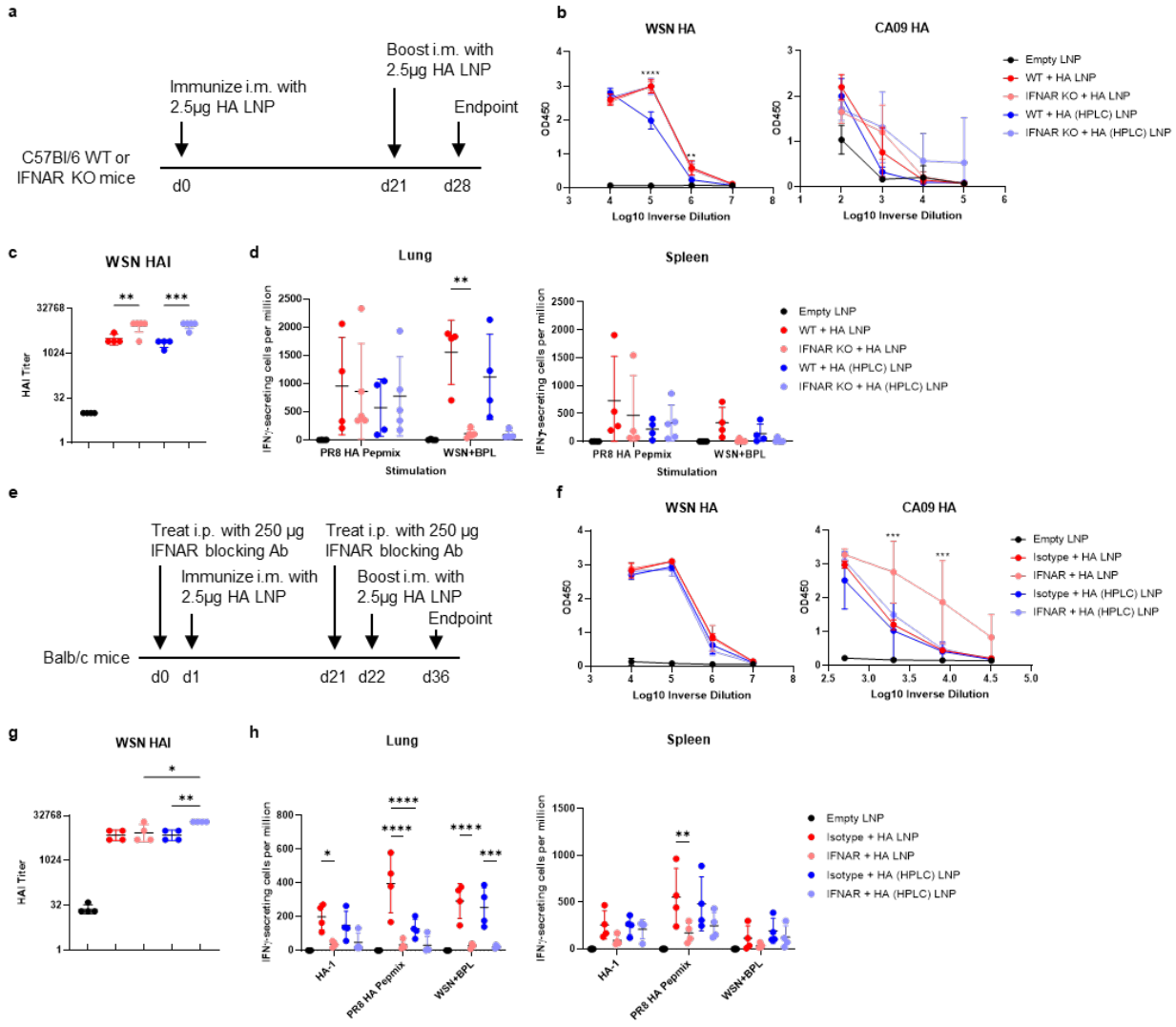

Figure 3-3: IFN-I, but not purification impacts HA T cells with little change in antibodies

(a) Immunization scheme for HA LNPs in C57Bl/6 WT and IFNAR KO mice used in (b-d)

(b) ELISA signals against homologous (WSN) and heterologous (CA09) HA

(c) ELISpot results from stimulating lung and spleen cells from immunized mice with overlapping peptides against PR8 HA or inactivated WSN virus

(d) Hemagglutinin inhibition titers against WSN virus

(e) Immunization scheme for HA LNPs in Balb/c mice used in (f-h)

(f) ELISA signals against homologous (WSN) and heterologous (CA09) HA

(g) Hemagglutinin inhibition titers against WSN virus

(h) ELISpot results from lung and spleen cells stimulated with an MHC-I restricted peptide, overlapping peptides against PR8 HA, or inactivated WSN virus

Statistical analysis: One way ANOVA (c and g) or two way ANOVA with Tukey's multiple comparisons test (b, d, f, and h). Difference between HA and HA (HPLC) in WT mice (b) or isotype and IFNAR antibody treatment with HA LNP (f) are shown. Only differences between HA and HA (HPLC) groups or WT and IFNAR KO with the same LNP are shown (c, d, g, and h). For (d), only WT + HA LNP stimulated with WSN+BPL in the lung was statistically different from empty LNP. For (g), both isotype-treated groups were not statistically different from empty LNP group. For (h), all IFNAR treated groups were not significantly different than empty LNP group. For (h) isotype-treated groups, only HA-1 stimulation in lung, PR8 HA pepmix stimulation for isotype + HA LNP in the lung, both WSN+BPL stimulations in the lung, and both PR8 HA pepmix stimulations in the spleen were significantly different from empty LNP. *$p<0.05$, **$p<0.01$, ***$p<0.001$, ****$p<0.0001$ Mean and standard deviation are displayed. N=4-5 mice per group.

Figure 3-4

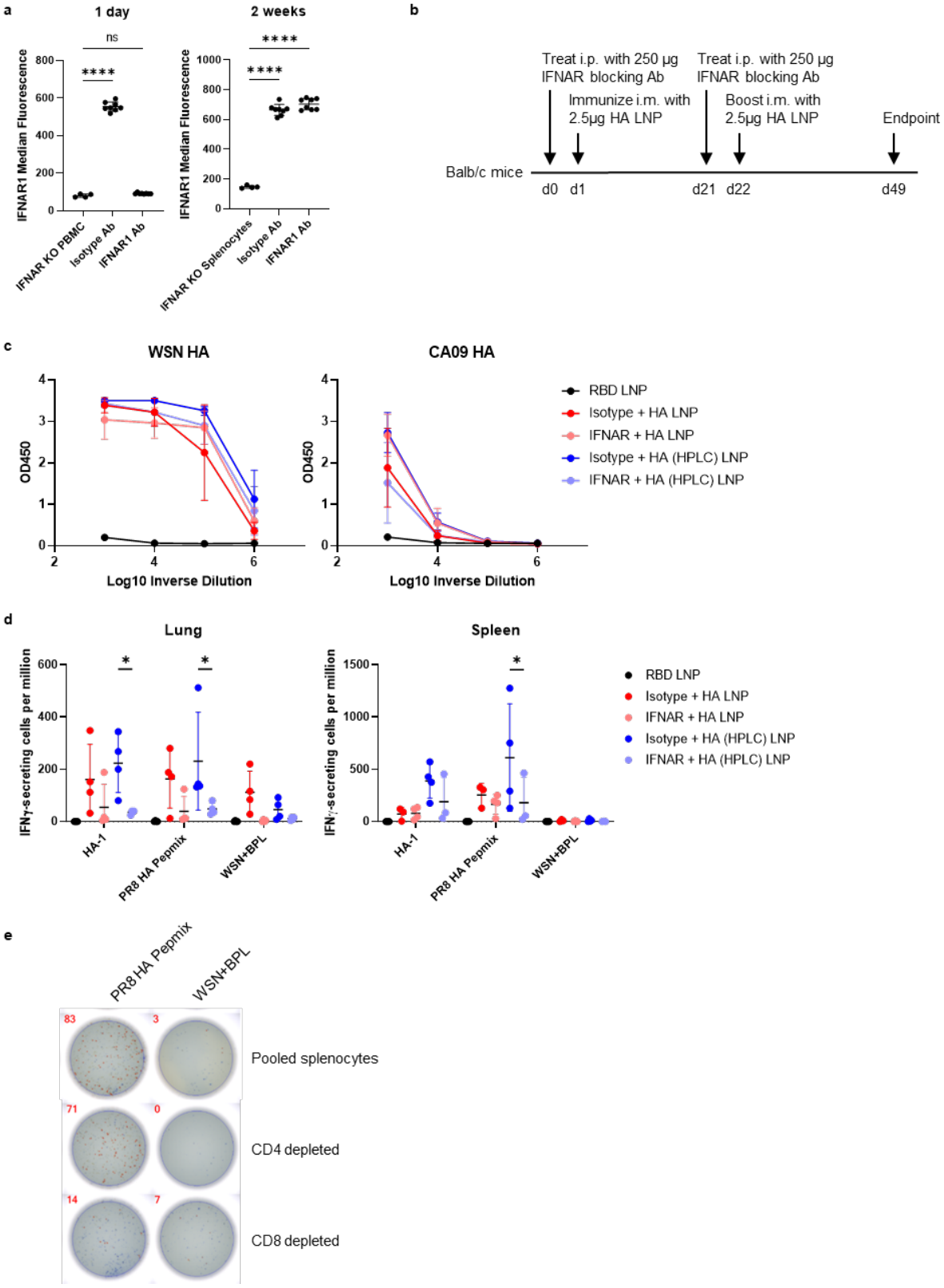
a
1 day
2 weeks
ns
****
IFNAR1 Median Fluorescence
IFNAR KO PBMC
Isotype Ab
IFNAR1 Ab
IFNAR KO Splenocytes
b
Treat i.p. with 250 µg IFNAR blocking Ab
Immunize i.m. with 2.5µg HA LNP
Treat i.p. with 250 µg IFNAR blocking Ab
Boost i.m. with 2.5µg HA LNP
Endpoint
Balb/c mice
d0 d1 d21 d22 d49
c
WSN HA
CA09 HA
OD450
Log10 Inverse Dilution
RBD LNP
Isotype + HA LNP
IFNAR + HA LNP
Isotype + HA (HPLC) LNP
IFNAR + HA (HPLC) LNP
d
Lung
Spleen
IFNγ-secreting cells per million
HA-1
PR8 HA Pepmix
WSN+BPL
e
PR8 HA Pepmix
WSN+BPL
83
3
71
0
14
7
Pooled splenocytes
CD4 depleted
CD8 depleted

Figure 3-4: Impact of IFNAR blockade on long term immunogenicity

(a) Flow cytometry results from staining PBMCs of mice treated with IFNAR blocking antibody or an isotype antibody

(b) Immunization scheme to look at immunogenicity after 1 month used in (c-e)

(c) ELISA signals against homologous (WSN) and heterologous (CA09) HA

(d) ELISpot results from stimulating lung and spleen cells from immunized mice with an MHC-I restricted peptide, overlapping peptides against PR8 HA, or inactivated WSN virus

(e) ELISpot results from pooled splenocytes depleted of CD4 or CD8 T cells and stimulated with overlapping peptides against PR8 HA or inactivated WSN virus

Statistical analysis: Two-way ANOVA with Tukey's multiple comparisons test. Only differences between isotype and IFNAR treatment or HA and HA (HPLC) immunization are shown. For (d), only isotype + HA (HPLC) group stimulated with HA-1 and PR8 HA pepmix in both organs are significantly different than RBD LNP. *$p<0.05$, **$p<0.01$, ***$p<0.001$ Mean and standard deviation are displayed. N=4 mice per group

Figure 3-5

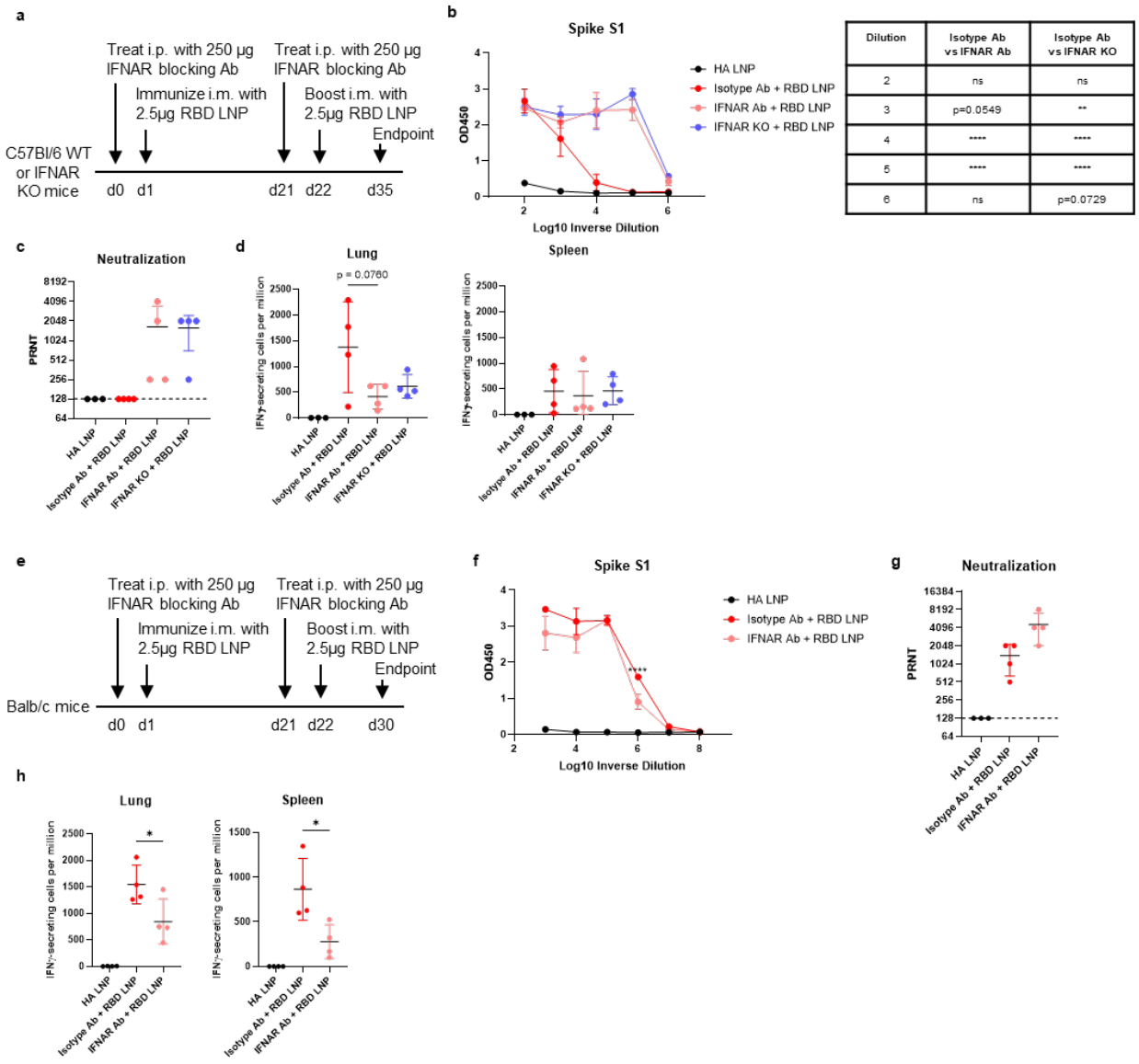

Dilution	Isotype Ab vs IFNAR Ab	Isotype Ab vs IFNAR KO
2	ns	ns
3	p=0.0549	**
4	****	****
5	****	****
6	ns	p=0.0729

Figure 3-5: Opposing impacts of IFN-I on RBD-specific antibody and T cell responses

(a) Immunization scheme for RBD LNPs in C57Bl/6 mice used in (b-d)

(b) ELISA data against Spike S1 protein

(c) Neutralization data against infectious SARS-CoV-2

(d) ELISpot results from lung and spleen cells stimulated with overlapping peptides against RBD

(e) Immunization scheme for RBD LNPs in Balb/c mice used in (f-h)

(f) ELISA data against Spike S1 protein

(g) Neutralization data against infectious SARS-CoV-2

(h) ELISpot results from lung and spleen cells stimulated with overlapping peptides against RBD

Statistical analysis: One way ANOVA (c, d, g, h) or two way ANOVA (b, f) with Tukey's multiple comparisons test. Difference between isotype and IFNAR antibody (e) is shown. Only differences between isotype-treated and IFNAR blockade or KO are shown (c, d, g, h). For (c), RBD LNP immunized groups were not significantly different than HA LNP group. For (d), only the isotype-treated lung was significantly different than HA LNP group. For (g), Isotype Ab + RBD LNP group is not significantly different than HA LNP group. For (h), IFNAR-treated group in the spleen was not significantly different than HA LNP. ns=not significant, *$p<0.05$, **$p<0.01$, ***$p<0.001$, ****$p<0.0001$ Mean and standard deviation are displayed. N=3 or 4 mice per group. Dashed line indicates limit of detection

Figure 3-6

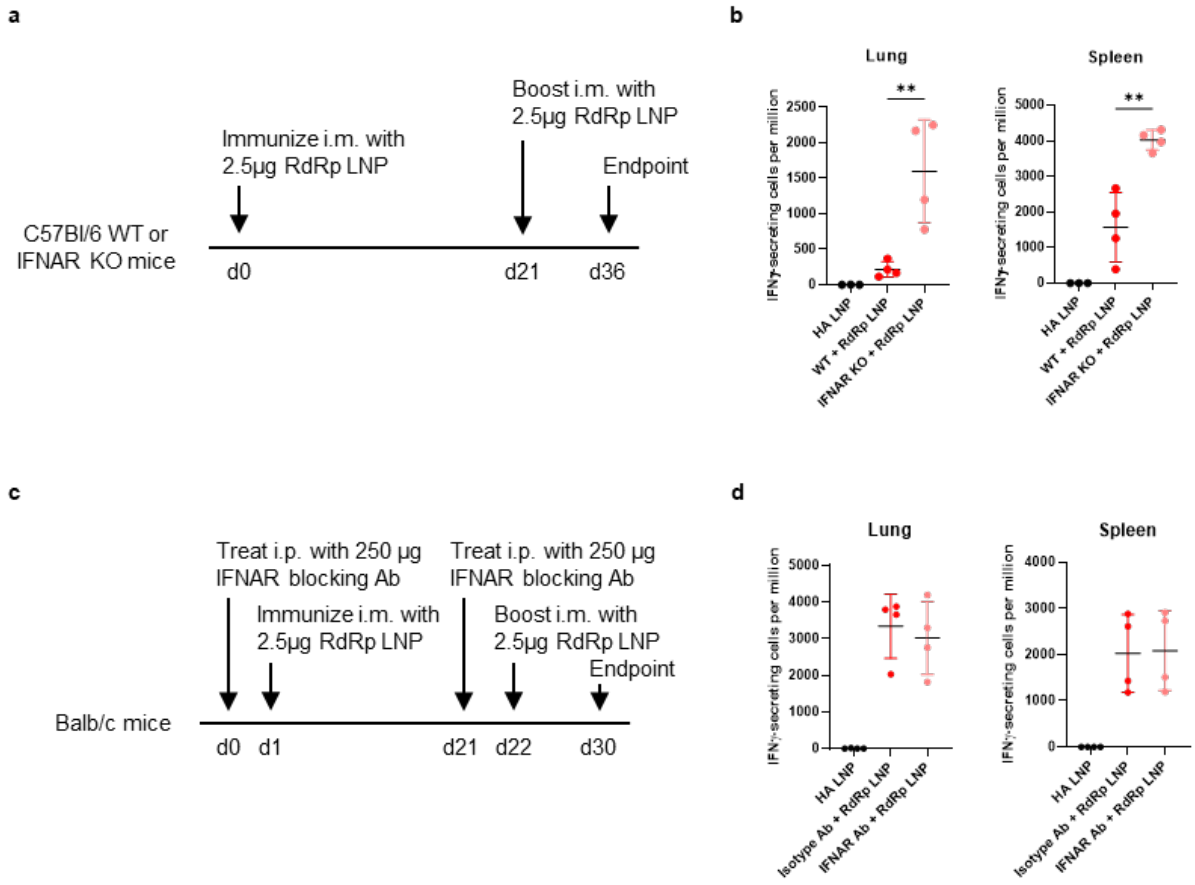

Figure 3-6: IFNAR signaling negatively impacts an RdRp mRNA-LNP optimized for T cell responses

(a) Immunization scheme for RdRp LNPs in C57Bl/6 mice used in (b)

(b) ELISpot results from lung and spleen cells stimulated with overlapping peptides from the RdRp

(c) Immunization scheme for RdRp LNPs in Balb/c mice used in (d)

(d) ELISpot results from lung and spleen cells stimulated with overlapping peptides from the RdRp

Statistical analysis: One way ANOVA with Tukey's multiple comparisons test. Only differences between WT or isotype-treated and IFNAR KO or IFNAR-treated groups are shown. All RdRp-immunized groups were significantly different from the HA LNP control group, except for WT

C57Bl/6 mice in the lung. *p<0.05, **p<0.01, ****p<0.0001 Mean and standard deviation are displayed. N=3 or 4 mice per group.

Figure 3-7

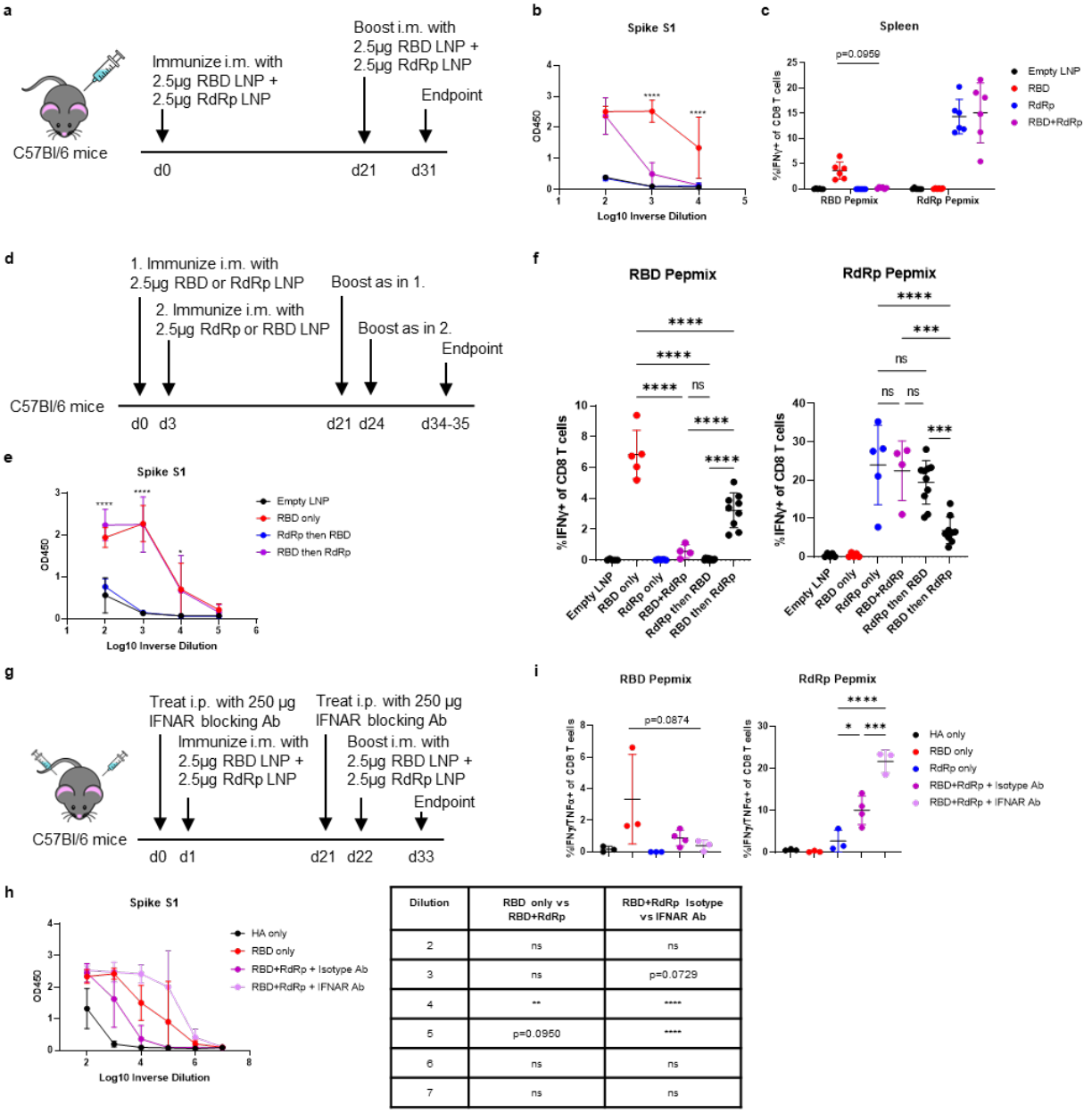

Dilution	RBD only vs RBD+RdRp	RBD+RdRp Isotype vs IFNAR Ab
2	ns	ns
3	ns	p=0.0729
4	**	****
5	p=0.0950	****
6	ns	ns
7	ns	ns

Figure 3-7: Altered immunogenicity of mRNA-LNPs administered together close in time

(a) Immunization scheme for coimmunization at the same site used in (b) and (c)

(b) ELISA results against Spike S1 protein

(c) Intracellular cytokine stimulation results from splenocytes stimulated with overlapping peptides from RBD or RdRp

(d) Immunization scheme for immunization separated by 3 days used in (e) and (f)

(e) ELISA results against Spike S1 protein

(f) Intracellular cytokine stimulation results from splenocytes stimulated with overlapping peptides from RBD or RdRp

(g) Immunization scheme for simultaneous immunization at different sites used in (h) and (i)

(h) ELISA results against Spike S1 protein

(i) Intracellular cytokine stimulation results from splenocytes stimulated with overlapping peptides from RBD or RdRp

Statistical analysis: One-way ANOVA (f, i) or two-way ANOVA (b, c, e, h) with Tukey's multiple comparisons test. Differences between RBD and RBD+RdRp (b), single antigen and coimmunization (c), RBD only and RdRp then RBD (e), or single and dual antigen (f, i) are shown. For (c), no groups stimulated with RBD pepmix was not significantly different than empty LNP and RBD immunized group was not significantly different than empty LNP with RdRp stimulation. For (f) RBD pepmix stimulations, RdRp only, RBD+RdRp, and RdRp then RBD groups were not significantly different than empty LNP. For (f) RdRp pepmix stimulations, RBD only and RBD then RdRp groups were not significantly different than empty LNP. For (i) RBD pepmix stimulation, no groups were significantly different than HA only group. For (i) RdRp pepmix stimulation, RBD only and RdRp only groups were not significantly different from HA only. *$p<0.05$, **$p<0.01$, ***$p<0.001$, ****$p<0.0001$ Mean and standard deviation are displayed. N=6 (a-c), 4-10 (d-f), or 3-4 (g-i) mice per group

Figure 3-8

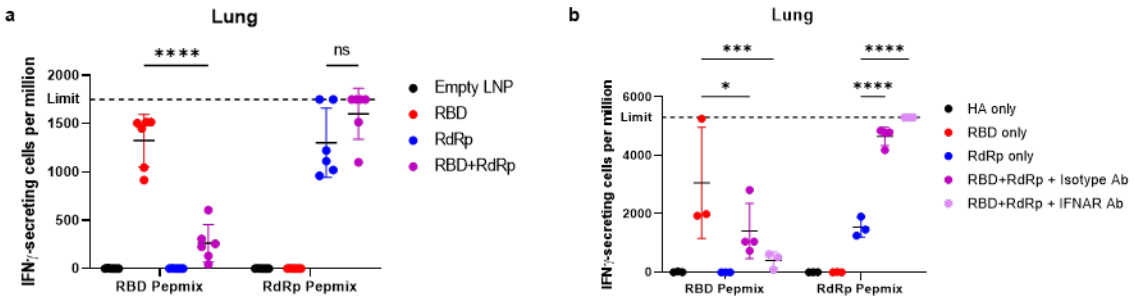

Figure 3-8: T cell responses in the lung after coimmunization

(a and b) ELISpot results from lung cells from mice immunized in Figure 6a (a) or Figure 6g (b) stimulated with overlapping peptides from RBD or RdRp

Statistical analysis: Two way ANOVA with Tukey's multiple comparisons test. Differences between single antigen and coimmunization groups are shown. For (a) RBD pepmix stimulation, RdRp and RBD+RdRp groups are not significantly different compared to empty LNP group. For (a) RdRp pepmix stimulation, RBD group is not significantly different than empty LNP group. For (b) RBD pepmix stimulation, all groups that contain RdRp are not significantly different than HA only. For (b) RdRp pepmix stimulation, RBD only and RdRp only groups are not significantly different than HA only group. ns=not significant, *p<0.05, ***p<0.001, ****p<0.0001 Limit=upper limit of detection Mean and standard deviation are displayed. N=6 (a) or 3-4 (b) mice per group

Materials and Methods

Mice and immunizations

All mouse experiments were conducted with the approval of the UCLA Institutional Animal Care and Use Committee and the Chancellor's Animal Research Committee. C57Bl/6J and Balb/cJ mice were purchased from the Jackson Laboratory (Bar Harbor, ME #000664 and #000651). IFN Alpha R-/- 129/Sv (IFNAR KO) mice (B&K Universal Ltd.) were a gift from Dr. Genhong Cheng (UCLA). IFNAR KO mice were back-crossed to the C57Bl/6 genetic background and maintained by the UCLA Division of Laboratory Animal Management.

For intramuscular injections, mice were restrained with a tailvein restrainer (Braintree Scientific, Braintree, MA #TV-RED 150-STD), cleaned with isopropanol wipes, and injected in the hindleg with 50μL with insulin syringes (Becton, Dickinson, and Company (BD), Franklin Lakes, NJ #329461). Intraperitoneal injections with IFNAR blocking antibody (clone MAR1-5A3), isotype-matched antibody (clone MOPC-21), or Thy1.2 antibody (clone 30H12) (BioXCell, Lebanon, NH #BE0241, #BE0083, and #BE0066, respectively) were performed with 200μL volumes in PBS.

mRNA-LNP

mRNA sequences were based on protein sequences from UniProtKB accession number P03454.1 (WSN HA) and GenBank accession number MN908947.3 (SARS-CoV-2 RBD and RdRp) and modified as described in the text. Sequences were optimized to minimize uridine content with Geneious software (Biomatters, Inc., San Diego, CA) and synthesized with ψ and a 5' CleanCap by TriLink Biotechnologies (San Diego, CA). Transcribed mRNA were encapsulated into LNP using a self-assembly process as previously described[69]; the ionizable cationic lipid and LNP composition are described in the patent application WO 2017/004143.

In vitro antigen expression

HEK293T cells were cultured in Dulbecco's Modified Eagle's Medium (DMEM) (Corning, Corning, NY #10017CV) supplemented with 10% fetal bovine serum (FBS) (Corning #35010CV) and 1X Penicillin/Streptomycin (Corning #30002CI) (complete DMEM) at 37°C and 5% CO_2. 150,000 293T cells were seeded overnight in 0.5mL culture medium in a 24-well plate (VWR, Radnor, PA #10062-896). The next day, culture medium was changed to culture medium containing the indicated amounts of LNP and recombinant human interferon alpha 2a (PBL Assay Science, Piscataway, NJ #11100-1). 24 hours post transfection, cells were lysed in RIPA buffer containing 1mM phenylmethylsulfonyl fluoride (PMSF) for 30 minutes at 4°C. 4X Laemmli buffer (Bio-Rad, Hercules, CA #1610747) with 10% beta-mercaptoethanol was added to lysates and samples were boiled at 95°C for 15 minutes. Lysates were run on a homemade 10% SDS-PAGE gel alongside a 10-250kDa molecular weight ladder (Thermo Fisher Scientific, Waltham, MA #26619). After proteins were transferred to a polyvinylidene difluoride membrane with semi-dry transfer (Bio-Rad #1704272), the membrane was blocked with 10% milk in phosphate buffered saline with 0.1% Tween-20 (PBS-T) for one hour at room temperature. The membrane was cut and probed with primary antibodies at a 1:1000 dilution in 2% milk in PBS-T overnight at 4°C. The next day, the membrane was washed thrice with PBS-T for 10 minutes, incubated with secondary antibody at a 1:10000 dilution for 2 hours at room temperature, and washed again thrice with PBS-T for 10 minutes. Chemiluminescent signal was detected with SuperSignal West Pico PLUS Chemiluminescent Substrate (Thermo Fisher Scientific #34580) using a Chemidoc XRS+ System (Bio-Rad #1708265).

Primary antibodies were used to detect the following proteins: Influenza A H1N1 HA (Genetex, Irvine, CA #GTX127357), SARS-CoV-2 Spike (Sino Biological, Wayne, PA #40591-T62), SARS-CoV-2 RdRp (Genetex #GTX135467), human IFIT1 (Cell Signaling Technology, Danvers, MA

#14769), and GAPDH (Thermo Fisher Scientific #MA5-15738). Horseradish peroxidase (HRP)-conjugated secondary antibodies were used to detect mouse and rabbit primary antibodies (Thermo Fisher Scientific, #62-6520 and #31460, respectively).

RNA expression by RT-PCR

Mice were anesthetized with 5% isoflurane in oxygen and bled retro-orbitally with heparin coated capillary tubes (Fisher Scientific, Waltham, MA #22-260950). RNA was isolated using the RNeasy mini kit (Qiagen, Hilden, Germany #74106) according to the manufacturer's instructions. Equal amounts of RNA from each mouse were reverse transcribed to complementary DNA (cDNA) with the High-Capacity cDNA Reverse Transcription Kit (Applied Biosystems, Waltham, MA #4368814). cDNA was diluted to 10ng input RNA per µL and 1uL was used for RT-PCR using the iTaq Universal SYBR Green Supermix (Bio-Rad #1725121) in a 10uL reaction volume on a CFX Connect Real-Time PCR Detection System (Bio-Rad #1855201). IFIT1 signal was detected with primers 5'-TGCTTTGCGAAGGCTCTGAAA-3' and 5'-TTCTGGATTTAACCGGACAGC-3' and actin signal was detected with primers 5'-GTATCCTGACCCTGAAGTACC-3' and 5'-TGAAGGTCTCAAACATGATCT-3'. IFIT1 to actin ratio was calculated with 2^ΔCt.

Verification of IFNAR blockade by flow cytometry

PBMCs were isolated by retro-orbital bleeding with heparin coated capillary tubes into EDTA-coated tubes (Sarstedt, Nümbrecht, Germany #41.1504.105). Red blood cells were removed by lysing twice with ACK lysing buffer (Thermo Fisher Scientific #A1049201) and PBMCs were resuspended in FACS buffer (PBS containing 2% FBS and 0.05% sodium azide). All wash steps were followed by centrifugation at 500g for 5 minutes to pellet cells. Cells were resuspended in 50µL DPBS containing a 1:25 dilution of Fc block (anti-CD16/CD32 clone 93, Thermo Fisher Scientific #14-0161-86) and incubated at 4°C for 10 minutes. 50µL of cell surface antibodies were

added and cells were further incubated for 30-60 minutes at 4°C. Cells were stained with the following antibodies at the indicated final dilutions: 1:100 IFNAR1-PE clone MAR1-5A3 (Leinco Technologies, Inc., St. Louis, MO #I-1188) and 1:200 CD45-APC-eFluor780 clone 30-F11 (Thermo Fisher Scientific #47-0451-82). Cells were washed twice with FACS buffer and analyzed on an LSR-II flow cytometer (BD). Flow cytometry data was analyzed using FlowJo (BD).

Generation of inactivated influenza virus

Inactivated WSN virus was generated by first seeding 10 million Madin-Darby canine kidney (MDCK) cells in complete DMEM in a 15cm dish overnight. Cells were washed with PBS and infected with WSN virus at a multiplicity of infection of 0.1-0.2 in serum-free DMEM. Cells were incubated at 37°C for 1 hour, with rocking every 15 minutes, then complete DMEM containing 20% FBS was added to a final FBS concentration of 10%. 2 days post infection, when most cells exhibited cytopathic effect (CPE), the supernatant was collected and clarified at 2000g for 10 minutes. The clarified supernatant was loaded into sterile ultracentrifuge tubes (Beckman-Coulter, Indianapolis, IN #C14292) and a 25% sucrose cushion in PBS was loaded underneath. Virus was pelleted at 80,000g for 1 hour at 4°C. The remaining supernatant was removed by aspiration and the pellet was incubated in PBS containing 100mM sodium phosphate (Fisher Scientific #S374-500) for 1 hour at 4°C. The pellet was resuspended and beta-propiolactone (BPL) (Alfa Aesar, Haverhill, MA #AAB2319703) was added to a final concentration of 0.1% (v/v). This solution was inverted at room temperature overnight to inactivate virus. BPL was removed by dialysis against DPBS at 4°C overnight using 15kDa molecular weight cut-off TUBE-O-DIALYZER (G-Biosciences, St. Louis, MO #786618). Dialyzed preparations were collected, separated into single-use aliquots, and stored at -80°C. Viral protein concentration was determined by standard Bradford assay with bovine serum albumin (BSA) as standards (Fisher Scientific #BP9703100). Inactivation was confirmed by comparing samples with and without BPL treatment in a tissue

culture infectious dose 50 (TCID50) assay, with no CPE observed in MDCK cells after incubation with BPL-treated virus.

Hemagglutinin Inhibition Assay (HAI)

HAI was performed according to a previously published protocol[70]. WSN virus was produced as described above and supernatants were aliquoted and stored at -80°C. Briefly, 4 hemagglutinin units (HAU) of virus were incubated with serially diluted immune serum inactivated with receptor destroying enzyme (RDE, Hardy Diagnostics, Santa Maria, CA #370013) in a V-bottom 96-well plate for 30 minutes at room temperature in a total volume of 50µL. Then 50µL of diluted turkey red blood cells (RBCs, Lampire Biological Laboratories, Pipersville, PA # 7249408) were added the plate was further incubated for 30 minutes at room temperature. Inhibition of hemagglutination was measured by RBCs forming a dot at the bottom of the well and HAI titer was the last dilution before inhibition stopped appearing.

SARS-CoV-2 plaque reduction neutralization test (PRNT)

Vero E6 cells were obtained from ATCC (Manassas, VA #CRL-158). Cells were cultured in EMEM growth media containing 10% fetal bovine serum (FBS) and penicillin (100 units/mL). SARS-Related Coronavirus 2 (SARS-CoV-2), Isolate USA-WA1/2020, was obtained from BEI Resources of National Institute of Allergy and Infectious Diseases (NIAID). All the studies involving live virus were conducted in UCLA BSL3 high-containment facility. SARS-CoV-2 was passaged once in Vero E6 cells and viral stocks were aliquoted and stored at -80°C. Virus titer was measured in Vero E6 cells by established plaque assay or TCID50 assay[71]. Heat inactivated (30 mins at 56°C) serum samples were two-fold serially diluted in a 96-well plate format and mixed with 100 pfu of SARS-CoV-2. The serum-virus mix were incubated for 1 hour at room temperature and were subsequently inoculated on to naïve Vero E6 cells. The cells were incubated at 37°C,

5%CO2 for additional 4 days. The cells were examined for viral cytopathic effect (CPE) and the highest serum dilution at which complete virus inhibition was considered as neutralization titer. The PRNT titer for all the serum samples were compiled and subjected to statistical analysis.

Enzyme-linked immunospot (ELISpot) Assay

Cells were obtained from spleens by passage through a 70µm cell strainer (Fisher Scientific #22-363-548) using a 3mL syringe plunger (Fisher Scientific #14-823-435). Red blood cells were lysed with ACK lysing buffer and cells were resuspended in Roswell Park Memorial Institute (RPMI) 1640 medium (Corning #10-040-CV) containing 10% FBS and 1X Penicillin/Streptomycin (complete RPMI). Cells from lungs were obtained by mincing the tissue with surgical scissors and digesting it with 2-5mg/mL collagenase A (Sigma-Aldrich #10103586001) in complete RPMI at 37°C for 60-80 minutes with mixing every 10 minutes. The digested tissue was processed in a manner identical to spleen samples to obtain lung cells.

ELISpot was performed using a mouse IFNγ/TNFα or mouse IFNγ ELISpot kit (Cellular Technology Limited (CTL), Shaker Heights, OH #mIFNgTNFa-1M/10 and #mIFNg-1M, respectively) according to the manufacturer's instructions. Negative control wells contained unstimulated cells and positive control wells were stimulated with a cocktail of phorbol 12-myristate 13-acetate (PMA) and ionomycin (Thermo Fisher Scientific #00-4970-03). Experimental wells were stimulated with 1µg/mL of the indicated reagents in complete RPMI. Cells were incubated at 37°C for 20-22 hours before plates were developed. Plates were scanned and spot counts were analyzed by CTL. The number of spots in negative control wells was subtracted from experimental wells to determine the number of antigen-specific spot-forming cells.

Cells were stimulated with overlapping peptide libraries for influenza A/PR8/1934 HA, SARS-CoV-2 Spike RBD, and SARS-CoV-2 RdRp (JPT Peptide Technologies GmbH, Berlin, Germany #PM-

INFA-HAPR, #PM-WCPV-S-RBD-2, and #PM-WCPV-NSP12-2, respectively). Individual peptides HA-1 (IYSTVASSL) and HA-2 (SFERFEIFPKE) were synthesized by Thermo Fisher Scientific at over 85% purity.

In vitro depletion of CD4 and CD8 T cells

Splenocytes from biological replicates were pooled and depleted of CD4 or CD8 T cells using the EasySep Mouse CD4 Positive Selection Kit II or the EasySep™ Mouse CD8a Positive Selection Kit II (Stemcell Technologies, Vancouver, BC, Canada #18952 and #18953, respectively) according to the manufacturer's directions.

Intracellular cytokine stimulation (ICS)

Splenocytes were prepared as described above. Stimulation was performed in 96-well U bottom plates in the presence of brefeldin A (Biolegend, San Diego, CA #420601) for 6 hours at 37°C. Cells were then stored at 4°C for up to 16 hours until staining. Cells were stained with anti-TCRbeta PerCP-Cy5.5 clone H57-597, anti-CD4 PE-Cy7 clone RM4-5, and anti-CD8 PE clone 53-6.7 (Biolegend #109228, #100528, and #100708) at a 1:100 dilution for 15 minutes on ice. Cells were washed with FACS buffer, then fixed and permeabilized with Cytofix/Cytoperm buffer (BD #554714) for 20 minutes on ice. Cells were washed with permeabilization buffer, then stained with anti-IFNγ APC clone XMG1.2 and anti-TNFα FITC clone MP6-XT22 (Biolegend #505810 and #506304) at a 1:50 dilution in permeabilization buffer for 30 minutes on ice. Cells were finally washed with permeabilization buffer and resuspended in FACS buffer before analysis.

Enzyme-linked immunosorbent assay (ELISA)

ELISA plates (Corning #07-200-721) were prepared by coating each well with 50µL recombinant WSN HA, CA09 HA, or SARS-CoV-2 Spike S1 (Sino Biological #11692-V08H, #11085-V08H, and

#40591-V08H, respectively) at a 1µg/mL concentration in carbonate-bicarbonate buffer (Sigma-Aldrich, Inc., St. Louis, MO #C3041-50CAP) overnight at 4°C. Coated 96-well plates were blocked with PBS containing 1% BSA (%w/v) (Fisher Scientific #BP9703100), and 0.05% Tween-20 (%v/v) (Fisher Scientific #BP337-500) at room temperature for 1 hour or overnight at 4°C. All serum samples and secondary antibodies were diluted in assay buffer consisting of PBS with 0.1% BSA and 0.025% Tween-20. Coated plates were washed with DPBS containing 0.1% Tween-20 (%v/v) (PBS-T) twice for 3 minutes. Plates were then washed twice quickly with PBS-T before the addition of 50µL serially diluted immune serum. 6-8 wells per plate were incubated with assay buffer containing no primary antibody as a background control. Plates were incubated for 1-2 hours at room temperature on an orbital shaker. Plates were washed with PBS-T twice for 3 minutes, then twice quickly before the addition of 50µL 1:4000 goat anti-mouse HRP secondary antibody (Thermo Fisher Scientific #62-6520). Secondary antibody was incubated for 1 hour at room temperature with shaking. Plates were then washed once with PBS-T for 3 minutes, then four times quickly. After one final wash with PBS (no Tween-20), 100µL 1-Step Ultra TMB ELISA Substrate (Thermo Fisher Scientific #34028) was added to each well. Plates were covered to protect them from light and incubated at room temperature for 30 minutes with shaking. Signal development was stopped by the addition of 100µL 1M sulfuric acid (Sigma-Aldrich #1603131000) and the optical density at 450nm (OD450) was measured with a ClarioStar plate reader (BMG Labtech, Cary, NC).

References

1. Hou, X., Zaks, T., Langer, R. & Dong, Y. Lipid nanoparticles for mRNA delivery. *Nat Rev Mater* **6**, 1078–1094 (2021).

2. McNab, F., Mayer-Barber, K., Sher, A., Wack, A. & O'Garra, A. Type I interferons in infectious disease. *Nat Rev Immunol* **15**, 87–103 (2015).

3. Gessani, S., Conti, L., Del Cornò, M. & Belardelli, F. Type I Interferons as Regulators of Human Antigen Presenting Cell Functions. *Toxins* **6**, 1696–1723 (2014).

4. Crouse, J., Kalinke, U. & Oxenius, A. Regulation of antiviral T cell responses by type I interferons. *Nat Rev Immunol* **15**, 231–242 (2015).

5. Ye, L. *et al.* Type I and Type III Interferons Differ in Their Adjuvant Activities for Influenza Vaccines. *J Virol* **93**, e01262-19 (2019).

6. Zhong, C. *et al.* Type I Interferon Promotes Humoral Immunity in Viral Vector Vaccination. *J Virol* **95**, e00925-21 (2021).

7. Proietti, E. *et al.* Type I IFN as a Natural Adjuvant for a Protective Immune Response: Lessons from the Influenza Vaccine Model. *J Immunol* **169**, 375–383 (2002).

8. Cull, V. S., Broomfield, S., Bartlett, E. J., Brekalo, N. L. & James, C. M. Coimmunisation with type I IFN genes enhances protective immunity against cytomegalovirus and myocarditis in gB DNA-vaccinated mice. *Gene Ther* **9**, 1369–1378 (2002).

9. Brar, G. *et al.* Deletion of immune evasion genes provides an effective vaccine design for tumor-associated herpesviruses. *npj Vaccines* **5**, 102 (2020).

10. Sun, S., Zhang, X., Tough, D. F. & Sprent, J. Type I Interferon-mediated Stimulation of T Cells by CpG DNA. *Journal of Experimental Medicine* **188**, 2335–2342 (1998).

11. Dondi, E., Rogge, L., Lutfalla, G., Uzé, G. & Pellegrini, S. Down-Modulation of Responses to Type I IFN Upon T Cell Activation. *J Immunol* **170**, 749–756 (2003).

12. Palacio, N. *et al.* Early type I IFN blockade improves the efficacy of viral vaccines. *Journal of Experimental Medicine* **217**, e20191220 (2020).

13. Kawasaki, T. & Kawai, T. Toll-Like Receptor Signaling Pathways. *Front. Immunol.* **5**, (2014).

14. Zhang, Z. *et al.* Structural Analysis Reveals that Toll-like Receptor 7 Is a Dual Receptor for Guanosine and Single-Stranded RNA. *Immunity* **45**, 737–748 (2016).

15. Alexopoulou, L., Holt, A. C., Medzhitov, R. & Flavell, R. A. Recognition of double-stranded RNA and activation of NF-κB by Toll-like receptor 3. *Nature* **413**, 732–738 (2001).

16. Karikó, K., Ni, H., Capodici, J., Lamphier, M. & Weissman, D. mRNA Is an Endogenous Ligand for Toll-like Receptor 3. *Journal of Biological Chemistry* **279**, 12542–12550 (2004).

17. Karikó, K., Buckstein, M., Ni, H. & Weissman, D. Suppression of RNA Recognition by Toll-like Receptors: The Impact of Nucleoside Modification and the Evolutionary Origin of RNA. *Immunity* **23**, 165–175 (2005).

18. Barral, P. M. *et al.* Functions of the cytoplasmic RNA sensors RIG-I and MDA-5: Key regulators of innate immunity. *Pharmacology & Therapeutics* **124**, 219–234 (2009).

19. Mu, X., Greenwald, E., Ahmad, S. & Hur, S. An origin of the immunogenicity of in vitro transcribed RNA. *Nucleic Acids Research* **46**, 5239–5249 (2018).

20. Hornung, V. *et al.* 5'-Triphosphate RNA Is the Ligand for RIG-I. *Science* **314**, 994–997 (2006).

21. Pichlmair, A. *et al.* RIG-I-Mediated Antiviral Responses to Single-Stranded RNA Bearing 5'-Phosphates. *Science* **314**, 997–1001 (2006).

22. Li, M. M. H., MacDonald, M. R. & Rice, C. M. To translate, or not to translate: viral and host mRNA regulation by interferon-stimulated genes. *Trends in Cell Biology* **25**, 320–329 (2015).

23. Lemaire, P. A., Anderson, E., Lary, J. & Cole, J. L. Mechanism of PKR Activation by dsRNA. *Journal of Molecular Biology* **381**, 351–360 (2008).

24. Kerr, I. M., Brown, R. E. & Hovanessian, A. G. Nature of inhibitor of cell-free protein synthesis formed in response to interferon and double-stranded RNA. *Nature* **268**, 540–542 (1977).

25. Anderson, B. R. *et al.* Incorporation of pseudouridine into mRNA enhances translation by diminishing PKR activation. *Nucleic Acids Research* **38**, 5884–5892 (2010).

26. Anderson, B. R. *et al.* Nucleoside modifications in RNA limit activation of 2'-5'-oligoadenylate synthetase and increase resistance to cleavage by RNase L. *Nucleic Acids Research* **39**, 9329–9338 (2011).

27. Foster, J. B. *et al.* Purification of mRNA Encoding Chimeric Antigen Receptor Is Critical for Generation of a Robust T-Cell Response. *Human Gene Therapy* **30**, 168–178 (2019).

28. Nelson, J. *et al.* Impact of mRNA chemistry and manufacturing process on innate immune activation. *Sci. Adv.* **6**, eaaz6893 (2020).

29. Baiersdörfer, M. *et al.* A Facile Method for the Removal of dsRNA Contaminant from In Vitro-Transcribed mRNA. *Molecular Therapy - Nucleic Acids* **15**, 26–35 (2019).

30. Karikó, K., Muramatsu, H., Ludwig, J. & Weissman, D. Generating the optimal mRNA for therapy: HPLC purification eliminates immune activation and improves translation of nucleoside-modified, protein-encoding mRNA. *Nucleic Acids Research* **39**, e142–e142 (2011).

31. Arunachalam, P. S. *et al.* Systems vaccinology of the BNT162b2 mRNA vaccine in humans. *Nature* **596**, 410–416 (2021).

32. Li, C. *et al.* Mechanisms of innate and adaptive immunity to the Pfizer-BioNTech BNT162b2 vaccine. *Nat Immunol* **23**, 543–555 (2022).

33. Kobiyama, K. *et al. Optimization of an LNP-mRNA vaccine candidate targeting SARS-CoV-2 receptor-binding domain*. http://biorxiv.org/lookup/doi/10.1101/2021.03.04.433852 (2021) doi:10.1101/2021.03.04.433852.

34. Byrd-Leotis, L., Galloway, S. E., Agbogu, E. & Steinhauer, D. A. Influenza Hemagglutinin (HA) Stem Region Mutations That Stabilize or Destabilize the Structure of Multiple HA Subtypes. *J Virol* **89**, 4504–4516 (2015).

35. Fonseca, J. A. *et al.* Inclusion of the murine IgGκ signal peptide increases the cellular immunogenicity of a simian adenoviral vectored Plasmodium vivax multistage vaccine. *Vaccine* **36**, 2799–2808 (2018).

36. Güthe, S. *et al.* Very Fast Folding and Association of a Trimerization Domain from Bacteriophage T4 Fibritin. *Journal of Molecular Biology* **337**, 905–915 (2004).

37. Kreiter, S. *et al.* Increased Antigen Presentation Efficiency by Coupling Antigens to MHC Class I Trafficking Signals. *J Immunol* **180**, 309–318 (2008).

38. Sahin, U. *et al.* Personalized RNA mutanome vaccines mobilize poly-specific therapeutic immunity against cancer. *Nature* **547**, 222–226 (2017).

39. Hobson, D., Curry, R. L., Beare, A. S. & Ward-Gardner, A. The role of serum haemagglutination-inhibiting antibody in protection against challenge infection with influenza A2 and B viruses. *Epidemiol. Infect.* **70**, 767–777 (1972).

40. Sant, A. J., DiPiazza, A. T., Nayak, J. L., Rattan, A. & Richards, K. A. CD4 T cells in protection from influenza virus: Viral antigen specificity and functional potential. *Immunol Rev* **284**, 91–105 (2018).

41. Nesterenko, P. A. *et al.* HLA-A∗02:01 restricted T cell receptors against the highly conserved SARS-CoV-2 polymerase cross-react with human coronaviruses. *Cell Reports* **37**, 110167 (2021).

42. Swadling, L. *et al.* Pre-existing polymerase-specific T cells expand in abortive seronegative SARS-CoV-2. *Nature* **601**, 110–117 (2022).

43. Karikó, K. *et al.* Incorporation of Pseudouridine Into mRNA Yields Superior Nonimmunogenic Vector With Increased Translational Capacity and Biological Stability. *Molecular Therapy* **16**, 1833–1840 (2008).

44. Vogel, A. B. *et al.* BNT162b vaccines protect rhesus macaques from SARS-CoV-2. *Nature* **592**, 283–289 (2021).

45. Corbett, K. S. *et al.* SARS-CoV-2 mRNA vaccine design enabled by prototype pathogen preparedness. *Nature* **586**, 567–571 (2020).

46. Polack, F. P. *et al.* Safety and Efficacy of the BNT162b2 mRNA Covid-19 Vaccine. *N Engl J Med* **383**, 2603–2615 (2020).

47. Baden, L. R. *et al.* Efficacy and Safety of the mRNA-1273 SARS-CoV-2 Vaccine. *N Engl J Med* **384**, 403–416 (2021).

48. Tahtinen, S. *et al.* IL-1 and IL-1ra are key regulators of the inflammatory response to RNA vaccines. *Nat Immunol* (2022) doi:10.1038/s41590-022-01160-y.

49. Chan, C. Y. Y. *et al.* Early molecular correlates of adverse events following yellow fever vaccination. *JCI Insight* **2**, e96031 (2017).

50. Quinn, K. M. *et al.* Antigen expression determines adenoviral vaccine potency independent of IFN and STING signaling. *J. Clin. Invest.* **125**, 1129–1146 (2015).

51. Pardi, N. *et al.* Nucleoside-modified mRNA vaccines induce potent T follicular helper and germinal center B cell responses. *Journal of Experimental Medicine* **215**, 1571–1588 (2018).

52. Pepini, T. *et al.* Induction of an IFN-Mediated Antiviral Response by a Self-Amplifying RNA Vaccine: Implications for Vaccine Design. *J.I.* **198**, 4012–4024 (2017).

53. Batista, F. D., Iber, D. & Neuberger, M. S. B cells acquire antigen from target cells after synapse formation. *Nature* **411**, 489–494 (2001).

54. Walsh, E. E. *et al.* Safety and Immunogenicity of Two RNA-Based Covid-19 Vaccine Candidates. *N Engl J Med* **383**, 2439–2450 (2020).

55. Saco, T. V., Strauss, A. T. & Ledford, D. K. Hepatitis B vaccine nonresponders. *Annals of Allergy, Asthma & Immunology* **121**, 320–327 (2018).

56. Pollard, C. *et al.* Type I IFN Counteracts the Induction of Antigen-Specific Immune Responses by Lipid-Based Delivery of mRNA Vaccines. *Molecular Therapy* **21**, 251–259 (2013).

57. De Beuckelaer, A. *et al.* Type I Interferons Interfere with the Capacity of mRNA Lipoplex Vaccines to Elicit Cytolytic T Cell Responses. *Molecular Therapy* **24**, 2012–2020 (2016).

58. Van Hoecke, L. *et al.* The Opposing Effect of Type I IFN on the T Cell Response by Non-modified mRNA-Lipoplex Vaccines Is Determined by the Route of Administration. *Molecular Therapy - Nucleic Acids* **22**, 373–381 (2020).

59. Tse, S.-W. *et al.* mRNA-encoded, constitutively active STINGV155M is a potent genetic adjuvant of antigen-specific CD8+ T cell response. *Molecular Therapy* **29**, 2227–2238 (2021).

60. Simmons, D. P. *et al.* Type I IFN Drives a Distinctive Dendritic Cell Maturation Phenotype That Allows Continued Class II MHC Synthesis and Antigen Processing. *J.I.* **188**, 3116–3126 (2012).

61. Kolumam, G. A., Thomas, S., Thompson, L. J., Sprent, J. & Murali-Krishna, K. Type I interferons act directly on CD8 T cells to allow clonal expansion and memory formation in response to viral infection. *Journal of Experimental Medicine* **202**, 637–650 (2005).

62. Cousens, L. P. *et al.* Two Roads Diverged: Interferon α/β– and Interleukin 12–mediated Pathways in Promoting T Cell Interferon γ Responses during Viral Infection. *Journal of Experimental Medicine* **189**, 1315–1328 (1999).

63. Kranz, L. M. *et al.* Systemic RNA delivery to dendritic cells exploits antiviral defence for cancer immunotherapy. *Nature* **534**, 396–401 (2016).

64. Corse, E., Gottschalk, R. A. & Allison, J. P. Strength of TCR–Peptide/MHC Interactions and In Vivo T Cell Responses. *J.I.* **186**, 5039–5045 (2011).

65. Wherry, E. J., Puorro, K. A., Porgador, A. & Eisenlohr, L. C. The induction of virus-specific CTL as a function of increasing epitope expression: responses rise steadily until excessively high levels of epitope are attained. *J Immunol* **163**, 3735–3745 (1999).

66. Awasthi, S. *et al.* Nucleoside-modified mRNA encoding HSV-2 glycoproteins C, D, and E prevents clinical and subclinical genital herpes. *Sci Immunol* **4**, (2019).

67. Chivukula, S. *et al.* Development of multivalent mRNA vaccine candidates for seasonal or pandemic influenza. *npj Vaccines* **6**, 153 (2021).

68. A Study of an Epstein-Barr Virus (EBV) Candidate Vaccine, mRNA-1189, in 18- to 30-Year-Old Healthy Adults. *ClinicalTrials.gov* https://clinicaltrials.gov/ct2/show/NCT05164094.

69. Maier, M. A. *et al.* Biodegradable Lipids Enabling Rapidly Eliminated Lipid Nanoparticles for Systemic Delivery of RNAi Therapeutics. *Molecular Therapy* **21**, 1570–1578 (2013).

70. Wu, Y. *et al.* Hemagglutination Inhibition (HI) Assay of Influenza Viruses with Monoclonal Antibodies. *BIO-PROTOCOL* **6**, (2016).

71. Sharma, A. *et al.* Human iPSC-Derived Cardiomyocytes Are Susceptible to SARS-CoV-2 Infection. *Cell Rep Med* **1**, 100052 (2020).

CHAPTER 4:

Targeting the conserved RNA-dependent RNA polymerase of SARS-CoV-2 for prophylactic vaccination

Abstract

The extension of the SARS-CoV-2 pandemic has been characterized by the continuous development of novel viral variants capable of escaping antibody immunity. One potential method to protect against these variants is the development of T cells that target a highly conserved viral antigen. We previously identified the RNA-dependent RNA polymerase (RdRp) as one such conserved antigen. Here, we generate an mRNA-LNP vaccine candidate for the development of RdRp-specific T cells. This mRNA-LNP is immunogenic and well tolerated in mouse models. However, no protection was demonstrated by these T cells in a SARS-CoV-2 infection model. Further studies are required to determine whether any protection can be conferred by RdRp-specific T cells.

Introduction

The continual evolution of SARS-CoV-2 variants of concern (VOCs) has allowed the virus to persist as a public health emergency[1,2]. Many of these variants have consistently displaced previously dominant strains in a geographic area[3–5]. This displacement can partially be explained by the evasion of neutralizing antibodies from both infected and vaccinated individuals, allowing new variants to infect immune individuals[6–10]. The dominance of these variants is especially concerning because the accumulated mutations in the Spike protein allows variants such as Omicron to evade therapeutic monoclonal antibodies, reducing the ability to stop the development of severe disease in susceptible individuals[11–14]. In addition, repeated infection allows for the evolution of additional mutations, renewing the cycle of escape variants and continuing the pandemic[15,16]. Thus, new strategies are needed to develop robust immunity to prevent the spread of novel variants.

Antibody escape variants are characterized by mutations in the viral Spike protein, which mediates entry into host cells and is the target of neutralizing antibodies[17–20]. However, these mutations that evade antibody responses do not necessarily escape T cells, which can cross-react to epitopes in other regions of the Spike protein[21–24]. Thus, T cells represent a potential pathway toward protective immunity in the face of constant viral evolution. Unlike antibodies, which can prevent viral infection, T cells kill infected cells to halt the production of new viral particles. T cells have also been identified as contributors to cross-protective immunity to different influenza strains[25]. Ideally, T cells that target a conserved protein could provide long-term immunity, as opposed to the Spike protein, which is under constant evolutionary pressure from antibodies. One such T cell target is the nucleocapsid (N) protein, which is present at high levels in infected cells and is a major target for T cell responses in infected individuals[26–29]. An adenovirus-based vaccine encoding the N protein can generate N-specific T cells that protect hamsters from lethal infection[30]. When combined with a Spike-encoding adenovirus vector, N-

encoding adenoviruses can also induce T cells that control infection of the brain in a murine model of SARS-CoV-2 neuroinvasion[31]. This combination has also been used in mRNA vaccines and was shown to provide additional protection superior to Spike only immunization against viral replication in animal models[32]. We previously identified another highly conserved viral protein, the viral RNA-dependent RNA polymerase (RdRp), also known as non-structural protein 12 (nsp12)[33]. RdRp is more highly conserved between pandemic and common cold human coronaviruses compared to nucleocapsid and we demonstrated that SARS-CoV-2 naïve individuals possessed SARS-CoV-2 RdRp-specific T cells[33]. These individuals possessed T cell receptors that cross-reacted with epitopes from other human coronaviruses, suggesting that these T cells were developed during a previous infection[33]. RdRp-specific T cells have also been identified in SARS-CoV-2 convalescent patients, suggesting that epitopes are presented as T cell targets during the course of infection[28,29]. Importantly, preexisting RdRp-specific T cells have been implicated in the development of an abortive infection instead of a symptomatic one in a close contact cohort[34], suggesting that they may possess some protective effect, at least in the cases of healthcare workers with personal protective equipment exposed to small amounts of virus in a patient care setting. Thus, the generation of RdRp-specific T cells could be a goal for T cell immunity against multiple future coronavirus variants.

Messenger RNA-containing lipid nanoparticles (mRNA-LNP) have emerged as powerful tools for prophylactic viral vaccines, as demonstrated by the Spike-encoding mRNA-LNP produced by Pfizer and Moderna[35,36]. Uptake of mRNA-LNP allows for translation of the mRNA cargo and direct presentation of antigenic peptides on major histocompatibility complex (MHC) molecules by antigen presenting cells[37]. In contrast to protein-based vaccines, this activity allows mRNA vaccines to efficiently prime CD8 T cells, an attribute that has been exploited for use in cancer immunotherapy[38,39]. In addition to *de novo* antigen synthesis for presentation, mRNA-LNP also provide their own adjuvant activity, potentially by stimulating inflammatory cytokines such as

interleukin-1 (IL-1) and interferons (IFNs)[40–42]. As a result, the commercial Spike mRNA vaccines have been demonstrated to generate long-term B and T cell responses after immunization[43,44]. Thus, mRNA-LNP provide a strong platform for the induction of long-lasting T cell responses toward conserved viral proteins.

Here, we investigate the use of mRNA-LNP encoding the SARS-CoV-2 Spike receptor binding domain (RBD) and RdRp. We demonstrate the immunogenicity of these mRNA-LNP to generate antigen-specific antibody and T cell responses in mice. Finally, we assess the protection afforded by these mRNA vaccines in a mouse model of SARS-CoV-2 infection.

Results

Detection of RBD and RdRp-specific T cells from infected patients

We confirmed that RBD and RdRp-specific T cells could be detected from SARS-CoV-2 infected individuals. We obtained peripheral blood mononuclear cells (PBMCs) from patients one month after SARS-CoV-2 infection or healthy immunized SARS-CoV-2 naïve healthcare workers. We polyclonally expanded CD8 T cells from these PBMCs and stimulated them with overlapping peptide libraries for the RBD or RdRp and assessed T cell responses by interferon gamma (IFNγ) ELISpot (Fig. 4-1). Vaccinated individuals had significantly more RBD-specific T cells compared to infected patients. However, RdRp-specific T cell responses were weak and similar between the two groups, suggesting that infection does not necessarily expand RdRp-specific T cells in this cohort.

Immunogenicity of RBD and RdRp mRNA-LNP

To test a vaccine strategy targeting the conserved RdRp protein, we generated two mRNA constructs for SARS-CoV-2 antigens (Fig. 4-2a). The RBD sequence was generated using amino

acids 319-541 from the Spike protein of the original Wuhan strain. It fused with the murine IgK signal sequence at the N-terminus to improve protein secretion and the foldon trimerization domain of bacteriophage T4 at the C-terminus to improve antibody responses[45,46]. The RdRp sequence was generated using the N-terminal 611 amino acids from the Wuhan strain. It was fused with an N-terminal MHC class I signal peptide and a C-terminal MHC-I trafficking domain (MITD) to enhance presentation to T cells[38,47]. These sequences were generated by *in vitro* transcription with silica membrane purification and encapsulated into LNP. We confirmed antigen expression from these mRNA-LNP by transfection into HEK293T cells (Fig. 4-2b).

To determine whether the RdRp mRNA-LNP was immunogenic, we immunized mice intramuscularly and analyzed T cells after a boosting immunization (Fig. 4-2c). We found that wildtype C57Bl/6 mice develop robust T cell immunity in the lungs and spleen against RdRp, as demonstrated by the production of IFNγ after stimulation with an RdRp overlapping peptide library (Fig. 4-2d). We also immunized mice transgenic for the human HLA-A2.1 molecule, which express a chimera of the extracellular domain of the human HLA-A2.1 molecule and the transmembrane and intracellular domain of the murine H-2D^{d} molecule. This mouse strain has been used to model immune responses to epitopes presented on HLA-A2 and provide a fuller T cell repertoire compared to unmodified HLA-A2.1 due to improved positive selection of murine T cells[48]. We found that HLA-A2.1 transgenic mice developed T cells that responded to two of three previously identified HLA-A2.1 restricted RdRp epitopes (Fig. 4-2e)[33]. We also performed a dose-escalation study to determine whether mice could tolerate large doses of mRNA-LNP and whether T cell responses could be further increased (Fig. 4-2f). We found that mRNA-LNP immunization resulted in transitory weight loss in C57Bl/6 mice with larger doses resulting in more pronounced and prolonged weight loss, especially after the boosting immunization (Fig. 4-2g). Surprisingly, there was no difference in RdRp-specific T cells at the endpoint, with higher doses actually trending toward lower T cell responses in our ELISpot assay, suggesting that the 2.5μg dose is sufficient

for robust T cell responses (Fig. 4-2h). Finally, we immunized mice that express the human angiotensin converting enzyme 2 (hACE2) from the keratin 18 promoter (K18-hACE2), which recapitulates severe COVID-19 infection in a mouse model[49–51]. We immunized these mice with both RBD and RdRp mRNA-LNP, with a two-week space between each immunization (Fig. 4-2i). This spacing eliminates interference between the two mRNA-LNP that occurs during co-immunization (Fig. 3-7). These mice developed IgG antibodies that bound to the Spike S1 protein, and there was no difference between mice immunized with RBD and those immunized with RBD and RdRp (Fig. 4-2j). These mice also developed RBD and RdRp-specific T cells after mRNA vaccination, with no difference between single and double-immunization groups (Fig. 4-2k). Thus, this data demonstrates that the RBD and RdRp-encoding mRNA-LNP are immunogenic in mouse models.

Challenge studies of RBD and RdRp-immunized mice

The K18-hACE2 mouse model allows for SARS-CoV-2 infection in a murine model that would otherwise not be infected. Due to the expression of hACE2 in multiple tissues, intranasal administration of the virus initiates viral replication in the lung, with neuroinvasion of the central nervous system later in the course of infection[50,51]. This model has been used to demonstrate the contribution of nucleocapsid-specific T cells to the protection of distal tissues such as the brain that is not provided by Spike-specific immunity[31]. In order to assay the protection afforded by RBD and RdRp immunization, we immunized K18-hACE2 mice and challenged them with $1x10^4$ plaque forming units (PFU) of plaque-isolated WA1 strain SARS-CoV-2 intranasally 20 days after the last immunization (Fig. 4-3a). We tracked weight loss in these mice and observed that 1/5 RdRp-immunized, 2/5 RBD-immunized, and 2/5-RBD+RdRp-immunized mice had not experienced a loss from the initial weight at the endpoint of 5 days post infection (dpi) (Fig. 4-3b). We harvested the lungs and brains from these mice and quantified viral genome copies in these tissues by RT-

PCR. There was no significant difference between mice immunized with RBD or RdRp and mice immunized with a negative control mRNA-LNP encoding for influenza hemagglutinin (Fig. 4-3c). In each group, we observed 1-2 mice that had much lower viral genome copies than their counterparts. We compared the viral genome data against the final weight data of these mice and observed that mice with lower viral genome copies in either the lung or brain demonstrated the highest relative weight (Fig 4-3d). This was expected, as viral replication would lead to disease evidenced as weight loss. Higher viral genome copies in the brain or lung also correlated with higher genome copies in the other site, but was not as obvious. Overall, this experiment did not demonstrate the RBD or RdRp immunization could provide protection in this model.

Because the first immunization experiment did not demonstrate protection against SARS-CoV-2 infection, we questioned whether higher levels of T cells could confer a more substantial impact. Therefore, we boosted immunized mice with an additional dose of RBD and/or RdRp mRNA-LNP and challenged them 9 days post boost (Fig. 4-3e), near the peak of the recall T cell response[52]. This third immunization also likely boosted neutralizing antibody levels, which are not detected after two immunizations in C57Bl/6 mice, the genetic background of the K18-hACE2 model (Fig. 3-5c). Mice were monitored until they reached a humane endpoint. All mice in the HA and RdRp only groups lost weight and were eventually euthanized, while all mice in the RBD only and RBD+RdRp groups did not exhibit any weight loss (Fig. 4-3f). There was a modest difference in survival between HA and RdRp only groups, with RdRp immunization conferring slightly longer survival than HA immunization (Fig. 4-3g). In order to assess whether RdRp co-immunization conferred any advantage over RBD immunization alone, we euthanized the mice from the RBD and RBD+RdRp groups at 12dpi, a timepoint when residual virus can still be found in the brains of infected nonimmunized mice[51]. We found minimal viral copies in the brain (Fig. 4-3h), suggesting that the infection was largely controlled at this time point in our immunized mice. Thus, it is unclear what advantage the RdRp immunization provided in this experimental model.

Discussion

The persistent emergence of SARS-CoV-2 variants with mutations that evade antibody immunity has resulted in multiple waves of infection. This immune evasion allows for infected and immunized individuals to be infected with new variants, prolonging the global pandemic and providing the opportunity for even more variants to develop. One strategy to combat this immune evasion is the development of T cells that can target a highly conserved viral antigen. Here, we investigated the potential for T cells generated by mRNA vaccination that target the viral RdRp to protect against SARS-CoV-2 infection.

We first confirmed that RdRp-specific T cells could be detected in infected individuals (Fig. 4-1). While we observed a range of responses toward RBD peptides in infected individuals, they were lower than those from individuals immunized with Spike mRNA vaccines. The responses toward RdRp peptides were lower than RBD peptides in both populations, with a significant fraction showing no response. This is consistent with published data showing that while RdRp is one of the viral antigens that contributes to a majority of T cell responses in infected individuals, it contributes a small amount to this majority compared to more dominant Spike and N-targeting responses[28,29]. Surprisingly, we also observed that two of three vaccinated samples showed T cell responses to RdRp despite lack of infection. This is likely due to cross-reactive T cell responses elicited by common cold coronaviruses and agreeing with our previous detection of RdRp-specific T cells in pre-pandemic samples[33,53].

In order to test whether RdRp would be an effective target for a T cell-based vaccine, we generated mRNA-LNP encoding for the N terminus of RdRp and optimized it for T cell responses (Fig. 4-2a)[38,47]. We found that this mRNA-LNP was immunogenic in mice. Importantly, it was able to generate epitope-specific T cells in HLA-A2.1 transgenic mice, suggesting that humans immunized with this mRNA-LNP would also generate or expand T cells against previously

identified epitopes that share a high degree of similarity to those found in other coronaviruses. This result support the use of RdRp mRNA-LNP to elicit a broad protection for SARS-CoV2 variants and potentially future related pandemic coronaviruses. In addition, we found that the RdRp mRNA-LNP generated much higher levels of IFNγ-secreting T cells compared to an RBD mRNA-LNP (Fig. 4-2k). This may be due to the differences in timing of the second dose and the experimental endpoint, as the RdRp mRNA-LNP was given 8 days before the endpoint, while the RBD mRNA-LNP was given 22 days before the endpoint. Thus, while RdRp-specific T cells could be at the peak of the immune response, the RBD-specific T cells have started to decay to the memory phase of the response[52]. However, this could also be a result of the difference in antigen design, as the RdRp mRNA was selected to enhance presentation to T cells on MHC molecules, while the RBD mRNA was designed for secretion to facilitate B cell receptor activation. Alternatively, this could be due to an intrinsic difference in the antigenicity of these two antigens or their ability to be expressed after immunization. Overall, we found that both mRNA-LNP were immunogenic and could be potentially combined for a new generation of mRNA vaccines.

The key test for the efficacy of an RdRp-based T cell vaccine is the protection from disease after SARS-CoV-2 infection. We confirmed that the mRNA-LNP were immunogenic in the K18-hACE2 transgenic mouse model that can be infected with SARS-CoV-2 and exhibits severe disease that includes neuroinvasion at later timepoints (Figs. 4-2i to 4-2k)[49–51]. However, when we infected mice immunized with RdRp mRNA-LNP and/or RBD mRNA-LNP, we did not observe significant protection, with only 1 or 2 mice in each group exhibiting lower viral genomes in the lung or brain at 5 dpi, and failed to show any separation from a negative control group immunized with HA mRNA-LNP (Fig. 4-3c). We attempted to increase the immune response by boosting the mice with a third dose of mRNA-LNP 9 days before challenge. While there was complete protection in the RBD only and RBD+RdRp groups, we only observed a minor delay in disease in mice that only received RdRp mRNA (Fig. 4-3g). In the groups with full protection from disease, we found

no difference in viral copies in the brain between the RBD and RBD+RdRp groups at 12dpi. Our data suggests that neuroinvasion was controlled after the virus reached the brain, as one mouse in the RBD only group had much higher viral copies than the others in the RBD only and RBD+RdRp groups. This contrasts with a previous report that found that Spike-specific immunity elicited by an adenovirus-based vaccine was unable to prevent brain infection[31]. However, due to the small group size, it is unclear whether RdRp-specific T cells contribute any additional protection to RBD-specific immunity.

The inability of RdRp T cells to protect transgenic K18-hACE2 mice from SARS-CoV-2 disease is an important topic for future studies. Vaccine-generated CD8 T cells against dominant T cell targets such as SARS-CoV-2 Spike or Zika virus NS3 have been shown to reduce viral burden during infection[54,55]. In the case of SARS-CoV-2, rhesus macaques were immunized with the adenovirus-based vaccine expression Spike and developed neutralizing antibodies as well as Spike-specific CD8 T cells. The immunization effectively reduced viral replication in macaques after challenge, but this reduction was impaired by depletion of CD8 T cells, demonstrating that Spike-specific CD8 T cells can contribute to protection even in the presence of neutralizing antibodies[54]. Moreover, despite the presence of few neutralizing antibodies against Omicron variants after two doses of the Pfizer BNT162b2 Spike mRNA vaccine[56], protection against hospital admission for COVID-19 was maintained during the Omicron wave in South Africa[57]. This observation supports the role of cellular immunity in protection afforded by the Spike-based vaccines. In addition, in health workers who remained seronegative after putative abortive infection, preferential expansion of RdRp-specific T cells was observed compared to those who had laboratory confirmed infection, indicating a protective role of these T cells[34].

In our study, two doses of RBD mRNA-LNP immunization in C57Bl/6 mice, elicited no neutralizing antibodies but T cell responses were detected. However, neither these RBD-specific T cells nor

the RdRp-specific T cells afforded any protection in the K18-ACE2 mouse challenge infection model. Even when mice were immunized with both mRNA-LNP to generate T cells targeting both RBD and RdRp, no protection was observed. Protection by CD8 T cells occurs through eliminating infected cells to reduce virion production. It is possible that the dose used in this study (10,000 PFU or >100 50% lethal dose (LD_{50}) in our hands) overwhelmed the immune system with a quickly replicating virus in a host that overexpresses the viral entry receptor. This is especially relevant as our two-dose immunization did not generate neutralizing antibodies unlike in Spike adenovirus studies[31,54], which may reduce the initial infectious dose for the first round of viral replication. As a result, this K18-ACE2 transgenic mouse model exhibited lethal disease, mimicking more severe SARS-CoV-2 infection in humans. However, humans, especially heath care workers, are more likely to be exposed to a much lower number of virions due to personal protective equipment. In those situations, T cells could play a more impactful role in stopping infection from progressing.

T cell-focused vaccines using adenovirus or mRNA-LNP to induce immunity targeting the highly expressed and immunodominant N protein have been described in the literature[30–32]. Generating T cells only against the N protein by an adenovirus-based vaccine resulted in an almost 4 log decrease in lung viral titers resulting in 12/16 mice surviving challenge from 300 PFU[30], a dose that is almost 2 orders of magnitude lower than the $1x10^4$ PFU used in our study. This lower dose may also be more relevant, as infectious doses as low as 10 50% tissue culture infectious dose units ($TCID_{50}$), approximately 7 PFU, have been shown to cause mild-to-moderate disease in young adult humans[58]. In studies where an inoculum dose closer to our study was used as a challenge infection, N-specific T cells alone had modest or no effects[31,32]. However, these T cells can help Spike-specific immunity control viral replication in the brains of mice or in a hamster model. Taken together, this suggests that RdRp-specific T cells may be more effective in mice challenged with a lower inoculum dose and in coordination with RBD-specific immunity.

Another aspect of concern is whether a sufficient number of peptide-MHCI complexes derived from RdRp are present on the surface of infected cells to activate T cell killing. While RdRp-specific T cells can be detected in individuals and RdRp is one of six main T cell targets, a significant portion of infected individuals do not have detectable CD8 T cells against RdRp (Fig. 4-1 and refs [29,34]), suggesting that it may not be efficiently presented in all individuals. RdRp is not expressed to a high level during viral replication, especially compared to structural proteins such as Spike and N. This relatively lower level of RdRp expression has been confirmed by mass spectrometry proteomics in infected cells[26]. In addition, HLA-based proteomic studies have not detected RdRp-specific epitopes bound to MHC-I molecules, despite the presence of RdRp in the infected cellular proteome[26,27]. Thus, although the RdRp mRNA-LNP has been designed to optimize priming to T cells, the low level of RdRp expression in infected cells might hinder the recognition and killing by vaccine-generated T cells. Nevertheless, it remains possible that T cells with high affinity TCRs to peptide-MHC complexes derived from RdRp could provide some protective effects, especially earlier in infection.

Our strategy of targeting the conserved RdRp of SARS-CoV-2 is not a completely new avenue of research. The inclusion of a small section of the RdRp has been tested as part of an intranasally administered adenovirus vectored vaccine candidate[59]. However, it is unclear how much protection is conferred by RdRp epitopes compared to the Spike and N proteins that were also delivered by this platform, especially because only about 200 bases of the RdRp sequence were included and an RdRp-only adenovirus was not tested. In addition, the conservation of the RdRp sequence between betacoronaviruses has enabled the use of a nucleoside analog, remdesivir, which inhibits viral replication by inhibiting viral RNA synthesis[60]. Remdesivir was first developed to treat infection by SARS-CoV-1 and MERS-CoV[61], but has now been shown to inhibit replication by SARS-CoV-2 with outcome benefits in clinical trials[62–64]. Importantly, while remdesivir-resistance mutations have been characterized, they remain rare[65,66], allowing for continued use

of this drug to minimize the risk of severe disease in vulnerable populations. Remdesivir is also effective against Omicron variants of SARS-CoV-2[67,68], which have developed mutations in the Spike glycoprotein to evade antibody immunity. Thus, the conservation of the RdRp not only within SARS-CoV-2 lineages but also with other betacoronaviruses make it an attractive target for therapeutics and for future vaccines.

Figures and Figure Legends

Figure 4-1

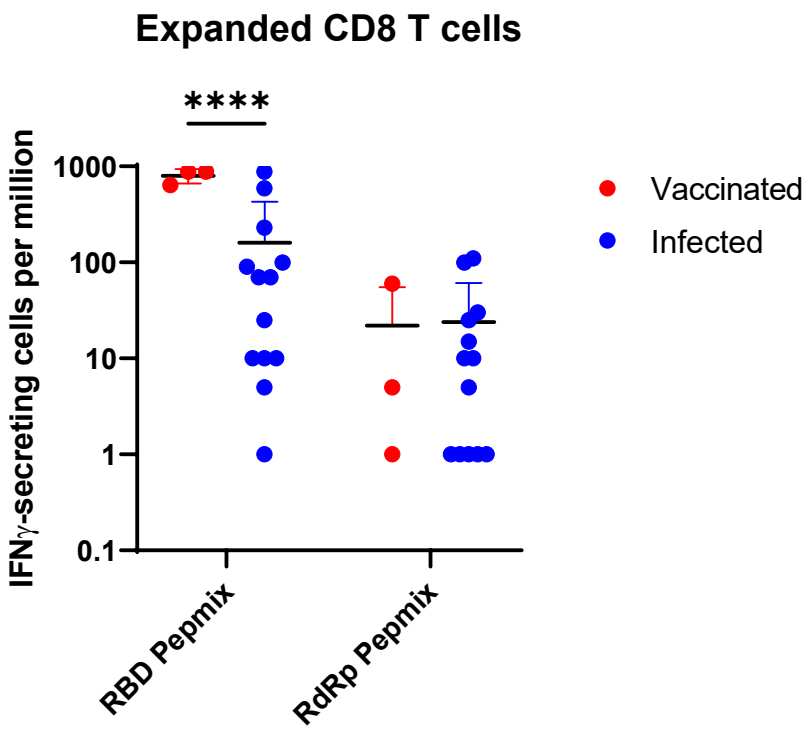

Figure 4-1: Detection of RdRp-specific T cells in SARS-CoV-2 convalescent patients

IFNγ ELISpot results from CD8 T cells expanded from human PBMC samples that were stimulated with overlapping peptide libraries from the SARS-CoV-2 Spike RBD or RdRp. Statistical analysis: Two way ANOVA with Sidak's test for multiple comparisons. ****p<0.0001. Mean and standard deviation are displayed. N=3 vaccinated and 13 infected patients

Figure 4-2

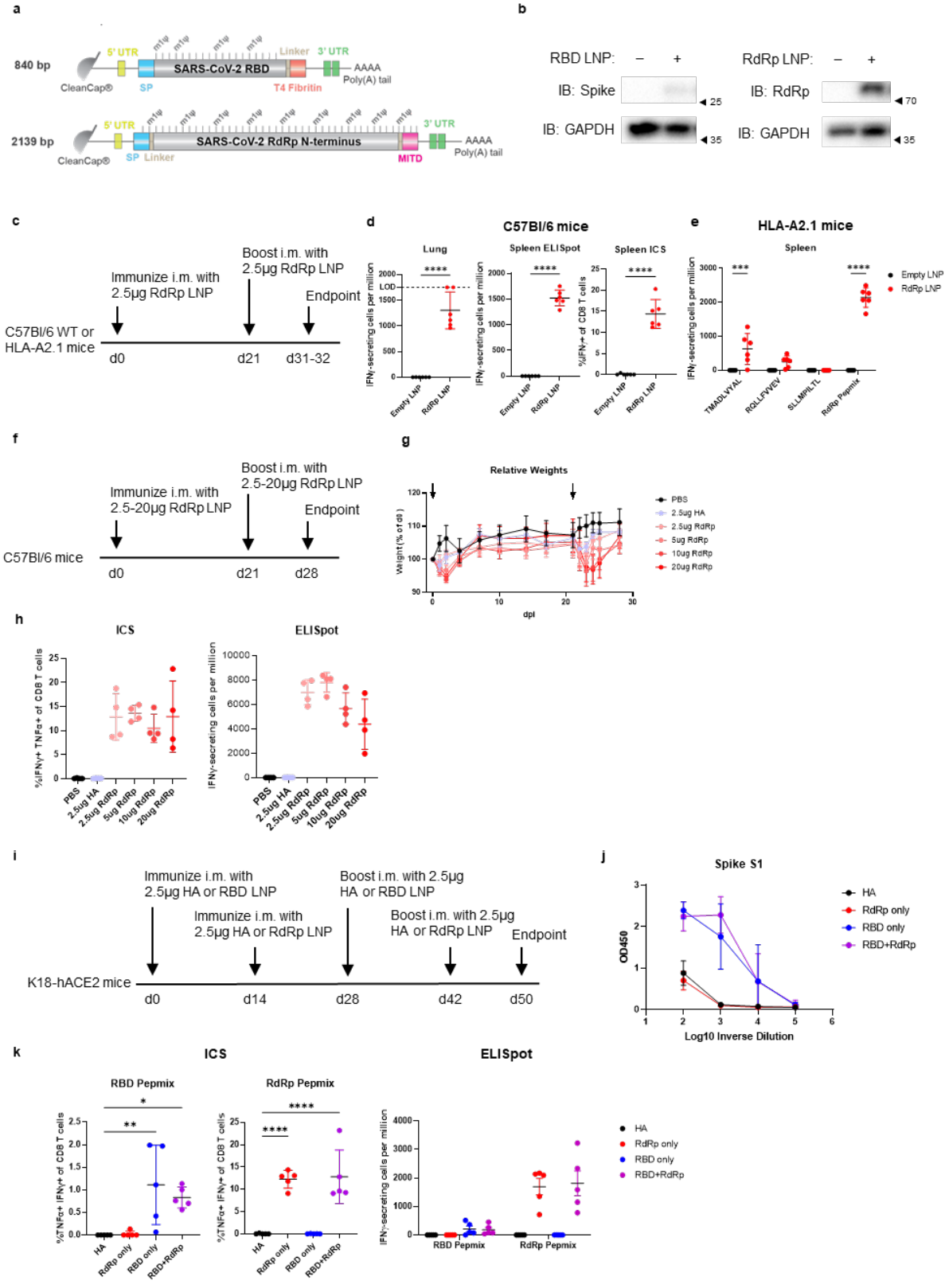
a
840 bp
5' UTR
SARS-CoV-2 RBD
Linker
3' UTR
AAAA
Poly(A) tail
CleanCap®
SP
T4 Fibritin
2139 bp
SARS-CoV-2 RdRp N-terminus
SP Linker
MITD
b
RBD LNP: – +
IB: Spike
IB: GAPDH
RdRp LNP: – +
IB: RdRp
IB: GAPDH
c
Immunize i.m. with 2.5µg RdRp LNP
Boost i.m. with 2.5µg RdRp LNP
Endpoint
C57Bl/6 WT or HLA-A2.1 mice
d0
d21
d31-32
d
C57Bl/6 mice
Lung
Spleen ELISpot
Spleen ICS
IFNγ-secreting cells per million
%IFNγ+ of CD8 T cells
Empty LNP
RdRp LNP
e
HLA-A2.1 mice
Spleen
TMADLVYAL
RQLLFVYEV
SLLMFPLTL
RdRp Pepmix
f
Immunize i.m. with 2.5-20µg RdRp LNP
Boost i.m. with 2.5-20µg RdRp LNP
Endpoint
C57Bl/6 mice
d0
d21
d28
g
Relative Weights
Weight (% of d0)
dpi
PBS
2.5ug HA
2.5ug RdRp
5ug RdRp
10ug RdRp
20ug RdRp
h
ICS
%IFNγ+ TNFα+ of CD8 T cells
ELISpot
IFNγ-secreting cells per million
i
Immunize i.m. with 2.5µg HA or RBD LNP
Immunize i.m. with 2.5µg HA or RdRp LNP
Boost i.m. with 2.5µg HA or RBD LNP
Boost i.m. with 2.5µg HA or RdRp LNP
Endpoint
K18-hACE2 mice
d0
d14
d28
d42
d50
j
Spike S1
OD450
Log10 Inverse Dilution
HA
RdRp only
RBD only
RBD+RdRp
k
ICS
ELISpot
RBD Pepmix
RdRp Pepmix
%TNFα+ IFNγ+ of CD8 T cells
IFNγ-secreting cells per million

Figure 4-2: Immunogenic mRNA-LNPs encoding the SARS-CoV-2 RBD and RdRp

(a) Diagrams showing the design of RBD and RdRp mRNA

(b) Western blots showing *in vitro* expression of RBD and RdRp mRNA-LNPs

(c) Immunization scheme to test immunogenicity of RdRp mRNA-LNP used in (d) and (e)

(d-e) ELISpot and ICS results from WT C57Bl/6 mouse lung and spleen cells (d) or HLA-A2.1 mouse spleen cells (e) stimulated with overlapping RdRp peptides. LOD=limit of detection

(f) Immunization scheme to test dose escalation of RdRp mRNA-LNP used in (g) and (h)

(g) Weight loss caused by RdRp mRNA-LNP immunization

(h) ICS and ELISpot results from splenocytes stimulated with overlapping RdRp peptides

(i) Immunization scheme to test immunogenicity of RBD and RdRp double immunization in K18-hACE2 mice used in (j) and (k)

(j) ELISA results of serum IgG antibodies against recombinant Spike S1 protein

(k) ICS and ELISpot results from splenocytes stimulated with overlapping RBD or RdRp peptides

Statistical analysis: Unpaired t test (d), two way ANOVA with Sidak's test for multiple comparisons (e), or one way ANOVA with Dunnett's test for multiple comparisons (k). *$p<0.05$, **$p<0.01$, ***$p<0.001$, ****$p<0.0001$. Mean and standard deviation are displayed. N=6 (c-e) or 4 (f-k) mice per group.

Figure 4-3

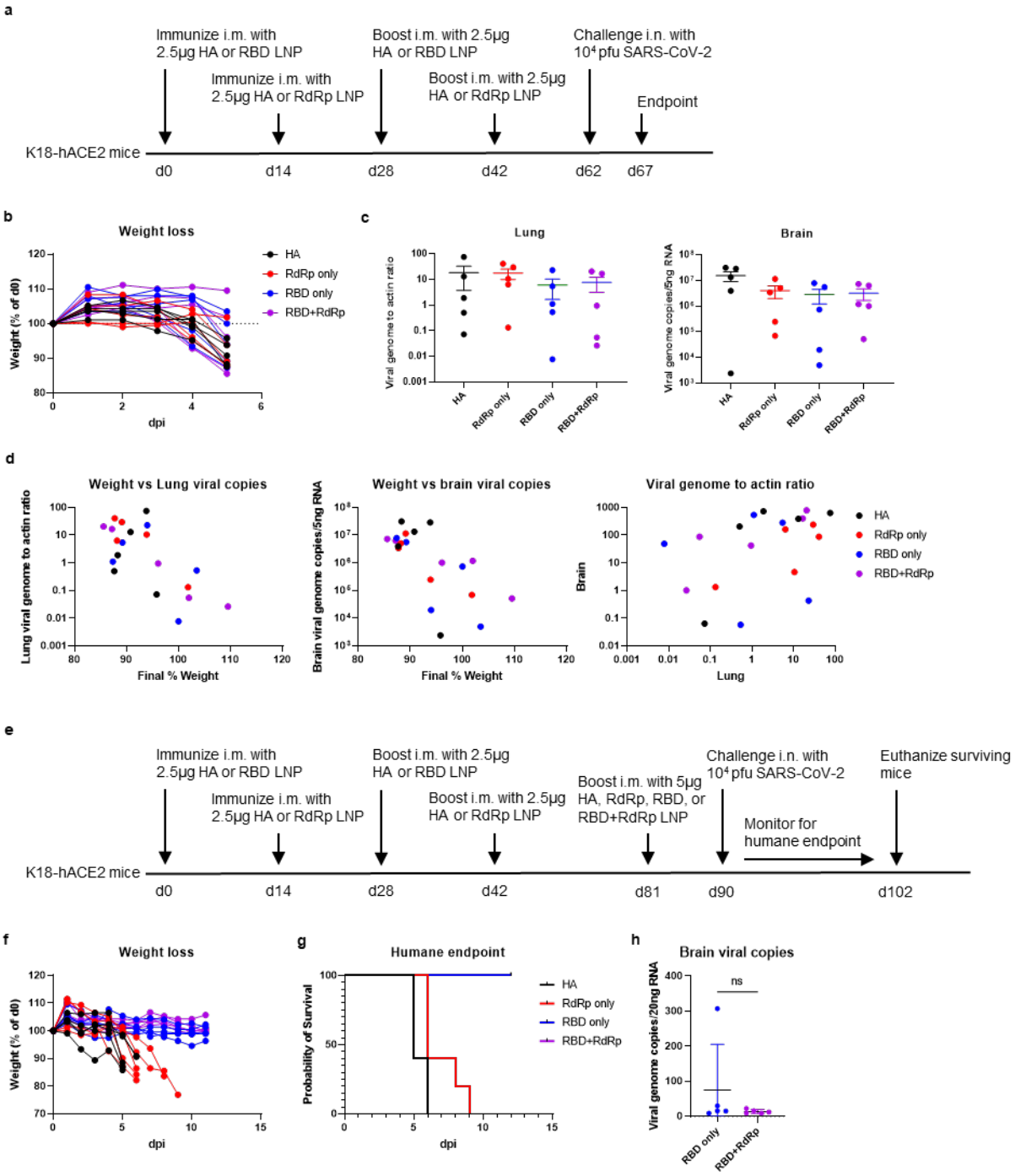

Figure 4-3: SARS-CoV-2 challenge of RBD and RdRp immunized mice

(a) Immunization scheme for protection generated by RBD and RdRp immunization used in (b-d)

(b) Weight loss data from immunized mice challenged with SARS-CoV-2

(c) Viral genome RNA copies in the lung and brain of mice 5 days post infection

(d) Correlation plots between viral genome copies in the lung or brain and final relative weight

(e) Immunization scheme for protection with a final immunization boost before infection used in (f-h)

(f) Weight loss data from infected mice

(g) Survival curves for mice reaching humane endpoint after infection

(h) Viral copies in the brain at 12dpi

Statistical analysis: unpaired t test (h). Mean and standard deviation are shown. N=5 mice per group.

Materials and Methods

Mice and Immunizations

All mouse experiments were conducted with the approval of the UCLA and USC Institutional Animal Care and Use Committees and the UCLA Chancellor's Animal Research Committee. C57Bl/6J, HLA-A2.1, and K18-hACE2 mice were purchased from the Jackson Laboratory (Bar Harbor, ME #000664, #004191, and #034860, respectively). For immunizations, mice were restrained with a tailvein restrainer (Braintree Scientific, Braintree, MA #TV-RED 150-STD), cleaned with isopropanol wipes, and injected in the hindleg with 50μL with insulin syringes (Becton, Dickinson, and Company (BD), Franklin Lakes, NJ #329461).

mRNA-LNP

mRNA sequences described in the text were optimized to minimize uridine content with Geneious software (Biomatters, Inc., San Diego, CA) and synthesized with ψ and a 5' CleanCap by TriLink Biotechnologies (San Diego, CA). Lipid nanoparticles were prepared using a self-assembly process as previously described[69]; the ionizable cationic lipid and LNP composition are described in the patent application WO 2017/004143.

Detection of antigen-specific T cells from human samples

Polyclonally expanded CD8 T cells were a gift from Ellie Taus and Otto Yang and were generated as previously described[70]. Briefly, cryopreserved PBMCs were stimulated with 50U/mL IL-2 and a CD3:CD4 bi-specific monoclonal antibody in RPMI for 14 days and the polyclonally expanded CD8 T cells were cryopreserved until use. T cells were stimulated with overlapping peptides for the RBD and RdRp (JPT Peptide Technologies GmbH, Berlin, Germany #PM-WCPV-S-RBD-2, and #PM-WCPV-NSP12-2, respectively) in RPMI (Corning, Corning, NY #10-040-CV) containing

10% fetal bovine serum (FBS) (Corning #35010CV) and 1X Penicillin/Streptomycin (Corning #30002CI) (complete RPMI). Unstimulated cells and cells stimulated with a cocktail of phorbol 12-myristate 13-acetate (PMA) and ionomycin (Thermo Fisher Scientific, Waltham, MA #00-4970-03) were used as controls. IFNγ-secreting T cells were detected with the Human IFN-γ Single-Color ELISPOT kit (Cellular Technology Limited (CTL), Shaker Heights, OH #hIFNg-1M-red) according to the manufacturer's instructions. Plates were scanned and analyzed by CTL and antigen-specific cells were calculated by subtracting spots from unstimulated controls from stimulated wells and normalizing to IFNγ-secreting cells per million.

In vitro antigen expression

HEK293T cells were cultured in Dulbecco's Modified Eagle's Medium (DMEM) (Corning #10017CV) supplemented with 10% fetal bovine serum (FBS) and 1X Penicillin/Streptomycin (complete DMEM) at 37°C and 5% CO_2. 150,000 293T cells were seeded overnight in 0.5mL culture medium in a 24-well plate (VWR, Radnor, PA #10062-896). The next day, culture medium was changed to culture medium containing 0.5µg mRNA-LNP. 24 hours post transfection, cells were lysed in RIPA buffer containing 1mM phenylmethylsulfonyl fluoride (PMSF) for 30 minutes at 4°C. 4X Laemmli buffer (Bio-Rad, Hercules, CA #1610747) with 10% beta-mercaptoethanol was added to lysates and samples were boiled at 95°C for 15 minutes. Lysates were run on a homemade 10% SDS-PAGE gel alongside a 10-250kDa molecular weight ladder (Thermo Fisher Scientific #26619). After proteins were transferred to a polyvinylidene difluoride membrane with semi-dry transfer (Bio-Rad #1704272), the membrane was blocked with 10% milk in phosphate buffered saline with 0.1% Tween-20 (PBS-T) for one hour at room temperature. The membrane was cut and probed with primary antibodies at a 1:1000 dilution in 2% milk in PBS-T overnight at 4°C. The next day, the membrane was washed thrice with PBS-T for 10 minutes, incubated with secondary antibody at a 1:10000 dilution for 2 hours at room temperature, and washed again

thrice with PBS-T for 10 minutes. Chemiluminescent signal was detected with SuperSignal West Pico PLUS Chemiluminescent Substrate (Thermo Fisher Scientific #34580) using a Chemidoc XRS+ System (Bio-Rad #1708265).

Primary antibodies were used to detect the following proteins: SARS-CoV-2 Spike (Sino Biological, Wayne, PA #40591-T62), SARS-CoV-2 RdRp (Genetex #GTX135467), and GAPDH (Thermo Fisher Scientific #MA5-15738). Horseradish peroxidase (HRP)-conjugated secondary antibodies were used to detect mouse and rabbit primary antibodies (Thermo Fisher Scientific, #62-6520 and #31460, respectively).

Enzyme linked immunospot (ELISpot) assay

Cells were obtained from spleens by passage through a 70μm cell strainer (Fisher Scientific, Waltham, MA, #22-363-548) using a 3mL syringe plunger (Fisher Scientific #14-823-435). Red blood cells were lysed with ACK lysing buffer (Thermo Fisher Scientific #A1049201) and cells were resuspended in complete RPMI. Cells from lungs were obtained by mincing the tissue with surgical scissors and digesting it with 2-5mg/mL collagenase A (Sigma-Aldrich #10103586001) in complete RPMI at 37^{o}C for 60-80 minutes with mixing every 10 minutes. The digested tissue was processed in a manner identical to spleen samples to obtain lung cells.

ELISpot was performed using a mouse IFNγ/TNFα or mouse IFNγ ELISpot kit (CTL #mIFNgTNFa-1M/10 and #mIFNg-1M, respectively) according to the manufacturer's instructions. Negative control wells contained unstimulated cells and positive control wells were stimulated with a cocktail of phorbol 12-myristate 13-acetate (PMA) and ionomycin. Experimental wells were stimulated with 1μg/mL RBD or RdRp Pepmix in complete RPMI. Cells were incubated at 37^{o}C for 20-22 hours before plates were developed. Plates were scanned and spot counts were

analyzed by CTL. The number of spots in negative control wells was subtracted from experimental wells to determine the number of antigen-specific spot-forming cells.

Intracellular cytokine staining (ICS)

Splenocytes were prepared as described above. Stimulation was performed in 96-well U bottom plates in the presence of brefeldin A (Biolegend, San Diego, CA #420601) for 6 hours at 37°C. Cells were then stored at 4°C for up to 16 hours until staining. Cells were stained with anti-TCRbeta PerCP-Cy5.5 clone H57-597, anti-CD4 PE-Cy7 clone RM4-5, and anti-CD8 PE clone 53-6.7 (Biolegend #109228, #100528, and #100708) at a 1:100 dilution for 15 minutes on ice. Cells were washed with FACS buffer, then fixed and permeabilized with Cytofix/Cytoperm buffer (BD #554714) for 20 minutes on ice. Cells were washed with permeabilization buffer, then stained with anti-IFNγ APC clone XMG1.2 and anti-TNFα FITC clone MP6-XT22 (Biolegend #505810 and #506304) at a 1:50 dilution in permeabilization buffer for 30 minutes on ice. Cells were finally washed with permeabilization buffer and resuspended in FACS buffer before analysis.

Enzyme-linked immunosorbent assay (ELISA)

ELISA plates (Corning #07-200-721) were prepared by coating each well with 50µL recombinant SARS-CoV-2 Spike S1 (Sino Biological #40591-V08H) at a 1µg/mL concentration in carbonate-bicarbonate buffer (Sigma-Aldrich, Inc., St. Louis, MO #C3041-50CAP) overnight at 4oC. Coated 96-well plates were blocked with PBS containing 1% BSA (%w/v) (Fisher Scientific #BP9703100), and 0.05% Tween-20 (%v/v) (Fisher Scientific #BP337-500) at room temperature for 1 hour or overnight at 4°C. All serum samples and secondary antibodies were diluted in assay buffer consisting of PBS with 0.1% BSA and 0.025% Tween-20. Coated plates were washed with DPBS containing 0.1% Tween-20 (%v/v) (PBS-T) twice for 3 minutes. Plates were then washed twice quickly with PBS-T before the addition of 50µL serially diluted immune serum. 6-8 wells per plate

were incubated with assay buffer containing no primary antibody as a background control. Plates were incubated for 1-2 hours at room temperature on an orbital shaker. Plates were washed with PBS-T twice for 3 minutes, then twice quickly before the addition of 50µL 1:4000 goat anti-mouse HRP secondary antibody (Thermo Fisher Scientific #62-6520). Secondary antibody was incubated for 1 hour at room temperature with shaking. Plates were then washed once with PBS-T for 3 minutes, then four times quickly. After one final wash with PBS (no Tween-20), 100µL 1-Step Ultra TMB ELISA Substrate (Thermo Fisher Scientific #34028) was added to each well. Plates were covered to protect them from light and incubated at room temperature for 30 minutes with shaking. Signal development was stopped by the addition of 100µL 1M sulfuric acid (Sigma-Aldrich #1603131000) and the optical density at 450nm (OD450) was measured with a ClarioStar plate reader (BMG Labtech, Cary, NC).

References

1. Harvey, W. T. *et al.* SARS-CoV-2 variants, spike mutations and immune escape. *Nat Rev Microbiol* **19**, 409–424 (2021).

2. Li, J., Lai, S., Gao, G. F. & Shi, W. The emergence, genomic diversity and global spread of SARS-CoV-2. *Nature* **600**, 408–418 (2021).

3. Hodcroft, E. B. *et al.* Spread of a SARS-CoV-2 variant through Europe in the summer of 2020. *Nature* **595**, 707–712 (2021).

4. Elliott, P. *et al.* Rapid increase in Omicron infections in England during December 2021: REACT-1 study. *Science* **375**, 1406–1411 (2022).

5. Bolze, A. *et al.* SARS-CoV-2 variant Delta rapidly displaced variant Alpha in the United States and led to higher viral loads. *Cell Reports Medicine* **3**, 100564 (2022).

6. Cai, Y. *et al.* Structural basis for enhanced infectivity and immune evasion of SARS-CoV-2 variants. *Science* **373**, 642–648 (2021).

7. McCallum, M. *et al.* SARS-CoV-2 immune evasion by the B.1.427/B.1.429 variant of concern. *Science* **373**, 648–654 (2021).

8. Mlcochova, P. *et al.* SARS-CoV-2 B.1.617.2 Delta variant replication and immune evasion. *Nature* **599**, 114–119 (2021).

9. McCallum, M. *et al.* Molecular basis of immune evasion by the Delta and Kappa SARS-CoV-2 variants. *Science* **374**, 1621–1626 (2021).

10. Zhang, J. *et al.* Membrane fusion and immune evasion by the spike protein of SARS-CoV-2 Delta variant. *Science* **374**, 1353–1360 (2021).

11. Planas, D. *et al.* Considerable escape of SARS-CoV-2 Omicron to antibody neutralization. *Nature* **602**, 671–675 (2022).

12. Liu, L. *et al.* Striking antibody evasion manifested by the Omicron variant of SARS-CoV-2. *Nature* **602**, 676–681 (2022).

13. Iketani, S. *et al.* Antibody evasion properties of SARS-CoV-2 Omicron sublineages. *Nature* **604**, 553–556 (2022).

14. Hachmann, N. P. *et al.* Neutralization Escape by SARS-CoV-2 Omicron Subvariants BA.2.12.1, BA.4, and BA.5. *N Engl J Med* **387**, 86–88 (2022).

15. Mascola, J. R., Graham, B. S. & Fauci, A. S. SARS-CoV-2 Viral Variants—Tackling a Moving Target. *JAMA* **325**, 1261 (2021).

16. Fontanet, A. *et al.* SARS-CoV-2 variants and ending the COVID-19 pandemic. *The Lancet* **397**, 952–954 (2021).

17. Li, Q. *et al.* The Impact of Mutations in SARS-CoV-2 Spike on Viral Infectivity and Antigenicity. *Cell* **182**, 1284-1294.e9 (2020).

18. Greaney, A. J. *et al.* Complete Mapping of Mutations to the SARS-CoV-2 Spike Receptor-Binding Domain that Escape Antibody Recognition. *Cell Host & Microbe* **29**, 44-57.e9 (2021).

19. Liu, Z. *et al.* Identification of SARS-CoV-2 spike mutations that attenuate monoclonal and serum antibody neutralization. *Cell Host & Microbe* **29**, 477-488.e4 (2021).

20. Rees-Spear, C. *et al.* The effect of spike mutations on SARS-CoV-2 neutralization. *Cell Reports* **34**, 108890 (2021).

21. Ferretti, A. P. *et al.* Unbiased Screens Show CD8+ T Cells of COVID-19 Patients Recognize Shared Epitopes in SARS-CoV-2 that Largely Reside outside the Spike Protein. *Immunity* **53**, 1095-1107.e3 (2020).

22. Tarke, A. *et al.* Impact of SARS-CoV-2 variants on the total CD4+ and CD8+ T cell reactivity in infected or vaccinated individuals. *Cell Reports Medicine* **2**, 100355 (2021).

23. Riou, C. *et al.* Escape from recognition of SARS-CoV-2 variant spike epitopes but overall preservation of T cell immunity. *Sci. Transl. Med.* **14**, eabj6824 (2022).

24. Keeton, R. *et al.* T cell responses to SARS-CoV-2 spike cross-recognize Omicron. *Nature* **603**, 488–492 (2022).

25. Altenburg, A. F., Rimmelzwaan, G. F. & de Vries, R. D. Virus-specific T cells as correlate of (cross-)protective immunity against influenza. *Vaccine* **33**, 500–506 (2015).

26. Weingarten-Gabbay, S. *et al.* Profiling SARS-CoV-2 HLA-I peptidome reveals T cell epitopes from out-of-frame ORFs. *Cell* **184**, 3962-3980.e17 (2021).

27. Nagler, A. *et al.* Identification of presented SARS-CoV-2 HLA class I and HLA class II peptides using HLA peptidomics. *Cell Reports* **35**, 109305 (2021).

28. Grifoni, A. *et al.* Targets of T Cell Responses to SARS-CoV-2 Coronavirus in Humans with COVID-19 Disease and Unexposed Individuals. *Cell* **181**, 1489-1501.e15 (2020).

29. Tarke, A. *et al.* Comprehensive analysis of T cell immunodominance and immunoprevalence of SARS-CoV-2 epitopes in COVID-19 cases. *Cell Reports Medicine* **2**, 100204 (2021).

30. Matchett, W. E. *et al.* Cutting Edge: Nucleocapsid Vaccine Elicits Spike-Independent SARS-CoV-2 Protective Immunity. *J.I.* **207**, 376–379 (2021).

31. Dangi, T., Class, J., Palacio, N., Richner, J. M. & Penaloza MacMaster, P. Combining spike- and nucleocapsid-based vaccines improves distal control of SARS-CoV-2. *Cell Reports* **36**, 109664 (2021).

32. Hajnik, R. L. *et al.* Dual spike and nucleocapsid mRNA vaccination confer protection against SARS-CoV-2 Omicron and Delta variants in preclinical models. *Sci. Transl. Med.* **14**, eabq1945 (2022).

33. Nesterenko, P. A. *et al.* HLA-A∗02:01 restricted T cell receptors against the highly conserved SARS-CoV-2 polymerase cross-react with human coronaviruses. *Cell Reports* **37**, 110167 (2021).

34. Swadling, L. *et al.* Pre-existing polymerase-specific T cells expand in abortive seronegative SARS-CoV-2. *Nature* **601**, 110–117 (2022).

35. Polack, F. P. *et al.* Safety and Efficacy of the BNT162b2 mRNA Covid-19 Vaccine. *N Engl J Med* **383**, 2603–2615 (2020).

36. Baden, L. R. *et al.* Efficacy and Safety of the mRNA-1273 SARS-CoV-2 Vaccine. *N Engl J Med* **384**, 403–416 (2021).

37. Pardi, N., Hogan, M. J., Porter, F. W. & Weissman, D. mRNA vaccines — a new era in vaccinology. *Nat Rev Drug Discov* **17**, 261–279 (2018).

38. Sahin, U. *et al.* Personalized RNA mutanome vaccines mobilize poly-specific therapeutic immunity against cancer. *Nature* **547**, 222–226 (2017).

39. Kranz, L. M. *et al.* Systemic RNA delivery to dendritic cells exploits antiviral defence for cancer immunotherapy. *Nature* **534**, 396–401 (2016).

40. Tahtinen, S. *et al.* IL-1 and IL-1ra are key regulators of the inflammatory response to RNA vaccines. *Nat Immunol* (2022) doi:10.1038/s41590-022-01160-y.

41. Li, C. *et al.* Mechanisms of innate and adaptive immunity to the Pfizer-BioNTech BNT162b2 vaccine. *Nat Immunol* **23**, 543–555 (2022).

42. Alameh, M.-G. *et al.* Lipid nanoparticles enhance the efficacy of mRNA and protein subunit vaccines by inducing robust T follicular helper cell and humoral responses. *Immunity* **54**, 2877-2892.e7 (2021).

43. Goel, R. R. *et al.* mRNA vaccines induce durable immune memory to SARS-CoV-2 and variants of concern. *Science* **374**, abm0829 (2021).

44. Mateus, J. *et al.* Low-dose mRNA-1273 COVID-19 vaccine generates durable memory enhanced by cross-reactive T cells. *Science* **374**, eabj9853 (2021).

45. Fonseca, J. A. *et al.* Inclusion of the murine IgGκ signal peptide increases the cellular immunogenicity of a simian adenoviral vectored Plasmodium vivax multistage vaccine. *Vaccine* **36**, 2799–2808 (2018).

46. Güthe, S. *et al.* Very Fast Folding and Association of a Trimerization Domain from Bacteriophage T4 Fibritin. *Journal of Molecular Biology* **337**, 905–915 (2004).

47. Kreiter, S. *et al.* Increased Antigen Presentation Efficiency by Coupling Antigens to MHC Class I Trafficking Signals. *J Immunol* **180**, 309–318 (2008).

48. Newberg, M. H. *et al.* Importance of MHC class 1 alpha2 and alpha3 domains in the recognition of self and non-self MHC molecules. *J Immunol* **156**, 2473–2480 (1996).

49. Winkler, E. S. *et al.* SARS-CoV-2 infection of human ACE2-transgenic mice causes severe lung inflammation and impaired function. *Nat Immunol* **21**, 1327–1335 (2020).

50. Oladunni, F. S. *et al.* Lethality of SARS-CoV-2 infection in K18 human angiotensin-converting enzyme 2 transgenic mice. *Nat Commun* **11**, 6122 (2020).

51. Yinda, C. K. *et al.* K18-hACE2 mice develop respiratory disease resembling severe COVID-19. *PLoS Pathog* **17**, e1009195 (2021).

52. Pennock, N. D. *et al.* T cell responses: naïve to memory and everything in between. *Advances in Physiology Education* **37**, 273–283 (2013).

53. Mateus, J. *et al.* Selective and cross-reactive SARS-CoV-2 T cell epitopes in unexposed humans. *Science* **370**, 89–94 (2020).

54. Liu, J. *et al.* CD8 T Cells Contribute to Vaccine Protection Against SARS-CoV-2 in Macaques. *Sci. Immunol.* eabq7647 (2022) doi:10.1126/sciimmunol.abq7647.

55. Elong Ngono, A. *et al.* CD8 $^{+}$ T cells mediate protection against Zika virus induced by an NS3-based vaccine. *Sci. Adv.* **6**, eabb2154 (2020).

56. GeurtsvanKessel, C. H. *et al.* Divergent SARS-CoV-2 Omicron–reactive T and B cell responses in COVID-19 vaccine recipients. *Sci. Immunol.* **7**, eabo2202 (2022).

57. Gray, G. *et al.* Effectiveness of Ad26.COV2.S and BNT162b2 Vaccines against Omicron Variant in South Africa. *N Engl J Med* **386**, 2243–2245 (2022).

58. Killingley, B. *et al.* Safety, tolerability and viral kinetics during SARS-CoV-2 human challenge in young adults. *Nat Med* **28**, 1031–1041 (2022).

59. Afkhami, S. *et al.* Respiratory mucosal delivery of next-generation COVID-19 vaccine provides robust protection against both ancestral and variant strains of SARS-CoV-2. *Cell* **185**, 896-915.e19 (2022).

60. Kokic, G. *et al.* Mechanism of SARS-CoV-2 polymerase stalling by remdesivir. *Nat Commun* **12**, 279 (2021).

61. Sheahan, T. P. *et al.* Broad-spectrum antiviral GS-5734 inhibits both epidemic and zoonotic coronaviruses. *Sci. Transl. Med.* **9**, eaal3653 (2017).

62. Wang, M. *et al.* Remdesivir and chloroquine effectively inhibit the recently emerged novel coronavirus (2019-nCoV) in vitro. *Cell Res* **30**, 269–271 (2020).

63. Beigel, J. H. *et al.* Remdesivir for the Treatment of Covid-19 — Final Report. *N Engl J Med* **383**, 1813–1826 (2020).

64. Gottlieb, R. L. *et al.* Early Remdesivir to Prevent Progression to Severe Covid-19 in Outpatients. *N Engl J Med* **386**, 305–315 (2022).

65. Gandhi, S. *et al.* De novo emergence of a remdesivir resistance mutation during treatment of persistent SARS-CoV-2 infection in an immunocompromised patient: a case report. *Nat Commun* **13**, 1547 (2022).

66. Stevens, L. J. *et al.* Mutations in the SARS-CoV-2 RNA-dependent RNA polymerase confer resistance to remdesivir by distinct mechanisms. *Sci. Transl. Med.* **14**, eabo0718 (2022).

67. Pitts, J. *et al.* Remdesivir and GS-441524 Retain Antiviral Activity against Delta, Omicron, and Other Emergent SARS-CoV-2 Variants. *Antimicrob Agents Chemother* **66**, e00222-22 (2022).

68. Takashita, E. *et al.* Efficacy of Antibodies and Antiviral Drugs against Omicron BA.2.12.1, BA.4, and BA.5 Subvariants. *N Engl J Med* **387**, 468–470 (2022).

69. Maier, M. A. *et al.* Biodegradable Lipids Enabling Rapidly Eliminated Lipid Nanoparticles for Systemic Delivery of RNAi Therapeutics. *Molecular Therapy* **21**, 1570–1578 (2013).

70. Taus, E. *et al.* Dominant CD8+ T Cell Nucleocapsid Targeting in SARS-CoV-2 Infection and Broad Spike Targeting From Vaccination. *Front. Immunol.* **13**, 835830 (2022).

CHAPTER 5:

Summary and Perspectives

Summary

The SARS-CoV-2 pandemic has launched lipid nanoparticle (LNP) technology into the scientific spotlight. Despite the many tragedies that have occurred because of the pandemic, one silver lining is the opportunities it has afforded for the study of this new vaccine technology. This dissertation examines the applications of LNP as both an adjuvant and an antigen delivery platform to provide insights on their future roles in society. First, we examined the ability of LNP to act as an adjuvant for KSHV VLVs to improve the immunogenicity of this multi-antigen vaccine platform. We showed that LNP are potent adjuvants for inducing both antibody and T cell responses after VLV immunization in mice. This strong antibody response led to our novel observation that antibodies specific for ORF4 can serve as a target for complement-mediated neutralization of KSHV, a response that may be beneficial to induce in a future KSHV vaccine. We also observed that encapsulation of a TLR agonist, polyUs, in LNP can enhance T cell responses against viral antigens compared to empty LNP, suggesting a method to further improve an already strong adjuvant platform.

We next examined the role of IFN-I in the immunogenicity of antigens delivered as mRNA LNP. Using three model viral antigens with different structural modifications, we found that the impact of IFN-I was antigen-dependent. Antibodies against HA were largely unaffected by IFN-I, but antibodies against RBD were markedly increased in C57Bl/6 mice in the absence of IFN-I signaling. We also demonstrated opposing impacts on T cells, with T cells against HA and RBD inhibited in the absence of IFN-I, while RdRp-specific T cells are unaffected or increased. Overall, this study indicated that the induction of IFN-I in future mRNA vaccines should be carefully considered in an antigen-dependent manner.

Finally, we investigated the use of mRNA LNP encoding the SARS-CoV-2 RdRp to generate T cell responses toward a conserved viral antigen. We found that RdRp mRNA LNP were highly

immunogenic, generating strong T cell responses toward the epitope rich N-terminus of RdRp. However, these T cells were unable to control viral replication in a transgenic mouse infection model. This could be due to poor presentation of RdRp epitopes by infected cells, a notion supported by low levels of RdRp-specific T cells found in SARS-CoV-2 convalescent patients. However, this could also be a result of a large challenge dose that could be remedied in future investigations. Overall, the goal of generating T cells against a conserved viral antigen was achieved, but the impact these T cells may have on disease is still unclear.

Towards a clinical KSHV vaccine

The road towards a KSHV vaccine is still quite long. The work described in chapter 2 of this dissertation provides an additional step toward the goal of stopping KSHV-associated diseases. We demonstrated that activating the complement system via antibodies specific for viral ORF4 may be a beneficial component of a future KSHV vaccine. To that end, we have filed an invention report describing our KSHV VLV vaccine platform, the adjuvant effect of polyUs-LNP, and the role of complement in KSHV neutralization in future vaccine development. However, this vaccine target and those currently under preclinical investigation still require validation in a challenge model of KSHV infection. Due to the restricted host range of KSHV, common small animal models cannot be used. Instead, mice can be infected with MHV-68, a rodent homolog of KSHV which has a lifecycle with pronounced lytic replication at early timepoints, and does not recapitulate what is expected in humans infected with KSHV[1]. This infection could still be useful using MHV-68 engineered to express KSHV glycoproteins, a project that is reportedly in development. Alternatively, KSHV can infect mice with humanized immune systems. However, this model requires high infectious doses[2,3] and immune responses to vaccines may not be ideal in humanized mice. Lastly, KSHV can infect non-human primates (NHPs) and cause KS-like disease[4]. This is likely the most relevant preclinical model to validate vaccine efficacy, but the

cost and scalability of NHP studies will likely restrict these studies to the most likely clinical candidates.

Even if a KSHV vaccine platform is shown to provide high levels of protection in preclinical studies, there will still be challenges that arise before it reaches the clinic. One such question is the target population for KSHV vaccination. One potential goal is to prevent KSHV acquisition by immunizing children in KSHV endemic regions where seropositivity is low in early childhood[5]. However, it is still unclear what immune responses are needed to prevent KSHV acquisition and how long protection would last after vaccination. Another route to pursue is preventing KSHV transmission, which occurs largely through saliva. Studies with KSHV, EBV, and hCMV have linked antibody levels to lack of infection in mother-child pairs[6–8]. Thus, it could be possible to immunize KSHV-infected individuals to enhance control of viral replication to reduce or prevent viral shedding. Natural KSHV infection does not induce robust neutralizing antibody or cellular immunity but remains largely asymptomatic in immunocompetent individuals[9–11]. This suggests that the seemingly “weak” natural KSHV immunity is sufficient to limit the virus but leaves room for vaccines to enhance immune control. One final option is for therapeutic vaccination against KSHV to suppress viral replication and minimize the number of latently infected cells in infected individuals. This will likely require the induction of virus-specific T cells that can recognize both lytic and latent antigens. However, it is unclear how much viral control will be needed to prevent KSHV-associated diseases and the development of such a T cell vaccine with demonstrated efficacy is still a while away.

Other challenges for a KSHV vaccine will come from the process of commercialization. Cell lines, such as iSLK cells used to make KSHV VLVs or CHO cells used for producing VLPs, must be validated and good manufacturing practice (GMP) standards must be developed to ensure consistency in vaccine production. Products must be tested for stability in areas without cold

storage chains and must be easily administered. Moreover, the vaccine will need to be produced at large scales, requiring huge investment from industry, government, or non-governmental organizations. As KSHV and KSHV-associated diseases are most prevalent in resource-limited areas such as sub-Saharan Africa and not in the Western world[12], there is little economic incentive for large vaccine manufacturers to invest in a KSHV vaccine. Thus, it may be on the backs of charitable and philanthropic organizations to bring a KSHV vaccine to the world. While large, these challenges are not insurmountable, and a widely used KSHV vaccine could be possible in the future.

The broad horizons of mRNA-LNP vaccinology

The work presented in this dissertation has demonstrated the power of LNP to generate strong adaptive immune responses. However, there is still much to be learned about this technology and its applications in vaccinology. Others have widely described LNP as inflammatory, potentially through IL-1 and IL-6 signaling[13,14], but preliminary studies from our lab also indicate that they can also generate IFN responses even in the absence of RNA cargo. Importantly, even commercial mRNA vaccines such as the one produced by Pfizer/BioNTech generate strong IFN-I responses[15]. This may appear in contrast with years of effort spent devising methods to reduce IFN-I signaling for improved antigen expression[16–19]. However, the discovery of modified nucleosides that reduce RNA sensing and diminish IFN-I induction has been a critical advancement for mRNA vaccines, because the very high level of IFN-I induced by unmodified mRNA severely undermines their safety and immunogenicity. What should be kept in mind are the potential negative effects of IFN-I induced by dsRNA byproducts and the LNP itself on the immunogenicity of mRNA vaccines and whether purification or different antigen designs can evade this interference. Thus, there is more to be learned about the role of innate immunity in the immunogenicity of mRNA-LNP vaccines.

It is clear from this work and published studies that innate immunity plays an important role in developing adaptive immune responses to mRNA vaccines. Increasing IL-1 signaling by genetically removing the IL-1 antagonist IL-1ra increases T cell responses to the Pfizer/BioNTech vaccine[13]. As shown in chapter 3, inhibition of IFN-I signaling through antibody blockade or genetic ablation can alter T cell responses in an antigen-dependent manner. However, it is still unclear what specific conditions are needed for these alterations to occur. For example, which cell types are required to respond to IL-1 and/or IFN-I for robust T cell responses? Cell type-specific removal of IL-1 receptor or IFNAR1 can be achieved in mice using the Cre-Lox system, allowing for discrimination of the roles of these innate cytokines on antigen presenting cells, T cells, and B cells. Timing should also be considered, as current mRNA vaccine regimes require at least two immunizations before individuals are considered protected. It could be possible that innate cytokines are more important in only the priming or boosting immunization instead of both. Further understanding of these cell type and temporal dynamics could help in the development of next-generation mRNA vaccines to properly use innate immunity to empower adaptive responses.

This dissection of IFN-I could be expanded to how individual IFN-I responses can impact the immunogenicity of an mRNA vaccine. In chapter 3, we noted that antibody responses to RBD were impacted by IFN-I in C57Bl/6 mice, but not in Balb/c mice. Pfizer's full-length Spike BNT162b2 did not demonstrate this difference in IFNAR KO mice and there were only minor differences when the two mouse strains were compared with Moderna's mRNA-1273[20,21]. In addition, humans immunized with BNT162b1 (RBD only) or BNT162b2 (full length Spike) demonstrated up to a 1 log range in binding and neutralizing antibody titers[22]. This suggests that genetic background or individual-specific contexts, including sensitivity to IFN-I, may impact the immunogenicity of an mRNA vaccine. One such modulator of a person's IFN-I sensitivity is the presence of anti-IFN antibodies. Anti-IFN antibodies can neutralize IFN activity, preventing the induction of antiviral gene programs and potentially leading to severe COVID-19[23,24]. These anti-

IFN antibodies can be found before SARS-CoV-2 infection, suggesting that they were not generated because of the infection and that they could impact IFN responses to prophylactic vaccines. While the role of IFN neutralizing antibodies on vaccine efficacy has not been widely studied, a recent report indicated that IFN-I deficiency from loss-of-function mutations in IFNAR or anti-IFN antibodies could result in severe adverse reactions to the live attenuated yellow fever vaccine[25]. Thus, it would reasonable to expect that anti-IFN antibodies would impact the immunogenicity of an mRNA vaccine, especially because commercial vaccines can trigger IFN-I gene signatures[15,20]. However, it is unclear if this modification in IFN-I signaling will be beneficial or detrimental for adaptive immune responses. With multiple mRNA vaccines in the commercial pipeline, time will soon tell whether the impacts of these IFN neutralizing antibodies are antigen-dependent as we demonstrated in mice.

One advantage of mRNA vaccines over traditional protein-based vaccines is the ability to quickly design new immunogens without the need to optimize the protein production for each antigen. The process of *in vitro* transcription is nearly identical for all mRNA sequences (assuming no issues arise in the secondary structure) with the exact same procedure for encapsulating them into LNP. This format also gives the opportunity for mRNA-encoded antigens to be modified to include other domains or to add on epitopes from other antigens. In chapter 3, we described antigen-specific impacts of IFN-I on mRNA-LNP immunogenicity. However, it is unclear whether these differences arise from the antigens themselves or from the modifications made to them. Additional work is needed to elucidate these differences, such as the ability of an MHC-I signal sequence and MITD domain to enhance T cell responses in the absence of IFN-I. The ease of mRNA transcription allows for the generation of antigens with swapped domains, such as RBD with the MHC-I signal sequence and a secreted RdRp, which will allow for the testing the impact of IFN-I on the antigens and their modifications.

The ease of generating new mRNA constructs for LNP formulations also facilitates the rapid production and testing of novel viral antigens. In chapter 4, we described the immunogenicity of an mRNA vaccine expressing the highly conserved SARS-CoV-2 RdRp. The immunogenicity of this RdRp mRNA-LNP has been described in an invention report for prophylactic immunization against SARS-CoV-2. While a robust RdRp-specific T cell response was generated, it was not protective. We discussed potential pitfalls and proposed a different challenge regime to confirm their role in preventing disease progression, since other studies have suggested that RdRp-specific T cells might play a role in protection[26]. Others have worked on the development of N specific T cell vaccines, which have shown efficacy in mice challenged with low infectious doses[27,28]. One potential benefit of RdRp is its earlier expression in the lifecycle, since it is needed to generate viral genomes. This is in contrast to N, which is a structural protein that is produced later when virions need to be formed. N is also subjected to antibody responses through display on the cell surface[29], potentially generating selective pressure that can result in T cell-evading mutations. However, RdRp is disadvantaged by its relatively lower expression level[30], which could reduce presentation on MHC-I to cytotoxic T cells. Overall, this study demonstrated the ability to test a new viral antigen for vaccine studies using mRNA-LNP technology, but the application of RdRp as a target for SARS-CoV-2 vaccination remains to be clarified.

Conclusions

The work described in the dissertation has utilized LNP technology for new and exciting purposes. It sets a foundation for an adjuvanted multivalent KSHV vaccine that generates antibodies with neutralizing and effector functions in addition to robust T cell responses. It demonstrates the effects of IFN-I on mRNA-LNP immunogenicity are not generalizable to all antigens. Finally, it describes a potential target for future SARS-CoV-2 mRNA vaccines that could provide broad

protection against current and future viral variants. Overall, it demonstrates the power and flexibility of LNP which will cement this technology into the future of vaccinology.

References

1. Nash, A. A., Dutia, B. M., Stewart, J. P. & Davison, A. J. Natural history of murine γ-herpesvirus infection. *Phil. Trans. R. Soc. Lond. B* **356**, 569–579 (2001).

2. Wang, L.-X. *et al.* Humanized-BLT mouse model of Kaposi's sarcoma-associated herpesvirus infection. *Proceedings of the National Academy of Sciences* **111**, 3146–3151 (2014).

3. McHugh, D. *et al.* Persistent KSHV Infection Increases EBV-Associated Tumor Formation In Vivo via Enhanced EBV Lytic Gene Expression. *Cell Host Microbe* **22**, 61-73.e7 (2017).

4. Chang, H. *et al.* Non-Human Primate Model of Kaposi's Sarcoma-Associated Herpesvirus Infection. *PLoS Pathog* **5**, e1000606 (2009).

5. Nalwoga, A. *et al.* Variation in KSHV prevalence between geographically proximate locations in Uganda. *Infect Agents Cancer* **15**, 49 (2020).

6. Poppe, L. K., Wood, C. & West, J. T. The Presence of Antibody-Dependent Cell Cytotoxicity–Mediating Antibodies in Kaposi Sarcoma–Associated Herpesvirus–Seropositive Individuals Does Not Correlate with Disease Pathogenesis or Progression. *J.I.* **205**, 2742–2749 (2020).

7. Minab, R. *et al.* Maternal Epstein-Barr Virus-Specific Antibodies and Risk of Infection in Ugandan Infants. *The Journal of Infectious Diseases* jiaa654 (2020) doi:10.1093/infdis/jiaa654.

8. Semmes, E. C. *et al.* Maternal Fc-mediated non-neutralizing antibody responses correlate with protection against congenital human cytomegalovirus infection. *Journal of Clinical Investigation* (2022) doi:10.1172/JCI156827.

9. Labo, N. *et al.* Heterogeneity and Breadth of Host Antibody Response to KSHV Infection Demonstrated by Systematic Analysis of the KSHV Proteome. *PLoS Pathog* **10**, e1004046 (2014).

10. Roshan, R. *et al.* T-cell responses to KSHV infection: a systematic approach. *Oncotarget* **8**, 109402–109416 (2017).

11. Nalwoga, A. *et al.* Kaposi's sarcoma-associated herpesvirus T cell responses in HIV seronegative individuals from rural Uganda. *Nat Commun* **12**, 7323 (2021).

12. Mesri, E. A., Cesarman, E. & Boshoff, C. Kaposi's sarcoma and its associated herpesvirus. *Nat Rev Cancer* **10**, 707–719 (2010).

13. Tahtinen, S. *et al.* IL-1 and IL-1ra are key regulators of the inflammatory response to RNA vaccines. *Nat Immunol* (2022) doi:10.1038/s41590-022-01160-y.

14. Alameh, M.-G. *et al.* Lipid nanoparticles enhance the efficacy of mRNA and protein subunit vaccines by inducing robust T follicular helper cell and humoral responses. *Immunity* **54**, 2877-2892.e7 (2021).

15. Arunachalam, P. S. *et al.* Systems vaccinology of the BNT162b2 mRNA vaccine in humans. *Nature* **596**, 410–416 (2021).

16. Karikó, K., Buckstein, M., Ni, H. & Weissman, D. Suppression of RNA Recognition by Toll-like Receptors: The Impact of Nucleoside Modification and the Evolutionary Origin of RNA. *Immunity* **23**, 165–175 (2005).

17. Karikó, K. *et al.* Incorporation of Pseudouridine Into mRNA Yields Superior Nonimmunogenic Vector With Increased Translational Capacity and Biological Stability. *Molecular Therapy* **16**, 1833–1840 (2008).

18. Karikó, K., Muramatsu, H., Ludwig, J. & Weissman, D. Generating the optimal mRNA for therapy: HPLC purification eliminates immune activation and improves translation of nucleoside-modified, protein-encoding mRNA. *Nucleic Acids Research* **39**, e142–e142 (2011).

19. Nelson, J. *et al.* Impact of mRNA chemistry and manufacturing process on innate immune activation. *Sci. Adv.* **6**, eaaz6893 (2020).

20. Li, C. *et al.* Mechanisms of innate and adaptive immunity to the Pfizer-BioNTech BNT162b2 vaccine. *Nat Immunol* **23**, 543–555 (2022).

21. Corbett, K. S. *et al.* SARS-CoV-2 mRNA vaccine design enabled by prototype pathogen preparedness. *Nature* **586**, 567–571 (2020).

22. Walsh, E. E. *et al.* Safety and Immunogenicity of Two RNA-Based Covid-19 Vaccine Candidates. *N Engl J Med* **383**, 2439–2450 (2020).

23. Bastard, P. *et al.* Autoantibodies against type I IFNs in patients with life-threatening COVID-19. *Science* **370**, eabd4585 (2020).

24. Bastard, P. *et al.* Autoantibodies neutralizing type I IFNs are present in ~4% of uninfected individuals over 70 years old and account for ~20% of COVID-19 deaths. *Sci Immunol* **6**, eabl4340 (2021).

25. Bastard, P. *et al.* Auto-antibodies to type I IFNs can underlie adverse reactions to yellow fever live attenuated vaccine. *Journal of Experimental Medicine* **218**, e20202486 (2021).

26. Swadling, L. *et al.* Pre-existing polymerase-specific T cells expand in abortive seronegative SARS-CoV-2. *Nature* **601**, 110–117 (2022).

27. Matchett, W. E. *et al.* Cutting Edge: Nucleocapsid Vaccine Elicits Spike-Independent SARS-CoV-2 Protective Immunity. *J.I.* **207**, 376–379 (2021).

28. Dangi, T., Class, J., Palacio, N., Richner, J. M. & Penaloza MacMaster, P. Combining spike- and nucleocapsid-based vaccines improves distal control of SARS-CoV-2. *Cell Reports* **36**, 109664 (2021).

29. López-Muñoz, A. D., Kosik, I., Holly, J. & Yewdell, J. W. Cell surface SARS-CoV-2 nucleocapsid protein modulates innate and adaptive immunity. *Sci. Adv.* **8**, eabp9770 (2022).

30. Weingarten-Gabbay, S. *et al.* Profiling SARS-CoV-2 HLA-I peptidome reveals T cell epitopes from out-of-frame ORFs. *Cell* **184**, 3962-3980.e17 (2021).